**The Thesis Committee for Takonporn Kunpitaktakun**
**Certifies that this is the approved version of the following thesis:**

# Architecture of Unusually Thick Bottomsets and Multidirectional Sediment Sourcing in Deep Lake Clinothems, Dacian Basin, Romania

**APPROVED BY**
**SUPERVISING COMMITTEE:**

**Supervisor:** _____
Ronald J. Steel

**Co-Supervisor:** _____
Cornel Olariu

**Co-Supervisor:** _____
William L. Fisher

# Architecture of Unusually Thick Bottomsets and Multidirectional Sediment Sourcing in Deep Lake Clinothems, Dacian Basin, Romania

**by**

**Takonporn Kunpitaktakun**

**Thesis**

Presented to the Faculty of the Graduate School of

The University of Texas at Austin

in Geological Sciences

of the Requirements

for the Degree of

**Master of Science in Geological Sciences**

**The University of Texas at Austin**

**August, 2017**

# Acknowledgements

I would like to thank Mr. Cornel Olariu, Dr. Ronald J. Steel and Dr. William L. Fisher for the support and advice and being the great advisers I could ever ask for. Secondly, I would like to thank PTTEP for the financial support for my master program and OMV Petrom for the data. Last but not least, I would like to thank my family and friends for emotional support and everything that they have done for me.

# Abstract

## Architecture of Unusually Thick Bottomsets and Multidirectional Sediment Sourcing in Deep Lake Clinothems, Dacian Basin, Romania

Takonporn Kunpitaktakun (MSGeoSci)

The University of Texas at Austin, 2017

Supervisor: Ronald J. Steel, Cornel Olariu and William L. Fisher

The models for basin floor fans formed at lowstand or highstand condition of sea level are now well known. In this project an additional complexity is added to deep water fan architecture where sediment is fed to an inland-lake basin floor from widely dispersed,multiple directions. Late Miocene clinoforms some 300-450 m high feed down onto the basin floor and are easily recognized in 3-D seismic of the western Dacian Basin, a para-Tethys basin in Romania. The basin was a closed lake basin during most of its existence. The basin margin clinoforms can be difficult to recognize even across closely spaced well logs but in seismic data the three clinoform segments are well imaged, namely a 100-150 m thick, lower interval with coarse sandy deposits, an overlying 150-200 m thick muddy succession and and an upper 50-100 m thick succession of sandy deposits.

The 3-D seismic data combined with seven well cross-sections are the main tools used here to investigate the architecture of the basin-floor fans. The submarine fans are surprisingly aggradational, reaching thicknesses 100-150 m in places, and the fans can be followed laterally on the seismic data for hundreds of kilometers. Spontaneous potential (SP) and resistivity logs of some 200 closely spaced (~300 m) wells have been correlated over an area of thick basin-floor

fans. Shelf, shelf edge, slope and basin floor depositional systems were mapped on seismic data and also recognized in well logs.

The well logs show that the fans are composed of vertically repeated 10-30 m thick sandstone units, interpreted here as fan lobes. The lobes have variable sandstone distribution with a range of coarsening or thinning upwards, blocky or ratty log patterns suggesting variable facies and depositional settings. Individual lobes extend from the lower slope and onto the basin floor. In the 'distal' area of one of the clinoforms the fans have thicker sandstone intervals,possibly representing lobes formed by sediment shed from a different directions Into this location on the basin floor.

We are able to document deepwater fan-lobe sandstones with different orientations and variable thicknesses through time, as these are linked with variable rates and directions of basin margin progradation. As a consequence, the complexity of fan lobes and feeding directions makes it likely that sediment was supplied from multiple catchment areas.

The unusual thickness of the Dachian Basin submarine fans relates both to the interfingering of differently oriented fans and to the tendency for a greater frequency of river-derived sediment-gravity flows reaching the basin floor of relatively fresh-water lakes. This high partitioning of sandy sediment into the clinothem bottomsets is likely to be similar in other enclosed lake basins.

# Table of Contents

# List of Figures

# Chapter 1: Introduction

The term clinoform refers to the sigmoidal geometry of the bounding surfaces of individual increments of shelf margin accretion, while the term clinothem refers to the rock deposited between two clinoform surfaces (Rich, 1951). The topset of basin margin clinothems is composed of fluvial and shallow marine deposits, the foreset or deepwater slope contains mainly mudstones and some sand-filled channels and the bottomset is composed of sandy basin-floor fan and other finer grained deposits (Johannessen and Steel, 2005). Clinoforms with a vertical amplitude of hundreds of meters thickness are present as infilling the Dacian Basin and these have been previously described and illustrated on seismic data with emphasize of the topset-foreset-bottomset separation and the depositional environments (Fong-ngern et al., 2015) (Figure 1). Leever et al. (2010) presented a regional seismic interpretation along multiple 2-D seismic lines and found different aged (Meotian to Pontian) clinoforms which prograded from multiple directions around the margin of Dacian Basin (Figure 2). Architecture of the basin floor fans that compose the bottomsets of clinoforms with multiple progradation directions is the focus of this thesis. In this study, (1) the seismic clinoform mapping is extended (compared to Fonfngern et al., 2015) toward the center of the basin, (2) the architecture of clinoform bottom sets are described using closely (hundreds of meters) spaced well logs. The working assumption while mapping is that different well logs patterns define variable basin floor depositional facies. Furthermore, this study aims to understand the direction of sediment feeding by using clinoform progradation directions, sandstone thickness maps, and Spontaneous Potential (SP) log characteristics distribution in each fan lobe, and 3) the sub-depositional environments of fan lobes are interpreted in order to generate the evolution of basin floor fans inside the study area.

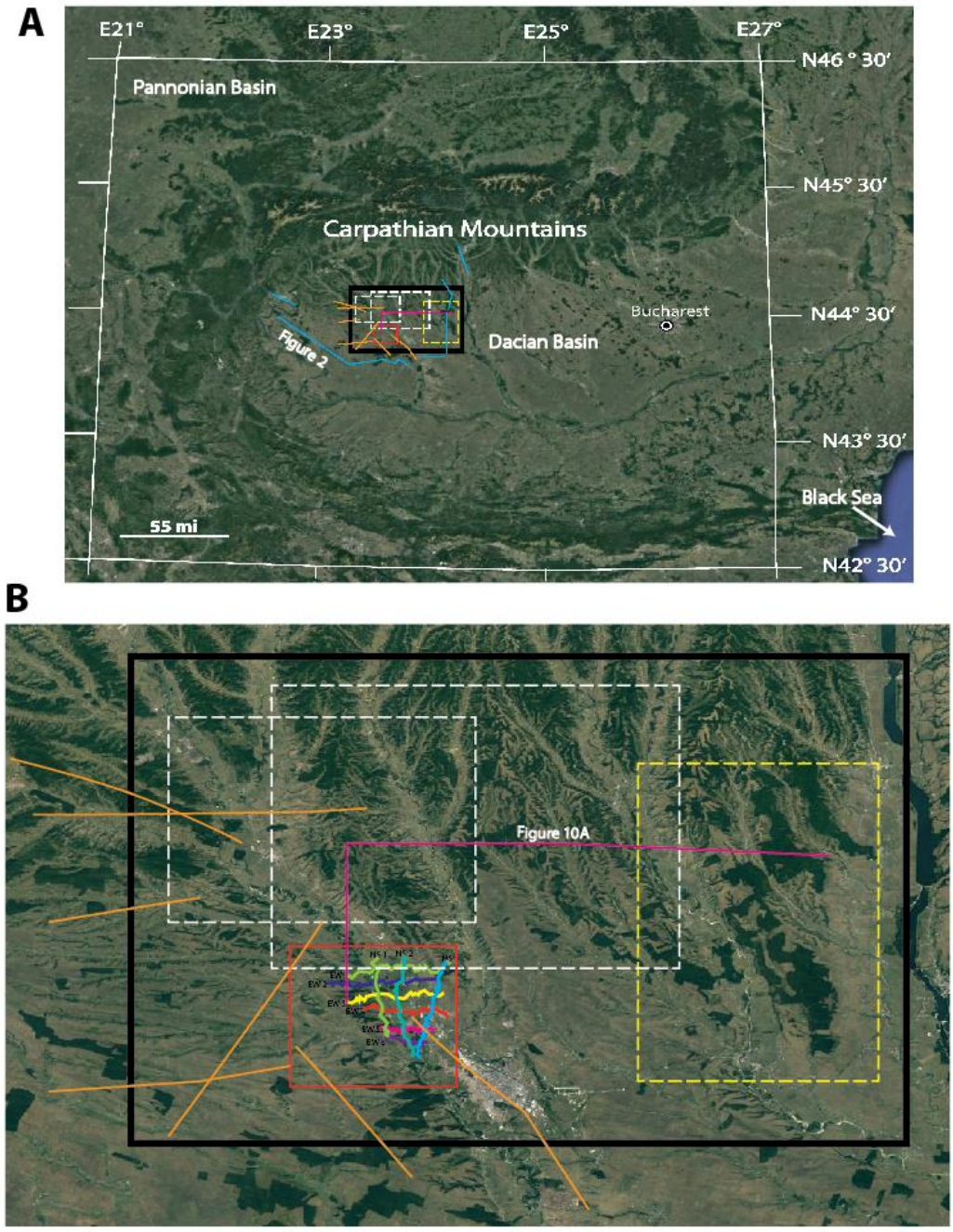


Figure 1: A) The study area in black rectangle. The yellow rectangle represents the seismic cube of Fong-ngern et al( 2015) The red rectangle represents the Bradesti 3D cube which is the main focus of this present study. The orange lines are selected 2D seismic lines, used here to define clinoform progradational patterns from around the study area. The pink line represents the seismic arbitrary line extended from Fong-ngern's (2015) study area to Bradesti 3D cube in Figure 10. The blue lines are the seismic sections in Figure 2. B) Enlarged study area shows well locations that are used for correlation inside Bradesti 3D cube.

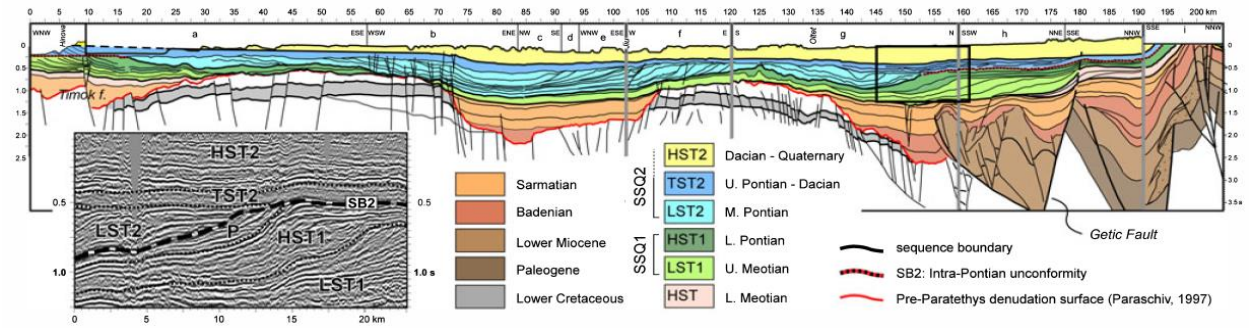


Figure 2: Regional seismic interpretation of the Dacian Basin illustrates clinoforms with ages ranging from Meotian (light green) to Pontian (blue) (Leever et al, 2010).

## GEOLOGICAL SETTING OF DACIAN BASIN

The Dacian Basin is the area covered from the foot of Eastern Carpathians and Southern Carpathian to the lower Danube River (Figure 3). The basin is bounded to the west by the transition from the Carpathians to the Balkan Mountains, and to the east by the Dobrogean High which is also the barrier between the Dacian Basin and the Black Sea Basin.

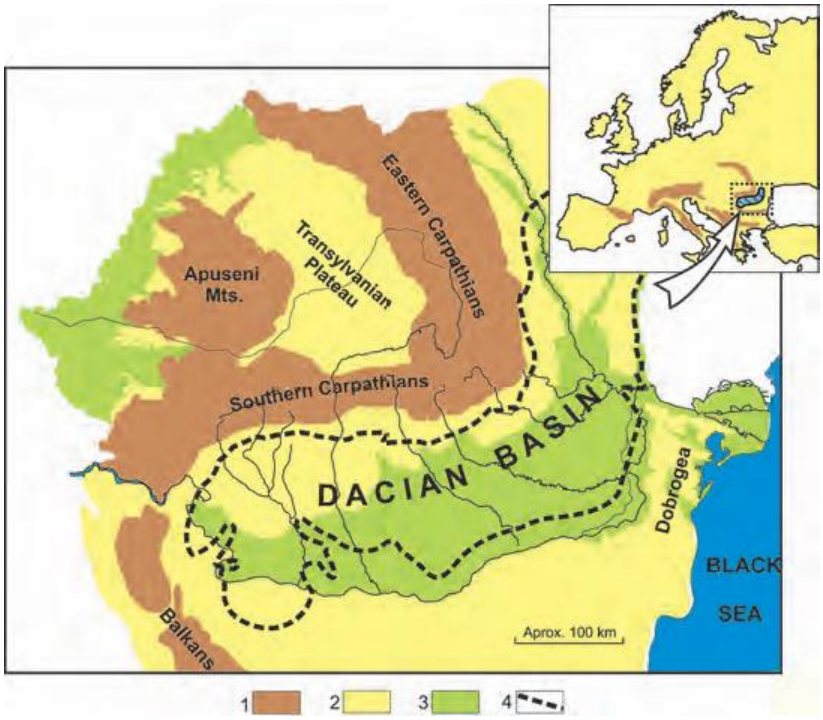


Figure 3: Maeotian Dacian Basin outline overlaying on Romania physical map. Upper-right corner is the Dacian Basin on the Europe map. Legend 1. Highland relief 2. Hilly relief 3. Lowland relief 4. Dacian Basin outline during Maeotian (Jipa &Olariu, 2009 after Saulea et al, 1969 and Hamor et al, 1988)

The Dacian Basin was formed during Sarmatian time (14 to 9 Ma) during the closure of the para-Tethys that was an extension of the Tethys Ocean between the African and Euro-Asian plates (Balla, 1987 and Ustaszewski et al, 2008). The Dacian Basin overlap with the Miocene Carpathian foredeep (Jipa & Olariu, 2009 after Popov et al, 2004 and Saulea et al, 1969) (Figure 4). The Dacian Basin formed due to increased subsidence rates during late Miocene (Matenco et al., 2003) caused by change in tectonic dynamics in early Miocene (Kreszek et al., 2013).

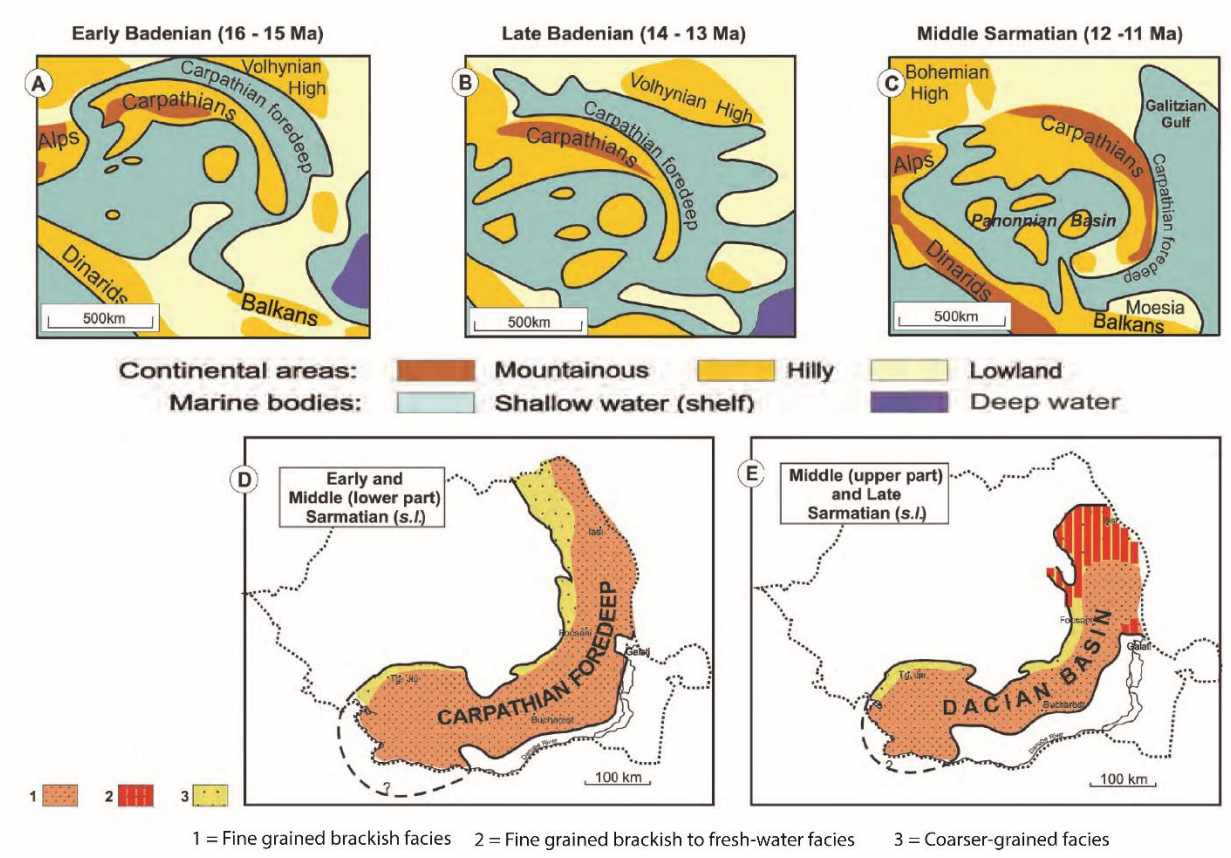


Figure 4: The evolution of the Carpathian foredeep during the Early Badenian (A), Late Badenian (B) and Middle Sarmatian (C). D is the paleogeographic of the Carpathian foredeep during the Middle Sarmatian. E is the paleogeographic of the Dacian Basin during the Late Sarmatian. (Jipa & Olariu, 2009 after Popov et al, 2004 and Saulea et al, 1969)

During the Maeotian (9 – 5.8 Ma), the paleogeography of uplifted area and basins changed dramatically in this area suggesting highly dynamic tectonics that influenced the depositional settings. The north of the Dacian Basin rose and created the Galati passage during Meotian that

limited the connection between the Dacian Basin and the Black Sea Basin or the Euxinian Basin (Figure 5). As a result, the Dacian Basin became the semi-enclosed basin. Since the Dacian Basin was separated from the Black Sea Basin, the brackish-water condition of Dacian Basin became more of lower salinity during the middle Miocene while the Euxinian Basin was still brackish to marine condition (Papaianopol, et al, 1995 and Ilyina et al, 1976).

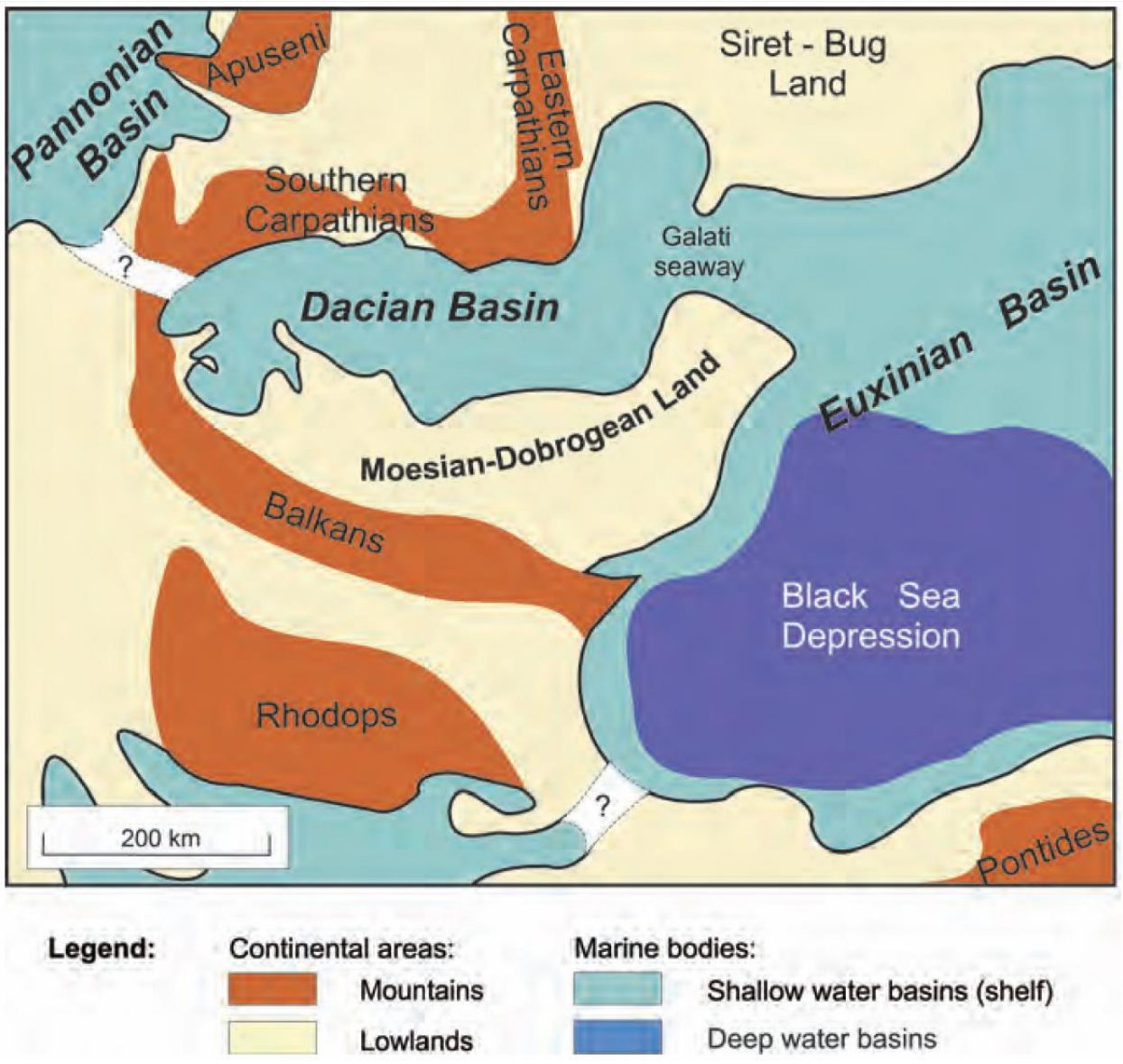


Figure 5: The paleogeography of the Dacian Basin during the Early Maeotian (Jipa & Olariu, 2009 after Ilyina et al, 1995)

Even though many studies have been done in outcrops or this area (Olteanu, 1989, Jipa, Stoica et al., 2007), the chronostratigraphic and geochronologic framework for the subsurface stratigraphy is not well established. The reason behind the lack of the subsurface chronostratigraphy is that relative recent imagining of the clinoforms in the basin do not match the widely used stratigraphic column model established from the outcrops (Figure 6).

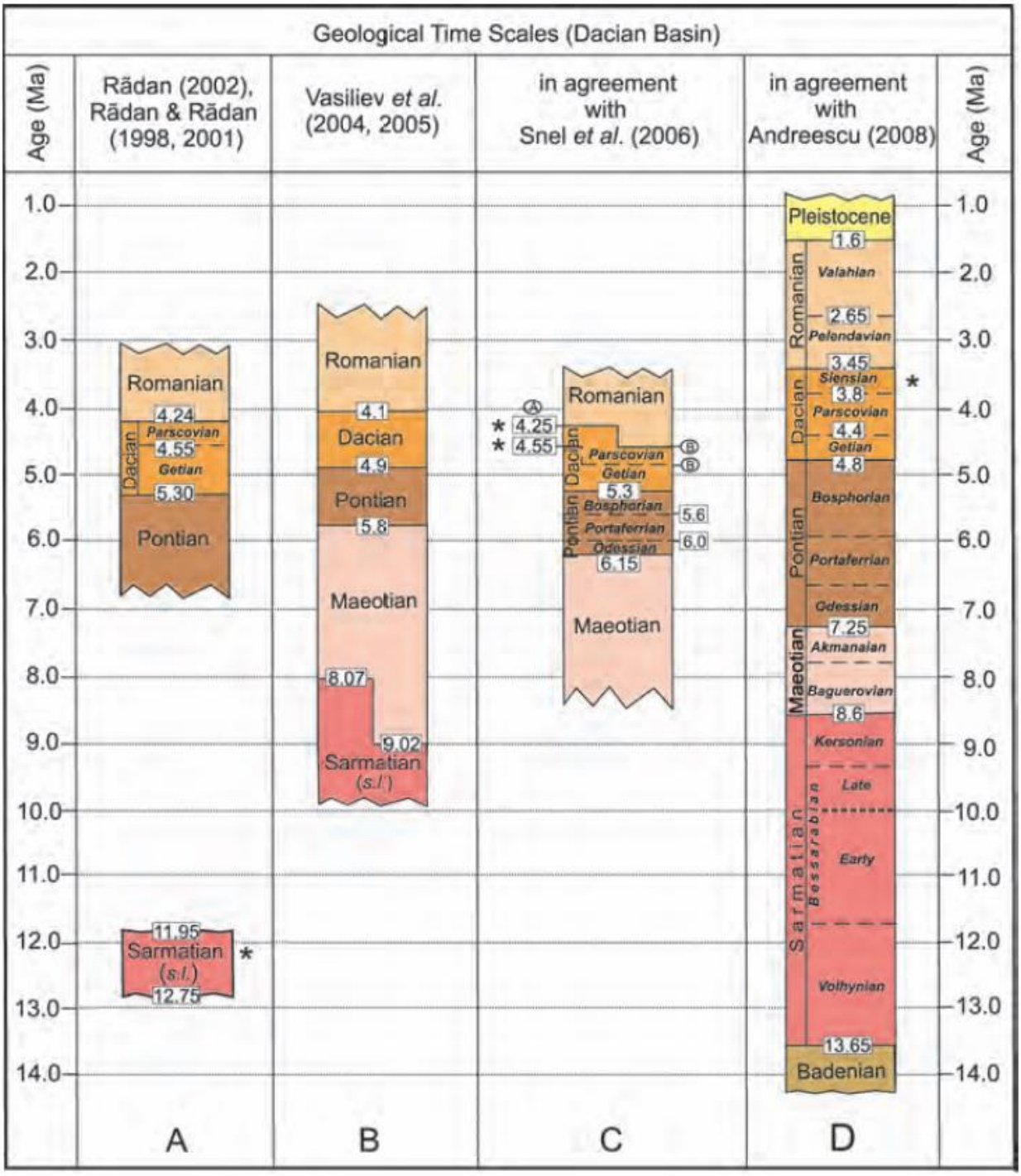


Figure 6: Geological time scale of the Dacian Basin (Jipa & Olariu, 2009)

Fong-ngern et al. (2015) mapped clinoforms in a 3-D seismic cube (Figure 1) and the result showed 400 m thick prograding clinoforms from northeast to southwest (Figure 7). On the mapped surface of a clinoform, the shelf edge and toe of slope were interpreted based on the changing of

gradient and they were illustrated in the dash lines (Figure 8A). The seismic amplitude maps of the clinoform in Figure 8B indicates coarser-grained in hot colors and finer-grained in cool colors. According to the amplitude maps, most of the coarse-grained has been deposited on shelf and basin floor. Furthermore, the age and depositional environment of clinoforms in this study are also interpreted as age ranged from Sarmatian to Pontian with topset interpreted as shelf or shallow water deposit, the foreset interpreted as slope deposits and the bottomsets interpreted as basin floor deposit (Figure 9).

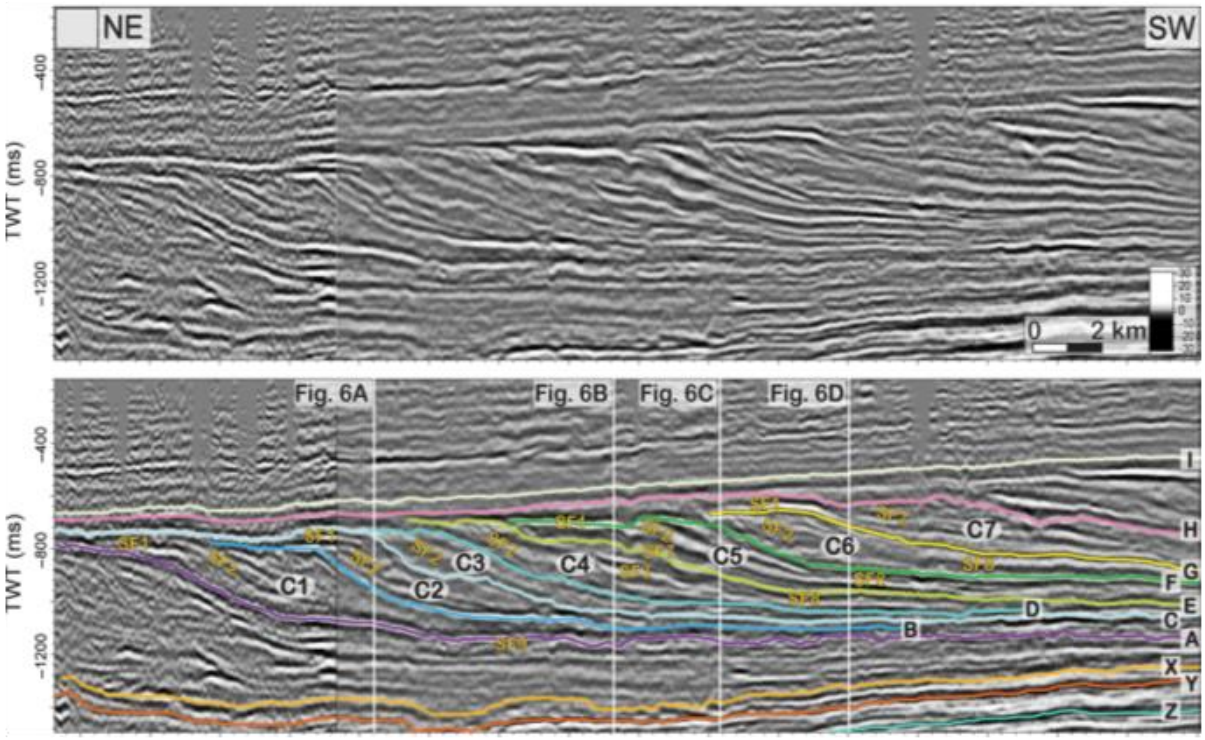


Figure 7: The depositional dip oriented seismic line that shows prograding of 400 m thick clinoforms from NE to SW (Fong-ngern et al, 2015)

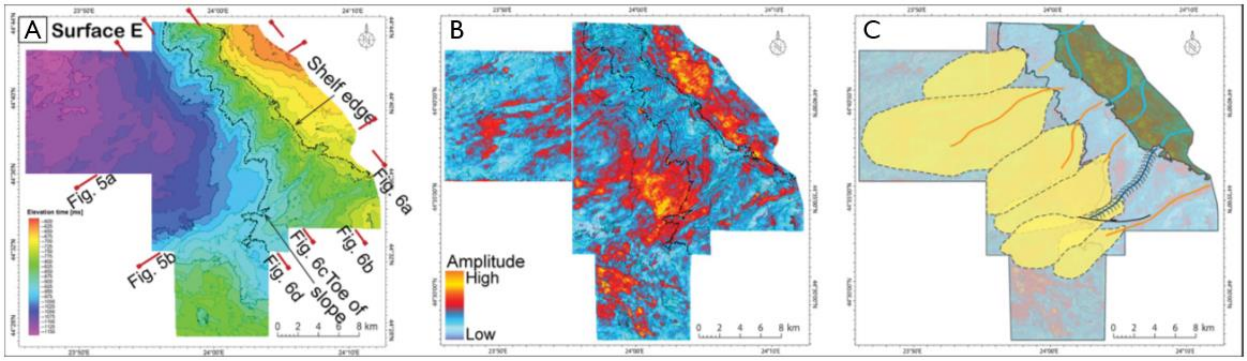


Figure 8: Image of a clinoform surface in 3-D. A: Surface depth of a clinoform. The dash lines represent change in gradient interpreted as shelf edge and toe of slope. B: the amplitude map of a clinoform. The hotter color indicates coarser grained than cooler color. C: the interpreted depositional environment of a clinoform. (Fong-ngern et al,2015)

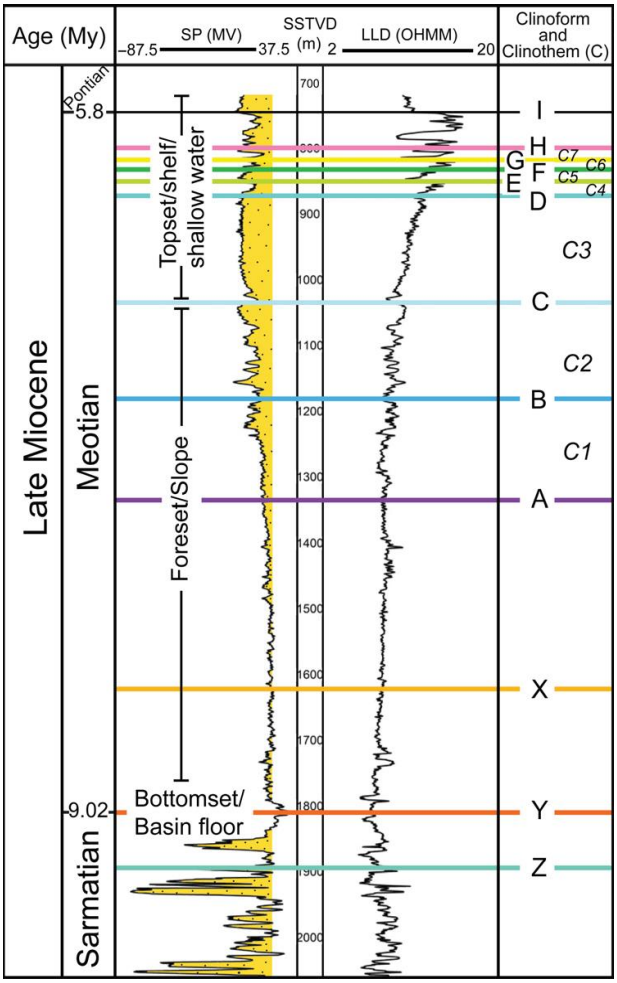


Figure 9: Example of a well log with characteristic patterns and the interpreted depositional environment and age of clinoforms (Fong-ngern et al, 2015)

# Chapter 2: Data and Methodology

Seismic and well log data are the main tools used in this study. The regional distribution of clinoforms and basin -floor fans were mapped on both 3-D seismic cube and 2-D seismic lines. After establishing the regional trend of clinoform progradation, the details of basin-floor fans were analysed using well log pattern characteristics, after the strata were correlated.

## SEISMIC DATA

Four seismic cubes were included in the clinoform mapping (Figure 1B). However, the detailed study was done in Bradesti 3-D cube because it allows best control of the well logs. Bradesti cube covers 170 square kilometers with the frequency ranges from 20 to 30 hertz. The depth of the examined stratigraphy was between 750 to 1400 ms.

## SEISMIC INTERPRETATION

Clinoforms were initially mapped as a continuation from the study area of Fong-ngern et al, (2015), to the current Bradesti 3-D cube. The seismic arbitrary line in Figure 10A illustrates the prograding, NE to SW clinoforms and shows well that the thick bottomsets of these clinoforms extend throughout the Bradesti 3-D cube. The seismic interpreted clinoforms are converted from time to depth domain using a velocity model which is the same as Fong-nger et al (2015) used in their study because the check-shot data in that seismic cube is available. After seismic interpretation and depth conversion, a correlated cross-section of wells was placed inside the Bradesti 3-D cube and the depth domain clinoforms were overlaid on the well section (Figure 10B). The bottomset of the clinoform series was thus matched with the 100-150m basin-floor fan sandstone interval in the well series. In the wells, the basin-floor fan sandstones can be seen to be overlain by >300 m thick mudstones interpreted as slope deposits. The black line in Figure 10A represents the top of the basin-floor fans and the white line marks their bottom. The fans can therefore be traced back landwards to the feeding clinoforms to the west (Figure 10A). The mudstone units capping most fan lobes are referred to as ‘abandonment surface mudstones’, and

are somewhat analogous to the flooding surfaces of the extensive muddy units seen on the shelf topset succession.

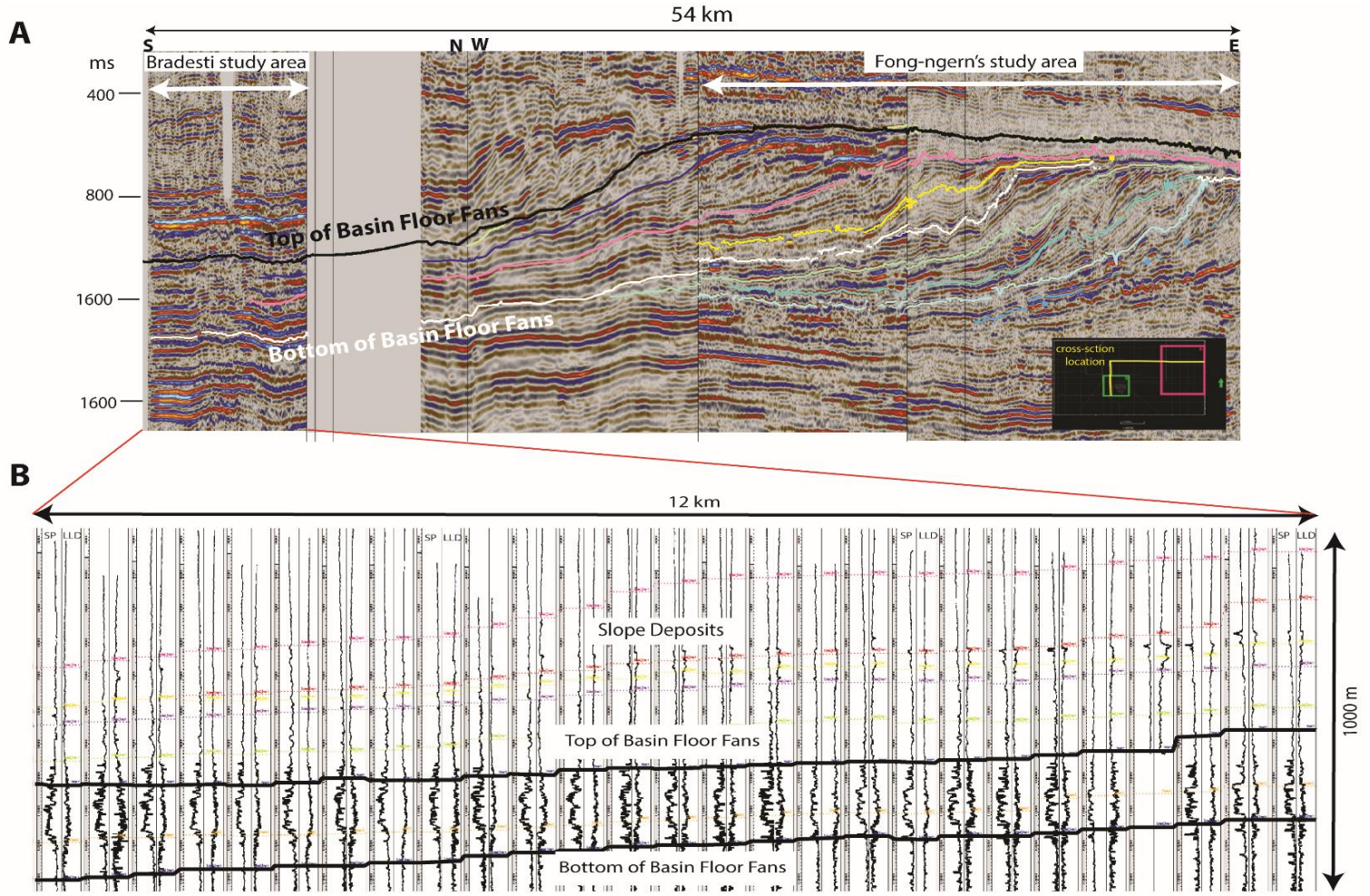


Figure 10: A) Arbitrary seismic line shows clinoforms prograding from the east (Fong-ngern's study area in pink rectangle) and emphasizes the thickness of the bottom set in the Bradesti 3D cube (in green rectangle). The back line represents the top of basin floor fans and the white line represents the bottom. The fans can be traced back from the basin-floor interval to the slope inside Bradesti 3D cube. B) The well cross-section inside Bradesti 3D cube.

The basal and upper horizons of the fan interval are extended across the 2-D seismic lines around the Bradesti area in order to map the clinoforms that were prograding from several directions. Different directions of clinoform progradation reflect a provenance range for the large scale sediment transport into the basin. Figure 1 illustrates the selected seismic 2D lines in orange color.

## WELL DATA

Some 217 well logs are located in the Bradesti area (Figure 10B) and penetrate the mapped clinoform bottomsets that are the focus of the study. The well logs were digitized from Raster (TIF) images and loaded in Petrel software allowing a tie between these and the seismic data, as well as allowing an interpretation of the key stratigraphic surfaces. The mapped stratigraphic surfaces, isochore and sandstone thickness maps were created using Petra. Spontaneous log (SP log) and resistivity log (LLD log) are the main tools for well correlation and for interpreting the characteristics of the fan lobes.

Well correlation is based on changes of well logs values and characteristic patterns. To illustrate, the lower SP values inside sandy interval reflect muddy surfaces (Figure 11) that might be related to reduced sediment supply on the shelf. The peaks in resistivity values inside muddy intervals possibly reflect condense sections or marine hiatus or low sedimentation rates (Loutit et al, 2012). Seventeen “muddy” surfaces are correlated throughout the area. An example of “muddy surface” picks that highlight separate fan-lobes is illustrated in Figure 11. Prelat et al termed these muddy surfaces as “fine-grained units” (interlobes). Since the sand thickness of each fan lobe varies laterally, the muddy surfaces characteristics also vary locally. The interval between two flooding surfaces are considered as one fan lobe similar to what was interpreted in other datasets (Prelat et al, 2009, Koo et al, 2016).

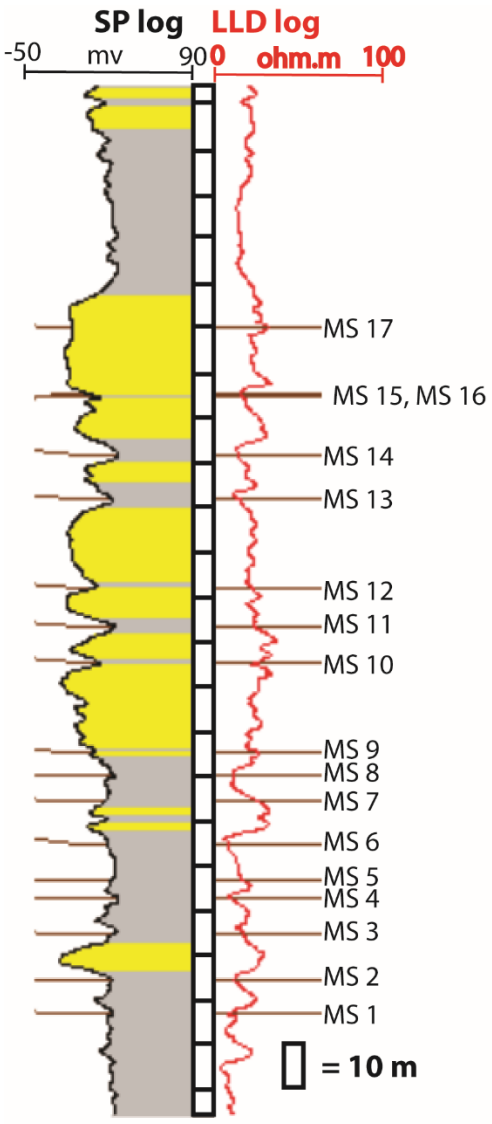


Figure 11: An arbitrary well showing the selection of seventeen thin muddy surfaces or lobe-abandonment surfaces, somewhat analogous (but likely of different origin) to flooding surfaces on the shelf.

## WELL CORRELATION

Six E-W cross sections and three N-S cross sections composing of 217 wells are generated inside the Bradesti 3-D cube (Figure 1). Characteristics of each well section are listed in table 1.

Table 1: well section information

| Well Section Name | Number of Wells | Total Distance |
|---|---|---|
| E-W1 | 30 | 8.2 km |
| E-W2 | 24 | 6.3 km |
| E-W3 | 31 | 6.5 km |
| E-W4 | 21 | 5.5 km |
| E-W5 | 31 | 3.3 km |
| E-W6 | 19 | 3.0 km |
| N-S1 | 24 | 5.4 km |
| N-S2 | 35 | 6.5 km |
| N-S3 | 41 | 6.5 km |

## MAPPING

Isochore and net sand maps were generated, using Petra software, for each of the fan lobes interpreted. The isochore map represents the vertical thickness of the fan lobe penetrated by wells. Since we do not have any image log or dip meter, we cannot correct for the structural dip to get the real fan lobe thickness. The net sand maps are based on SP log cutoff of 40 mv, based on various wells and the variety of drilling mud resistivity. Then, the SP log pattern of each fan lobe is overlaid on the net sand map in order to use the fan lobe thinning direction and SP log-pattern characteristics to understand the lobe progradation direction and depositional setting.

# Chapter 3: Results

## CLINOFORM THICKNESS INTERPRETATION FROM SEISMIC DATA

The bottom and top of a chosen set of clinoforms (including basin floor fans) are interpreted in different seismic 3-D cubes (Figures 12A and 12C) then converted to depth domain by a velocity model (Figure 12B and 12D). The top and bottom of the same set of clinoforms in a series of well logs are tied into the seismic mapped clinoforms which can be seen to be prograding into the Dacian Basin from the northeast.

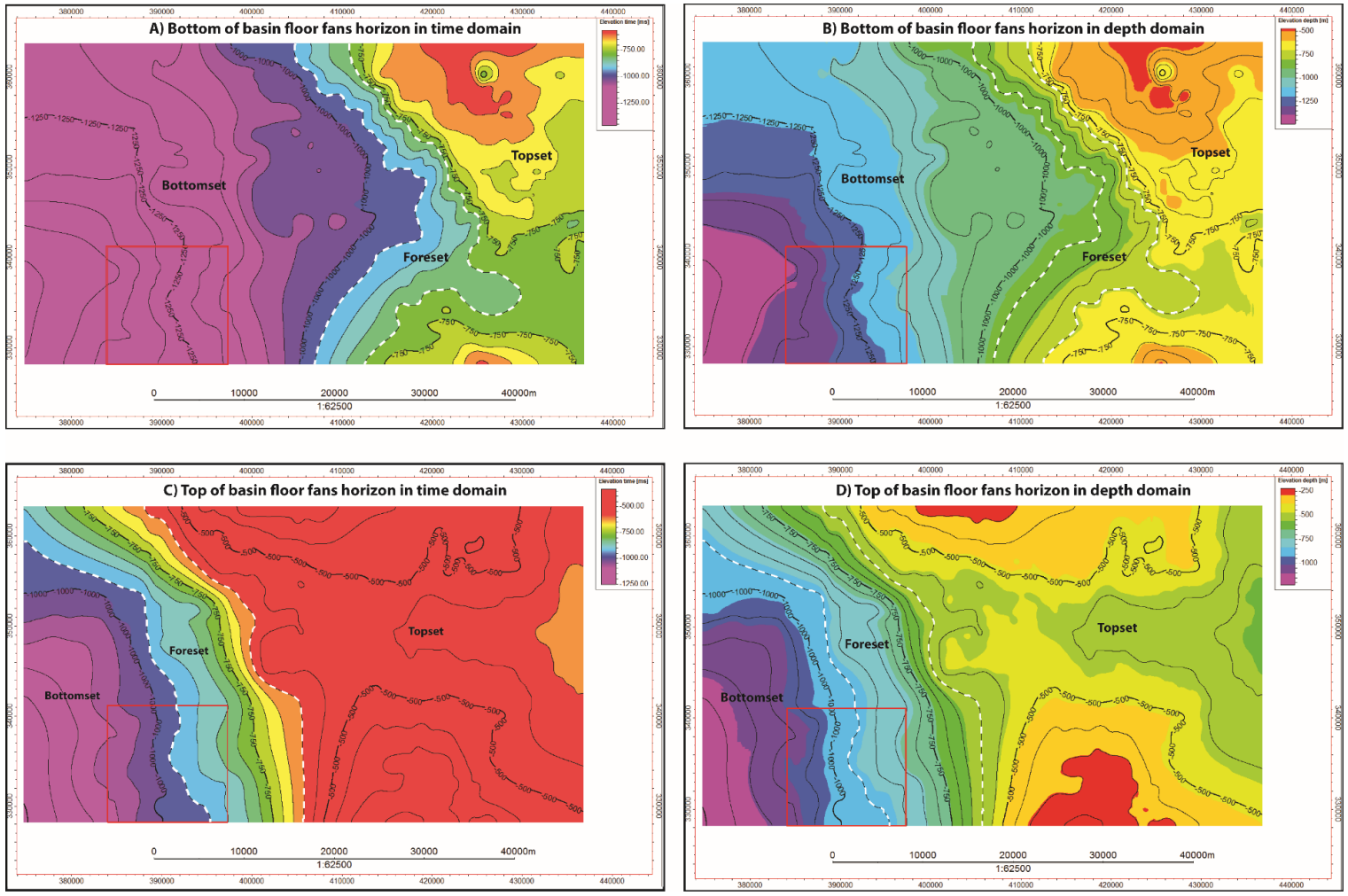


Figure 10: A) Depth map, picking the base of the basin-floor fan series in time domain with Bradesti 3D cube in red rectangle. B) Depth map, picking the base of the basin-floor fan series in depth domain with Bradesti 3D cube in red rectangle C) Depth map, picking the top of the basin-floor fan series in time domain with Bradesti 3D cube in red rectangle D) Depth map picking the top of the basin-floor fan series in depth domain with Bradesti 3D cube in red rectangle

The thickness map (Fig. 13A) of the selected series of clinothems is generated as the difference between the two depth maps, for example between the black and white reflectors in Figure 10A. The average thicknesses of topset, slope and bottomset are 100 m, 500m and 300m, respectively. This highlights an architecture of a clinothem set with meagre topsets, surprisingly thick bottomsets and strong shelf-margin progradation (Figure 13B).

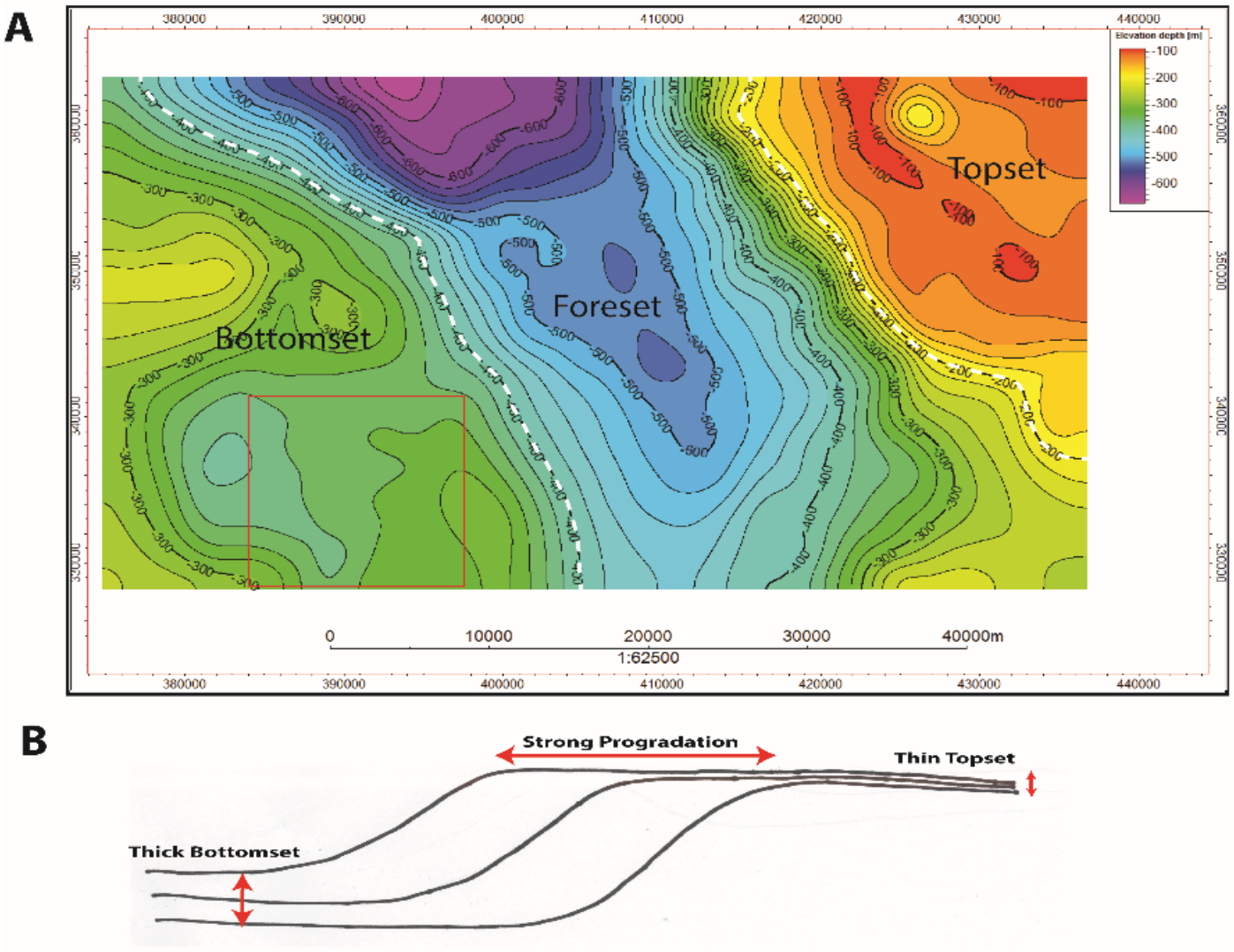


Figure 11: A) Thickness map of the chosen set of clinothems (see base and top of clinoforms set in Fig. 10A) B) Schematic drawing of clinoforms in the study area

In order to understand the changing depositional environments down and along the mapped clinoforms and to highlight the grainsize distribution along the bottomsets, seismic amplitude maps were generated in the Bradesti area. The seismic amplitude maps were generated by dividing the combined thickness of the series of clinothems (black to white horizons in Figure 10A) into 100 intervals, with an amplitude map generated for each interval. The amplitude slices were numbered from interval 100 at the bottom and interval 1 at the top. The hotter color indicates coarser grain size. The examples of amplitude intervals 98 to 94 show the progradation of coarse-grained lobes from the east to the west and some lobate features in intervals 96 and 94 (Figure 14). However, the amplitude slice from the middle interval 50 does not demonstrate anysignificant features (Figure 15). The reason might be the low reflection coefficient inside amalgamated sandstone units.

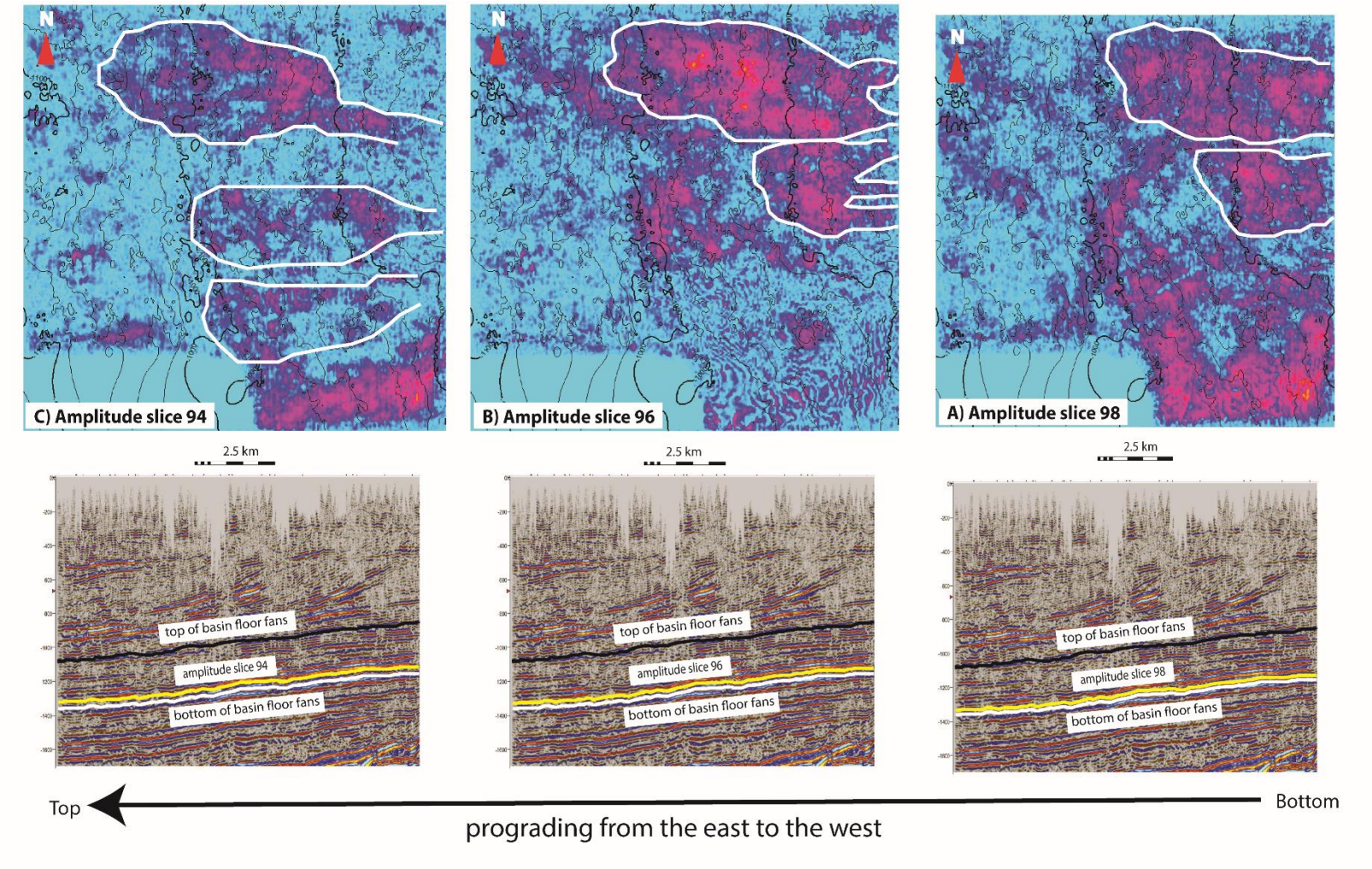


Figure 12: Amplitude slice interval 94, 96 and 98 in Bradesti 3D cube showing lobate features prograding form the east to the west. The hotter color indicates coarser grain size.

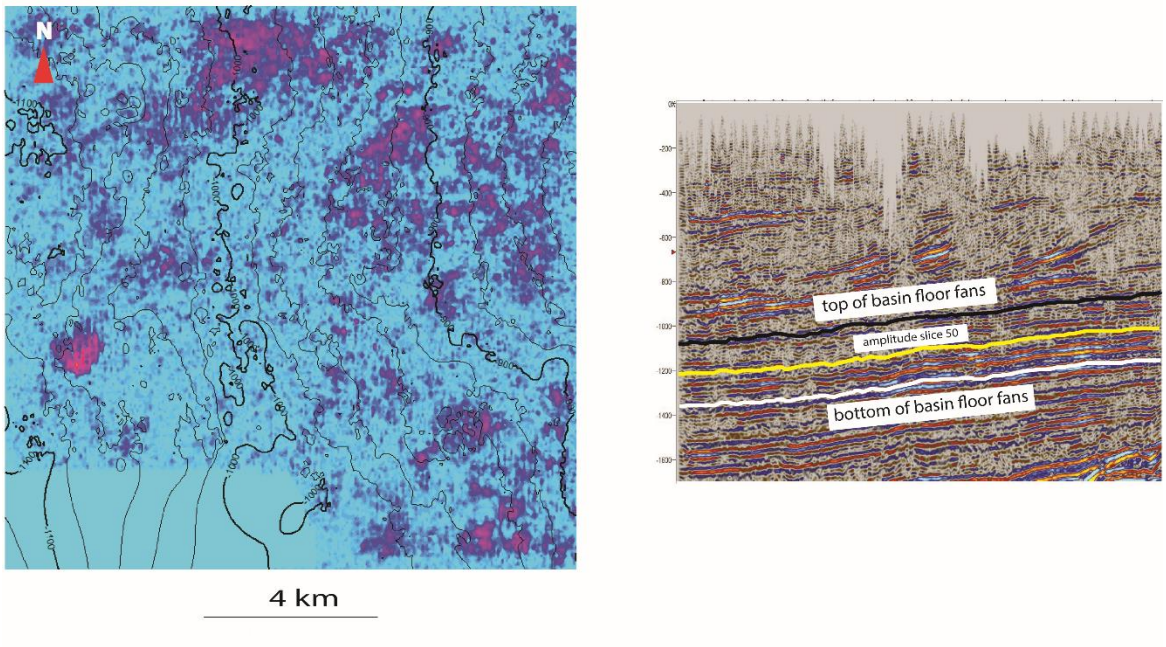


Figure 13: Amplitude slice interval 50 in the middle of basin floor fans in Bradesti 3D cube. The hotter color indicates coarser grain size.

Interpretation of selected 2-D seismic lines with different orientations show clearly that clinoforms prograded the basin margin from several directions (Figure 16), but at different times. For example, seismic line C shows clinoforms prograding from the west (Figure 17), whereas seismic line F show clinoforms prograding from the south (Figure 18). The yellow arrows illustrate the clinform progradation direction of each 2-D seismic line (Figure 16).

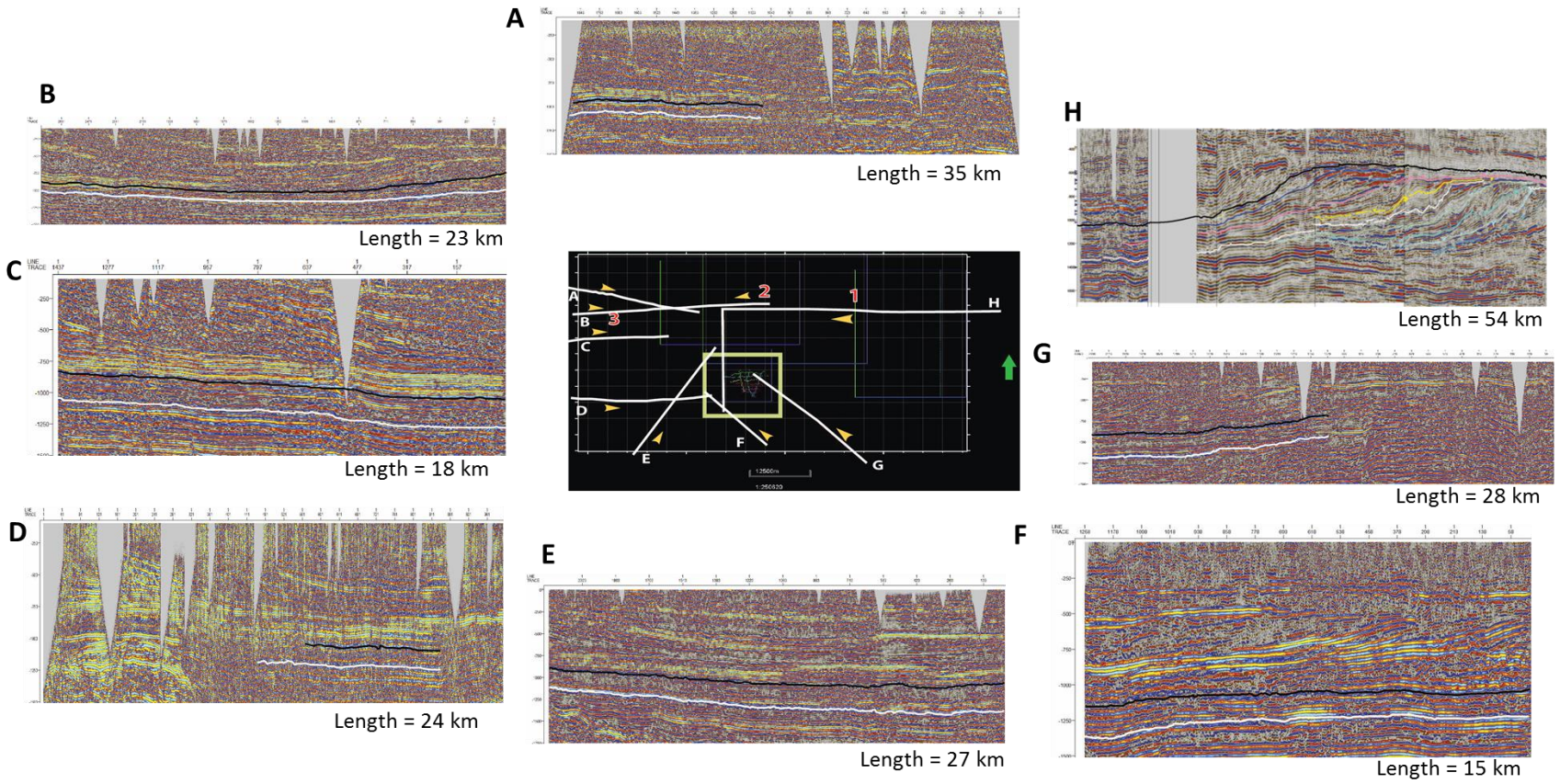


Figure 14: Seismic lines show clinoforms prograding from several directions. Yellow arrows indicate the direction of prograding in each line. The yellow rectangle is Bradesti 3D cube.

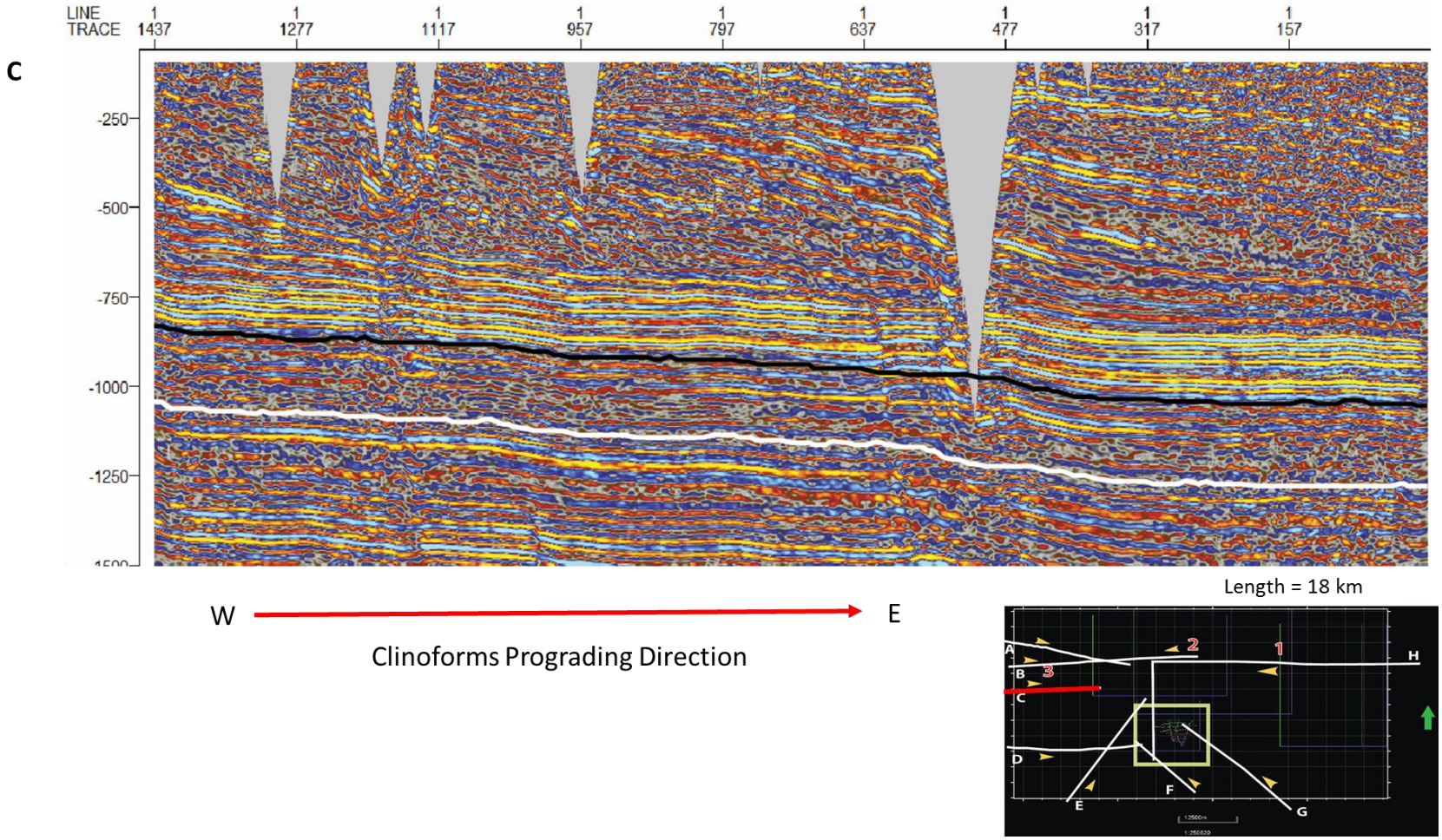


Figure 15: Seismic line C illustrating clinofroms prograding from the west to the east

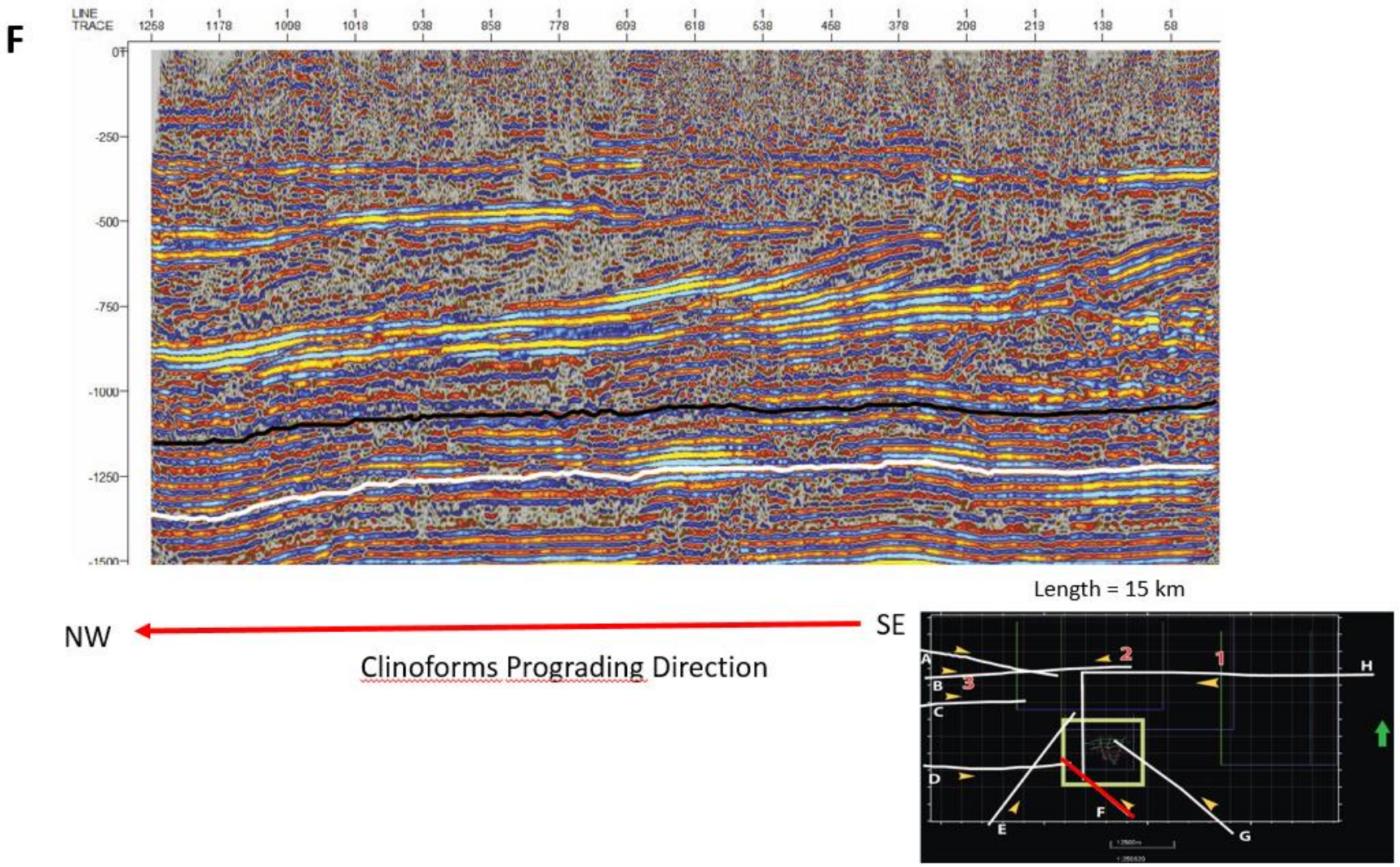


Figure 16: Seismic line F illustrating clinoforms prograding from the northwest to the southeast

The relative age of clinoforms can be identified from the seismic data as the seismic lines intersect providing information on multiple directions. Seismic data show more than one direction of prograding clinoforms, for instance seismic line B (Figure 19) which is located in the northern part of Bradesti 3-D cube has clinoforms prograding from both east and west side but the clinoforms prograding from the west are younger, as they overlie the clinoforms prograding from the east. Figure 19 gives a schematic illustration of those clinoforms that have amalgamated bottomsets in seismic line B.

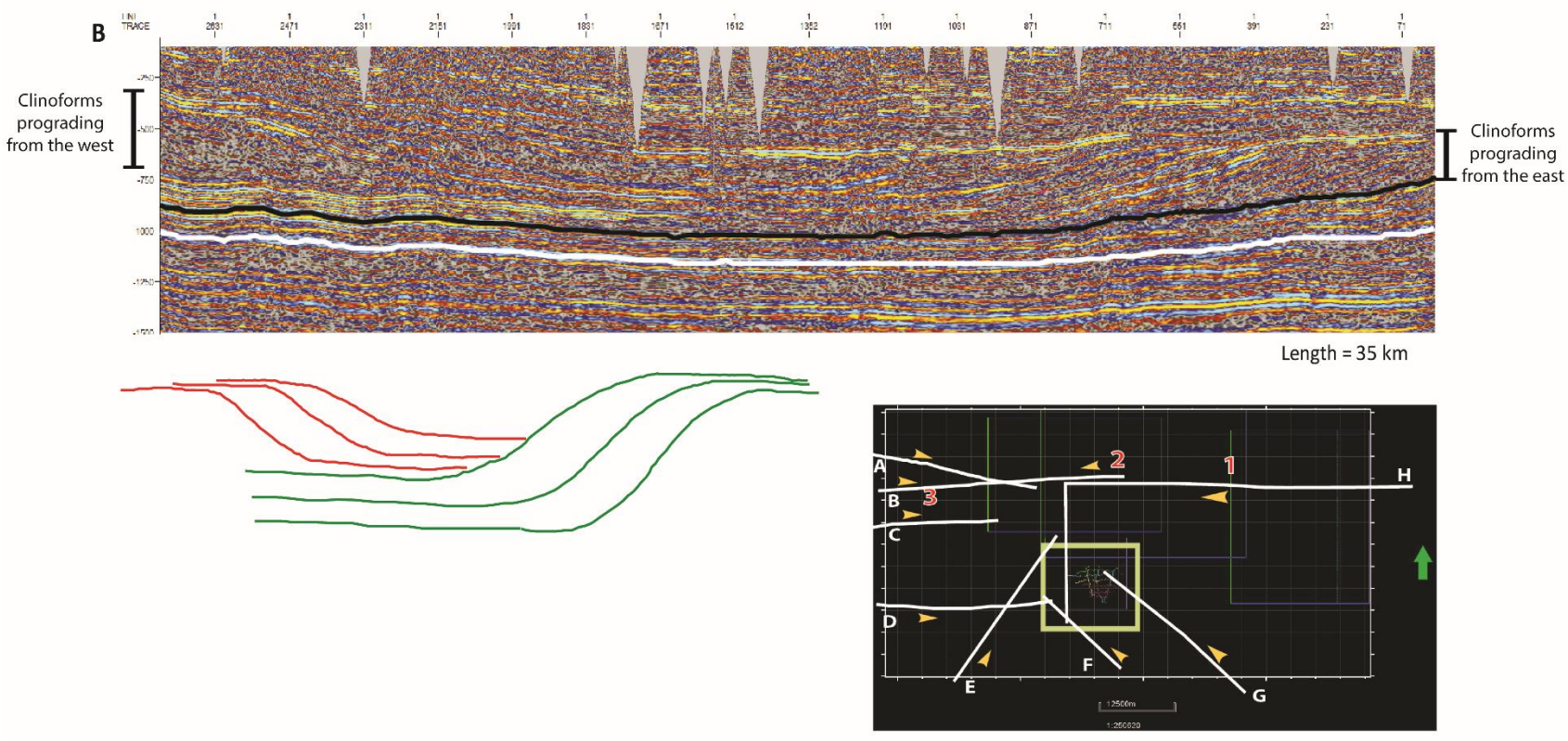


Figure 17: seismic line B shows clinofroms prograding from the west and from the east and the schematic drawing of amalgamated bottom sets of clinoforms in seismic line B

## BASIN FLOOR FANS IN WELL DATA

According to the well correlation data, the thickness of amalgamated clinoform bottomsets interpreted as amalgamated basin-floor fans ranges from 100 to 150 m and the individual fan-lobe thickness ranges mainly from 10 to 30 m (Figure 20). The SP log for individual fan lobes shows a range of characteristic patterns as coarsening upward, fining upward, blocky and irregularly ratty (Figure 20). Well cross-sections E-W2 (Figure 21A) and N-S2 (Figure 21B) illustrate in detail such examples. The well correlation figures shows that the fan lobes have different SP and Resistivity log characteristics and even inside the same fan lobe. For example, in Fan lobe 16 between FS16 and FS17 (the uppermost fan lobe) in well section E-W2 there is mostly a coarsening-upward pattern in the east, but this then changes to fining upward and blocky toward the west (Figure 21A). The thinning direction of Fan lobe 16 is also illustrated in Figures 26 and 27; Fan lobe 16 thins towards the West in E-W2l section and toward the North in N-S2 section (Figure 21A and 21B). Therefore, the overall thinning direction of Fan lobe 16 is towards the NE.

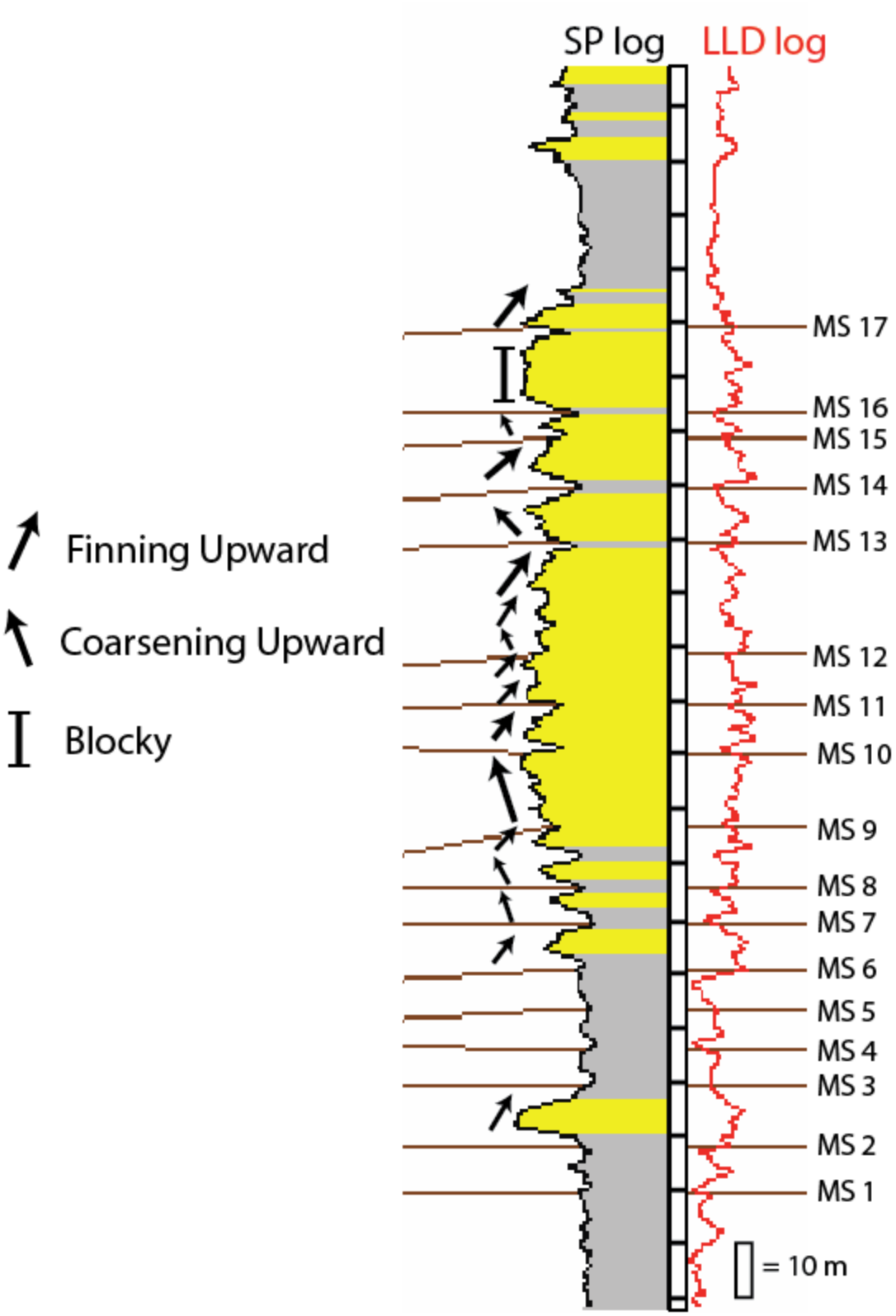


Figure 18: Examples of the range of well log patterns developed for fan lobes

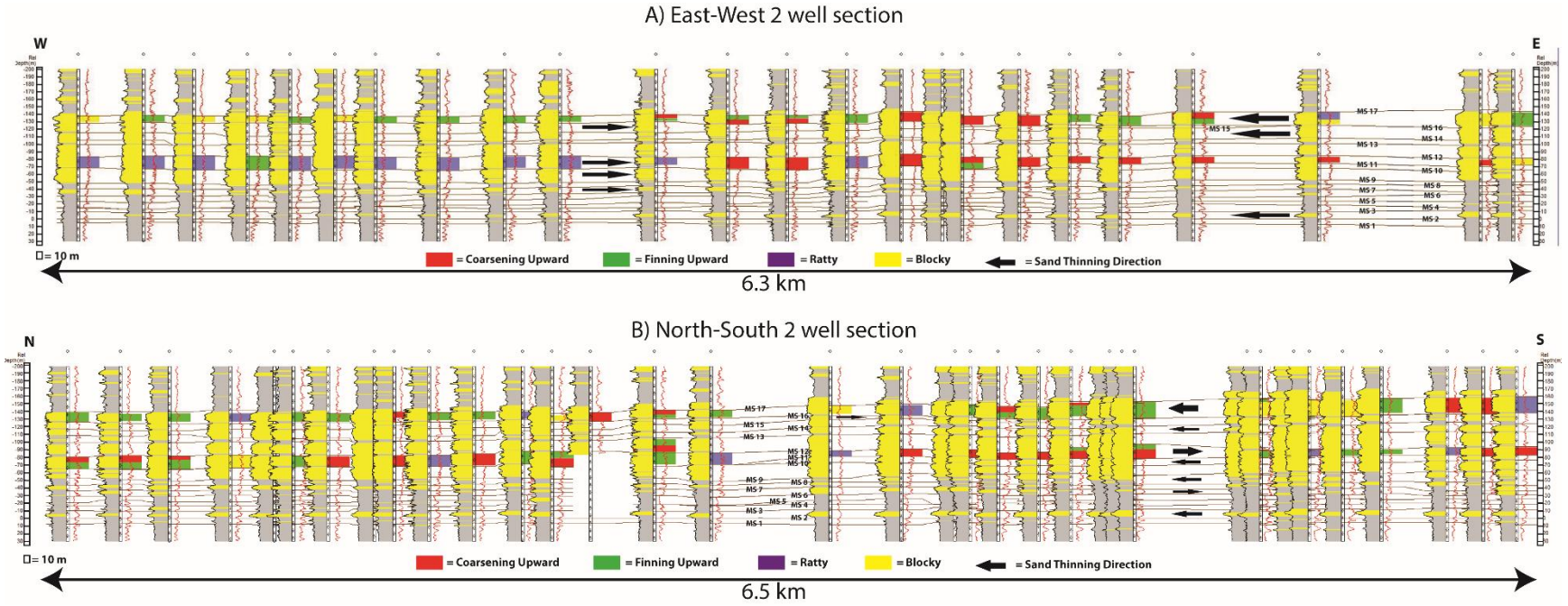


Figure 19: A) East-West 2 well section. For location see Figure 1B. B) North – South 2 well section. For location see Figure 1B.

In addition to sandstone thickness trends and geometries, well log characteristics can be used to interpretdepositional sub-environments of the basin floor fans. Koo et al. (2016) did a study on basin floor fan-lobe-complexes in Maastrichtian basin-floor fans in the Washakie Basin, Wyoming. They found that the gamma ray log characteristics of fan lobes changes quickly within different parts of the lobe, as was also previously discussed in Prelat and Hodgson (2013). To illustrate, Figure 22 shows log characteristics of a fan lobe in a dip direction from proximal (a) to distal (g) parts. The relationship between gamma ray log characteristics and sub-depositional environment are as follows; the muddy intervals are interpreted as distal lobe facies, the fining upward and thinning bed sets and can be interpreted as decreasing energy from center of lobe to lobe margin; the coarsening-upward pattern is interpreted as increasing energy from lobe margin to center; the blocky log pattern is interpreted as amalgamated sandy fan lobes in proximal and center of basin-floor fans, and the interbedded sand and shale intervals are interpreted as slope channels and overbank deposits. The detail of log characteristics are summarized in Figure 23. The results of the Koo et al. (2015) study is applied to the basin-floor well logs in the Dacian Basin. The lithological characteristics can be read despite the fact that the well logs used in Dacian Basin are SP rather than gamma-ray logs. The sub-depositional environment of each fan lobe together with the thinning direction of sandstones are used to generate the basin floor fan evolution in the study area.

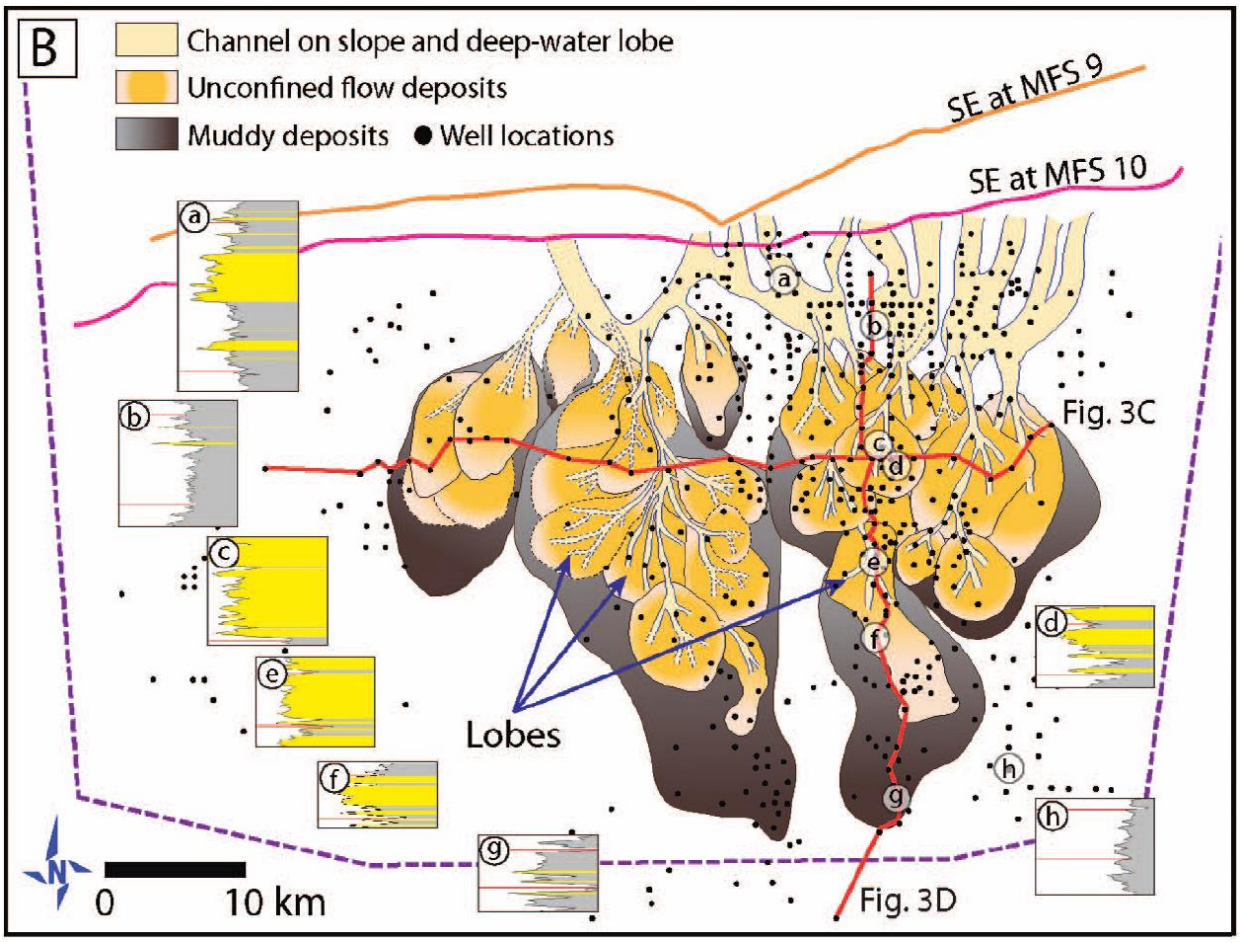


Figure 20: Gamma ray log motifs of architectural elements of deep water lobe complexes (Koo et al, 2017)

| Log Motif | Description | Deposits | Interpretation |
|---|---|---|---|
| 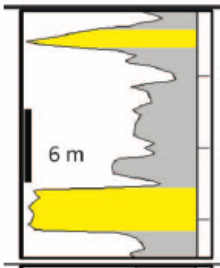 | Relatively sharp-based units with a fining-upward log motif; low GR within thick high-GR interval | Erosional surface overlain by thin sandstones and underlain by muds | Slope channels and overbank deposits |
| 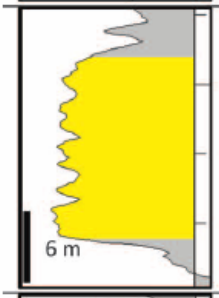 | Blocky log motifs with low GR in lower section; upward increasing GR at uppermost tops | Amalgamated sandstones in lower section; slightly upward-fining and thinning bed sets in the upper section | Amalgamated channels dominant in proximal and center of lobe |
| 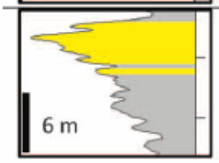 | Upward-decreasing and thickening GR; upward increasing GR at uppermost top | Upward-coarsening and thickening bed sets; the uppermost section displays upward-fining and thinning bed sets | Increasing energy from lobe margin to center of lobe |
| 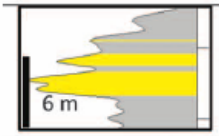 | Bell-shaped log motif; upward-increasing GR | Upward-fining and thinning bed sets | Decreasing energy from center of lobe to lobe margin |
| 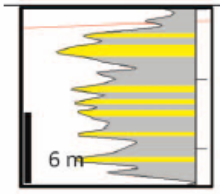 | Serrated log motif with high and low GR peaks with gentle upward-decreasing increasing GR | Interbedded thin sandstones and mudstones, but predominantly mudstones | Channel levee close lobe axis if preserved, dominant in lobe fringes |
| 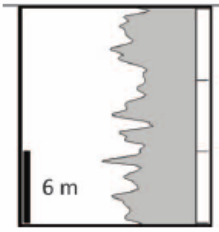 | Blocky log motif; moderate to high GR with gentle upward decreasing or increasing GR | Structureless and laminated mudstones with thin siltstones and sandstones | Muddy slope, inter-lobe anywhere on top of lobe if preserved, but dominant in distal lobes |

Figure 21: Interpreted facies from gamma ray log characteristic (Koo et al, 2017)

**INTERPRETATION OF INDIVIDUAL FAN LOBES 1-16**

To better understand the deposits of the Dacian fan lobes, a generalized schematic of fan lobe sub-depositional environments can be used (Figure 24). The sub-depositional environment

from proximal to distal part of fan lobe are interpreted based on the grainsize composition (sand and mud) and the presence of overall thinning trend of the lobes. The well log characteristics are considered in the interpretation but are given less importance as an interpretation tool to determine the sub-depositional environment because of the complex and highly variable well log characteristic distribution throughout the fan lobe. This issue will be emphasized in the following section.

The sub-depositional environments from proximal to distal area are divided into four parts (Figure 24). The most proximal sub-depositional environment is channelized with variable thickness, producing amalgamated sandstones. The second sub-depositional environment is the central part of the fan lobe with amalgamated sandstones but without any obvious sandstone thinning direction (thick sandstone without thinning trend). The third sub-depositional environment is the edge of any sandy fan lobe that shows thinning direction on sandstone thickness maps. The most distal part of the fan lobe is the muddy distal fan which consists of mainly mudstone with less sandstone toward the basin. The muddy distal fan of zone 4 shows a thinning of mud/sand body. The zone 5 muddy area does not have obvious thinning direction of mudstone/sandstone and will be considered as pelagic mud on the basin floor or the inter-lobe area.

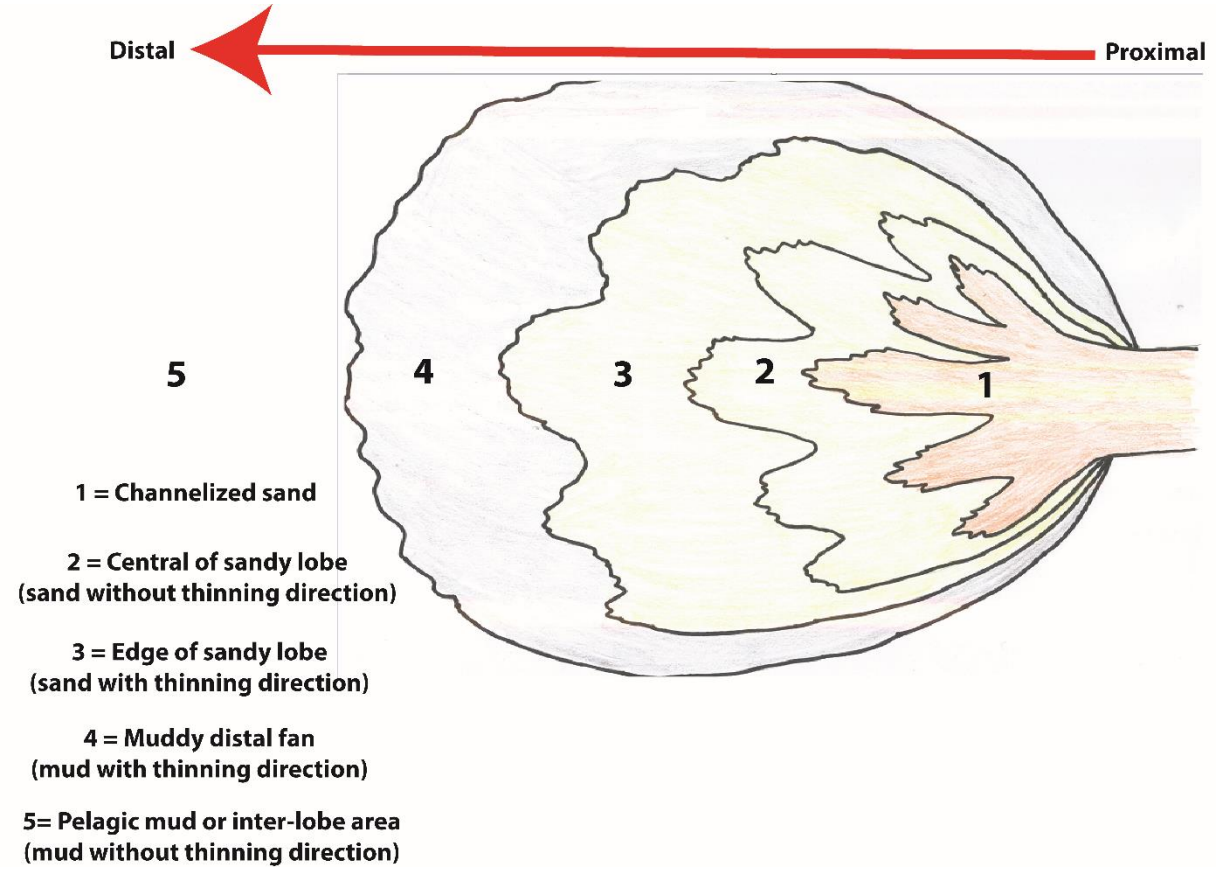


Figure 22: Schematic ideal drawing of sub-depositional environments on a fan lobe.

In the next section, the maps of individual fan-lobes are shown and progradation direction interpreted based on total thickness (isochore maps) for fan lobes that have little sandstone; fan lobes 1, 3, 4 ,5 and 6, while net sand maps as well as log patterns are used in the rest of fan lobes.

Fan lobe 1 lies between muddy surface 1 and muddy surface 2 (Figure 25A) at the base of basin-floor fans, and is therefore the oldest fan lobe mapped. Fan lobe 1 is composed of mudstone with net sandstone thickness less than 3 m (Figure 25C). The isochore map of fan lobe 1 in Figure 25B shows that the thickness of fan lobe ranged from 3 to 12 m. Fan lobe 1 is thinning toward the west and the SP log charateristics are mostly fining upward and muddy. The sub-depositional environment of this fan lobe in the study area is most likely to be a muddy distal fan lobe and the direction of sediment feeding is from the east to the west (Figure 25D).

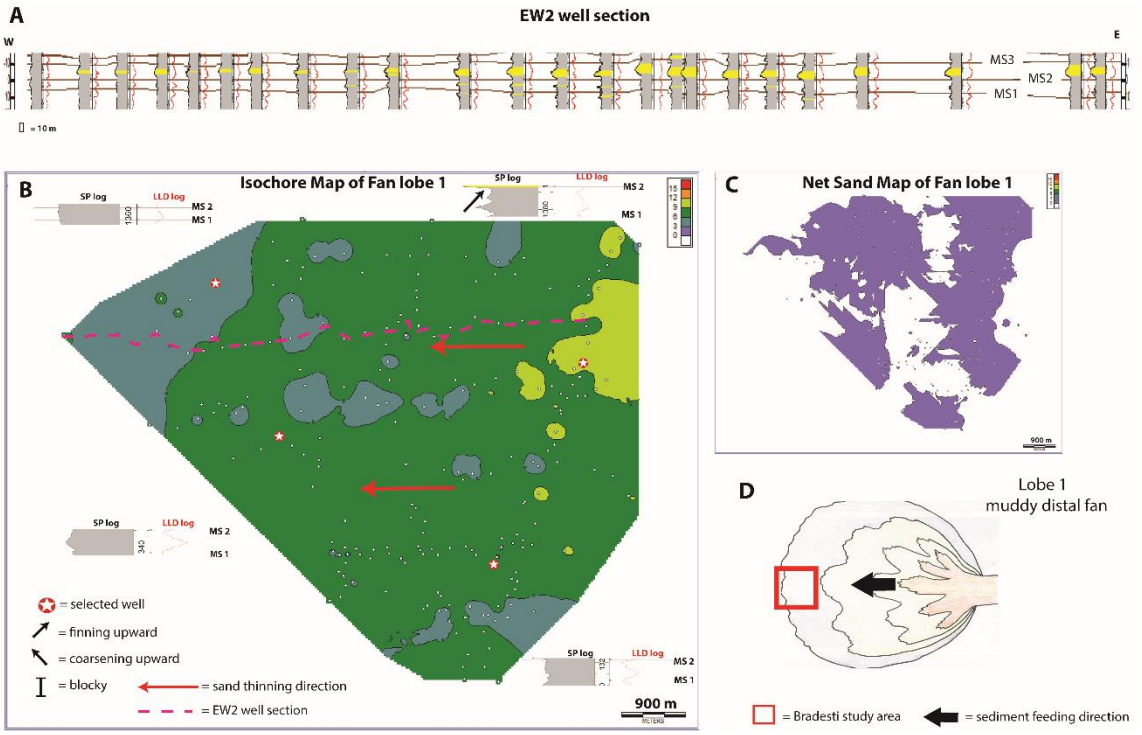


Figure 23: A) East-West 2 well section shows well log characteristic of Fan lobe 1 from the east to the west. B) isochore map of Fan lobe 1 with 3 m contour interval C) net sand map of Fan lobe 1 with 3 m contour interval D) sub-depositional environment of Fan lobe 1 inside the study area (red rectangle)

Fan lobe 2 lies between muddy surface 2 and muddy surface 3 (Figure 26A). Fan lobe 2 is composed of more sandstone than Fan lobe 1 (Figure 26B). The isochore map of Fan lobe 2 indicates overall thickness from 6 to 15 m (Figure 26C). The net sand map shows an average sand thickness of 6 m with thinning toward the west (Figure 26B). The SP log characteristic on this lobe are consistent throughout the study area, i.e., coarsening upward at the bottom and fining upward at the top that can be interpreted as a forward-stepping and back-stepping of the distal lobe fringe (Koo et al., 2015). The sub-depositional environment of this fan lobe inside the study area is muddy distal fan but closer to the center of the lobe than Fan lobe 1. The sediment feeding direction is from the east to the west (Figure 26D).

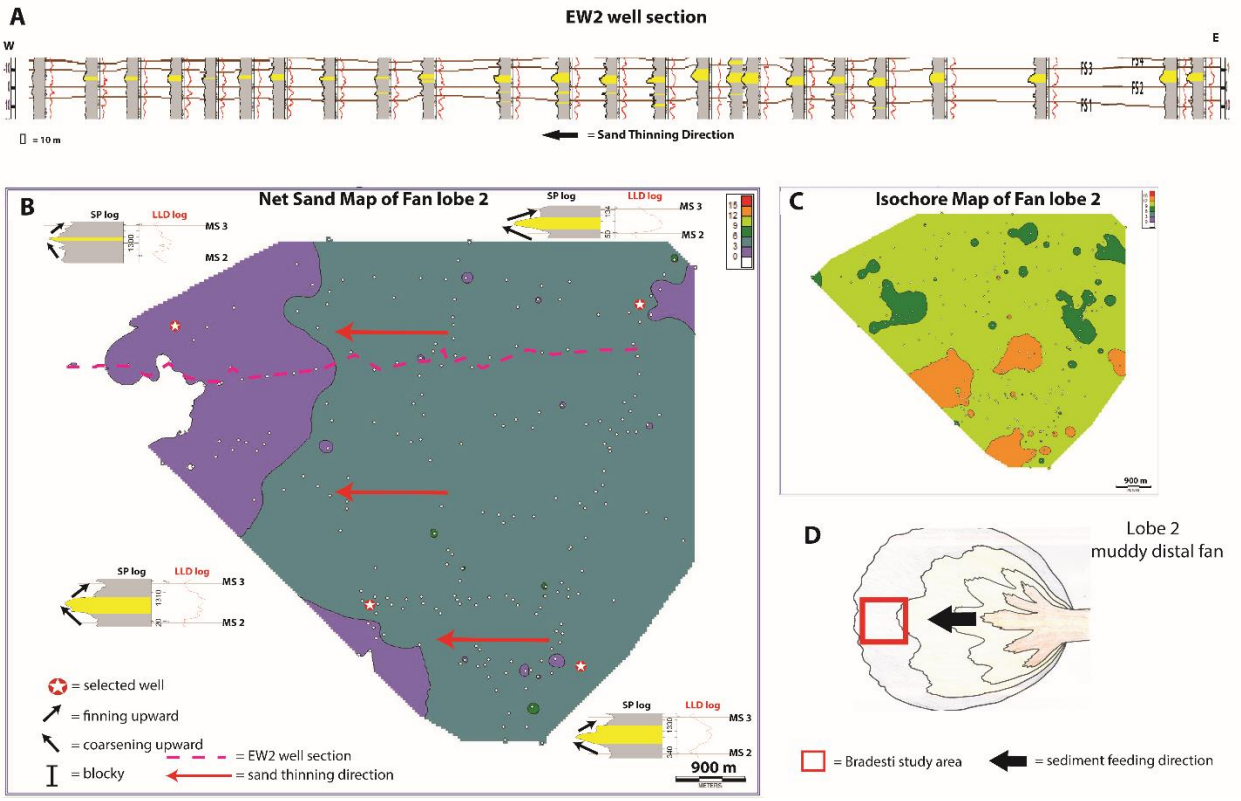


Figure 24: A) East-West 2 well section shows well log characteristic of Fan lobe 2 from the east to the west. B) net sand map of Fan lobe 2 with 3 m contour interval C) isochore map of Fan lobe 2 with 3 m contour interval D) sub-depositional environment of Fan lobe 2 inside the study area (red rectangle).

Fan lobe 3 lies between muddy surface 3 and muddy surface 4. Fan lobe 3 (Figure 27A) is mainly composed of mudstone with a bit more sandstone in the northeastern area. The isochore map of Fan lobe 3 indicates overall thickness from 3 to 12 m (Figure 27B). The net sand map shows average sand thickness less than 3 m and thinning toward the southwest. (Figure 27C). The SP log characteristic of this lobe is fining upward throughout the study area suggesting back-stepping of the lobe in this area. The sub-depositional environment of this fan lobe inside the study area is muddy distal fan. The sediment feeding direction is from the northeast to the southwest (Figure 27D).

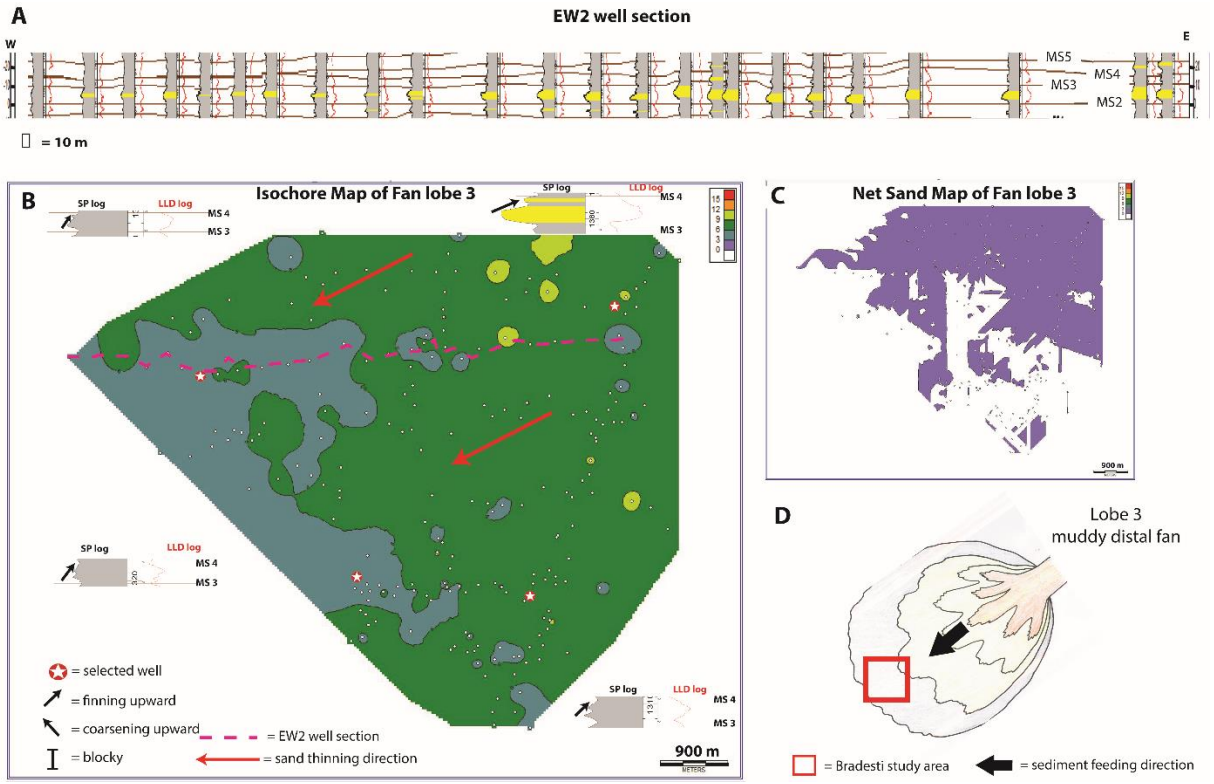


Figure 25: A) East-West2 well section shows well log characteristic of Fan lobe 3 from the east to the west. B) isochore map of Fan lobe 1 with 3 m contour interval C) net sand map of Fan lobe 3 with 3 m contour interval D) sub-depositional environment of Fan lobe 3 inside the study area (red rectangle).

Fan lobe 4 lies between muddy surface 4 and muddy surface 5 (Figure 28A) and is mainly composed of mudstone. The isochore map of Fan lobe 4 indicates an overall thickness from 0 to 9 m (Figure 28B). The net sand map shows average sand thickness less than 3 m and thinning toward the west. (Figure 28C). The SP log characteristics of this lobe are some “weak” fining upward trends. The sub-depositional environment of this fan lobe inside the study area is muddy distal fan. The sediment feeding direction is from the east to the west (Figure 28D).

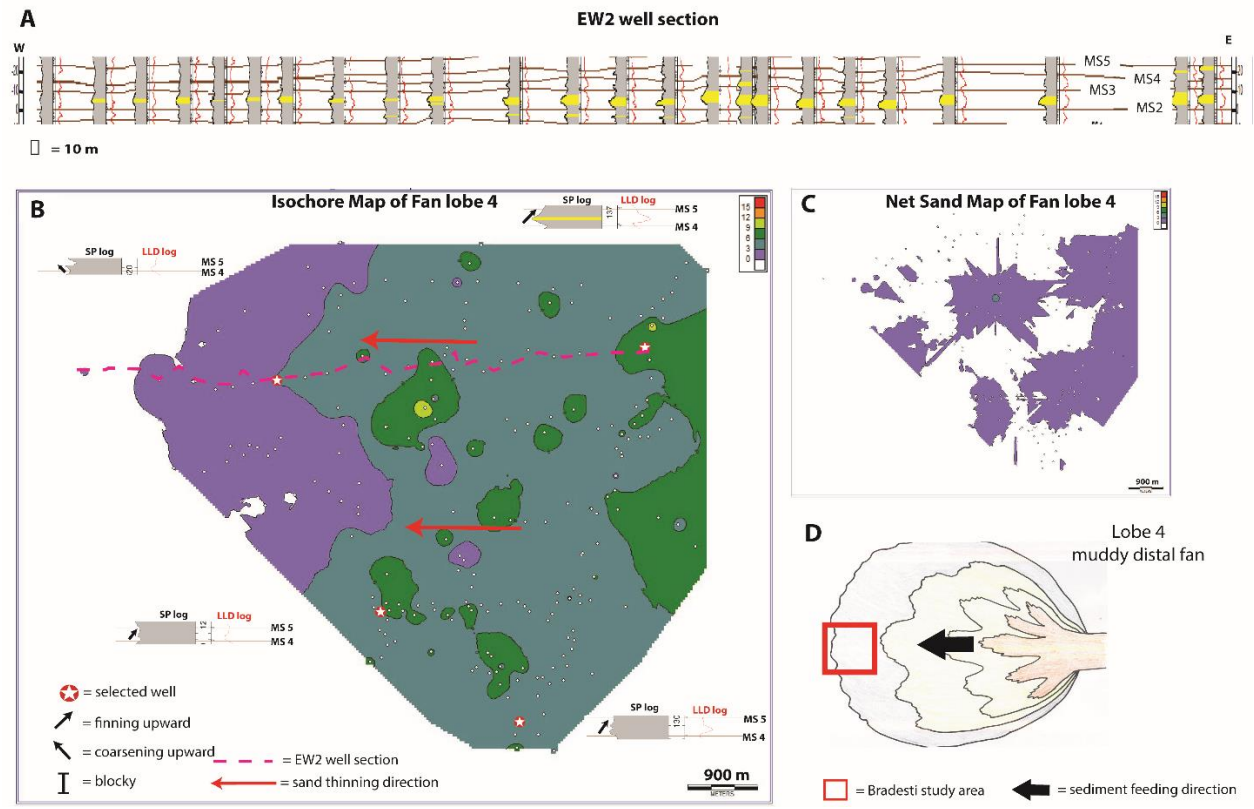


Figure 26: A) East-West2 well section shows well log characteristic of Fan lobe 4 from the east to the west. B) isochore map of Fan lobe 4 with 3 m contour interval C) net sand map of Fan lobe 4 with 3 m contour interval D) sub-depositional environment of Fan lobe 4 inside the study area (red rectangle).

Fan lobe 5 lies between muddy surface 5 and muddy surface 6 (Figure 29A) and is overall composed of mudstone. The net sand map indicates no sandstone in this lobe (Figure 29C). Therefore, there is no thickness trend to interpret the sediment feeding direction. The isochore map of Fan lobe 5 indicates overall thickness from 3 to 12 m (Figure 29B). The SP log characteristics of this lobe are mostly fining upward. The sub-depositional environment of this fan lobe inside the study area is pelagic mud on the basin floor or inter-lobe area (Figure 29D).

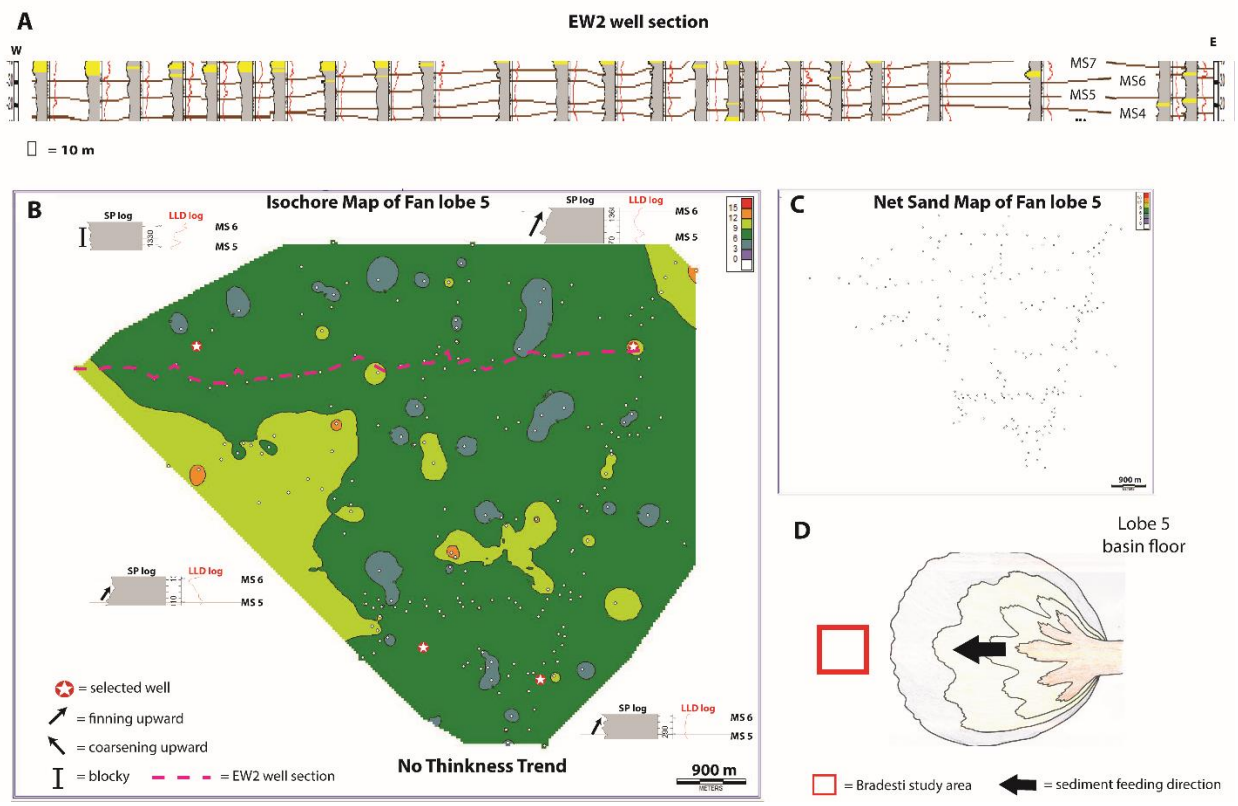


Figure 27: A) East-West2 well section shows well log characteristic of Fan lobe 5 from the east to the west. B) isochore map of Fan lobe 5 with 3 m contour interval C) net sand map of Fan lobe 1 with 3 m contour interval D) sub-depositional environment of Fan lobe 5 inside the study area (red rectangle).

Fan lobe 6 lies between muddy surface 6 and muddy surface 7 (Figure 30A). Fan lobe 6 is mainly composed of mudstone with thin "interbedded" sandstone. The isochore map of Fan lobe 6 indicates overall thickness from 3 to 15 m (Figure 30B). The net sand map indicates sandstone thickness ranged from 3 to 9 m on the extreme NE area of the map (Figure 30C). The SP log characteristics of this lobe are mostly "ratty" and fining upward. The sub-depositional environment of this fan lobe inside the study area is distal fan lobe. The sediment feeding direction is unclear in this lobe but it likely to be fed from the east/ north-east to west since this was the dominated direction in the previous fan lobes (Figure 30D).

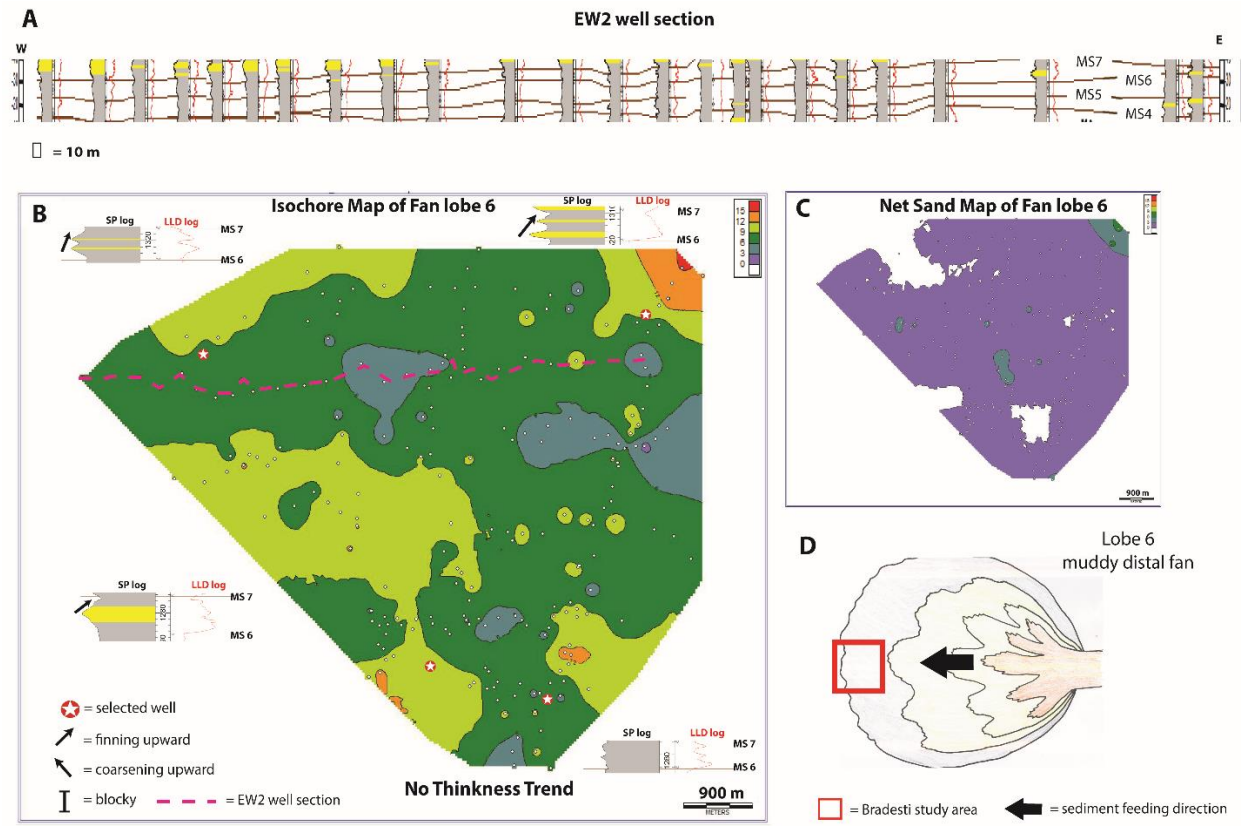


Figure 28: A) East-West2 well section shows well log characteristic of Fan lobe 6 from the east to the west. B) isochore map of Fan lobe 6 with 3 m contour interval C) net sand map of Fan lobe 6 with 3 m contour interval D) sub-depositional environment of Fan lobe 6 inside the study area (red rectangle)

Fan lobe 7 lies between muddy surface 7 and muddy surface 8 (Figure 31A) and it is mainly composed of mudstone with thin interbedded sandstone. The isochore map of Fan lobe 7 indicates overall thickness from 3 to 12 m (Figure 31C). The net sand map shows sandstone thickness from 0 to 6 m and thinning toward the east (Figure 31B). The SP log characteristics of this lobe are mostly coarsening upward, suggesting forward-stepping of the lobe. The sub-depositional environment of this fan lobe inside the study area is muddy distal fan. The sediment feeding direction is from the west to the east (Figure 31D).

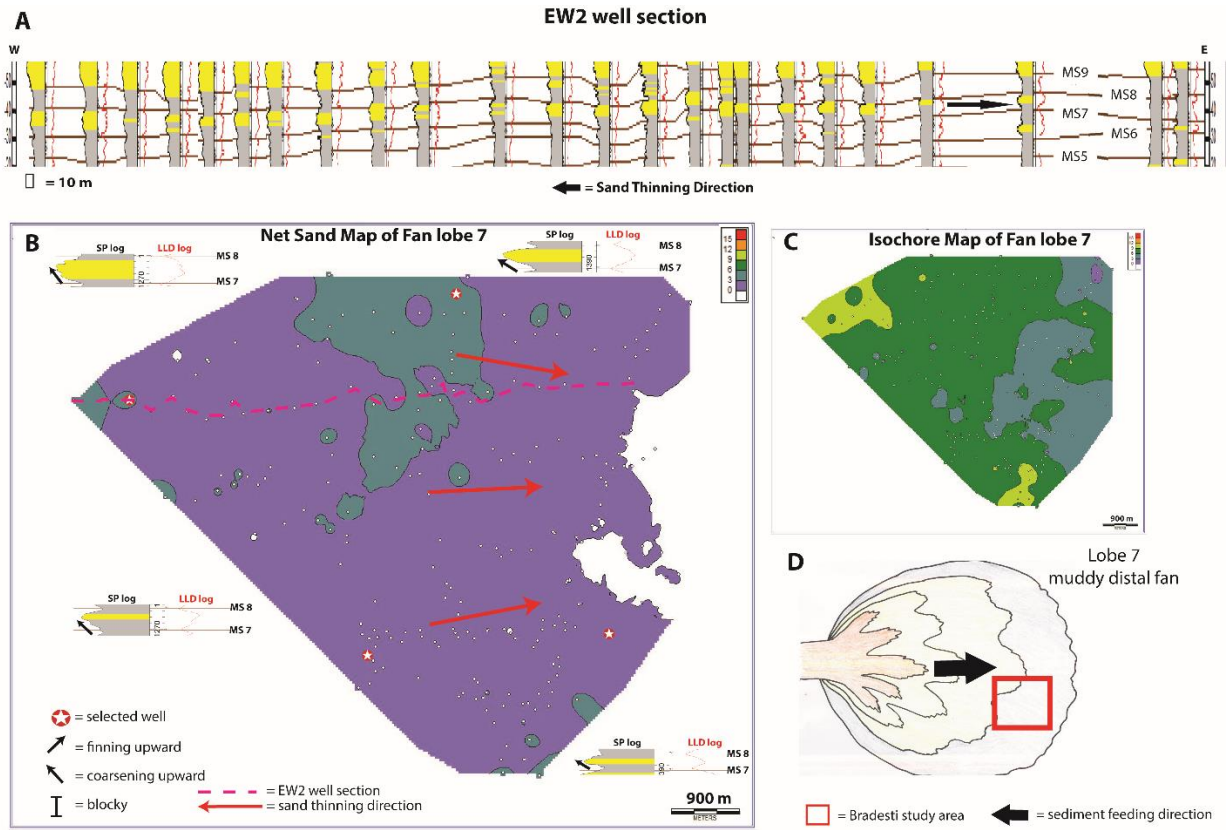


Figure 29: A) East-West2 well section shows well log characteristic of Fan lobe 7 from the east to the west. B) net sand map of Fan lobe 7 with 3 m contour interval C) isochore map of Fan lobe 7 with 3 m contour interval D) sub-depositional environment of Fan lobe 7 inside the study area (red rectangle)

Fan lobe 8 lies between muddy surface 8 and muddy surface 9 (Figure 32A) and is mainly composed of mudstone with interbedded sandstone. The isochore map of Fan lobe 8 indicates overall thickness from 3 to 15 m (Figure 32C). The net sand map shows sandstone thickness from 3 to 6 m and thinning toward the north (Figure 32B). The SP log characteristics of this lobe are mostly coarsening upward in the south and coarsening to fining upward to the north. The sub-depositional environment of this fan lobe inside the study area is muddy distal fan. The sediment feeding direction is from the south to the north (Figure 32D).

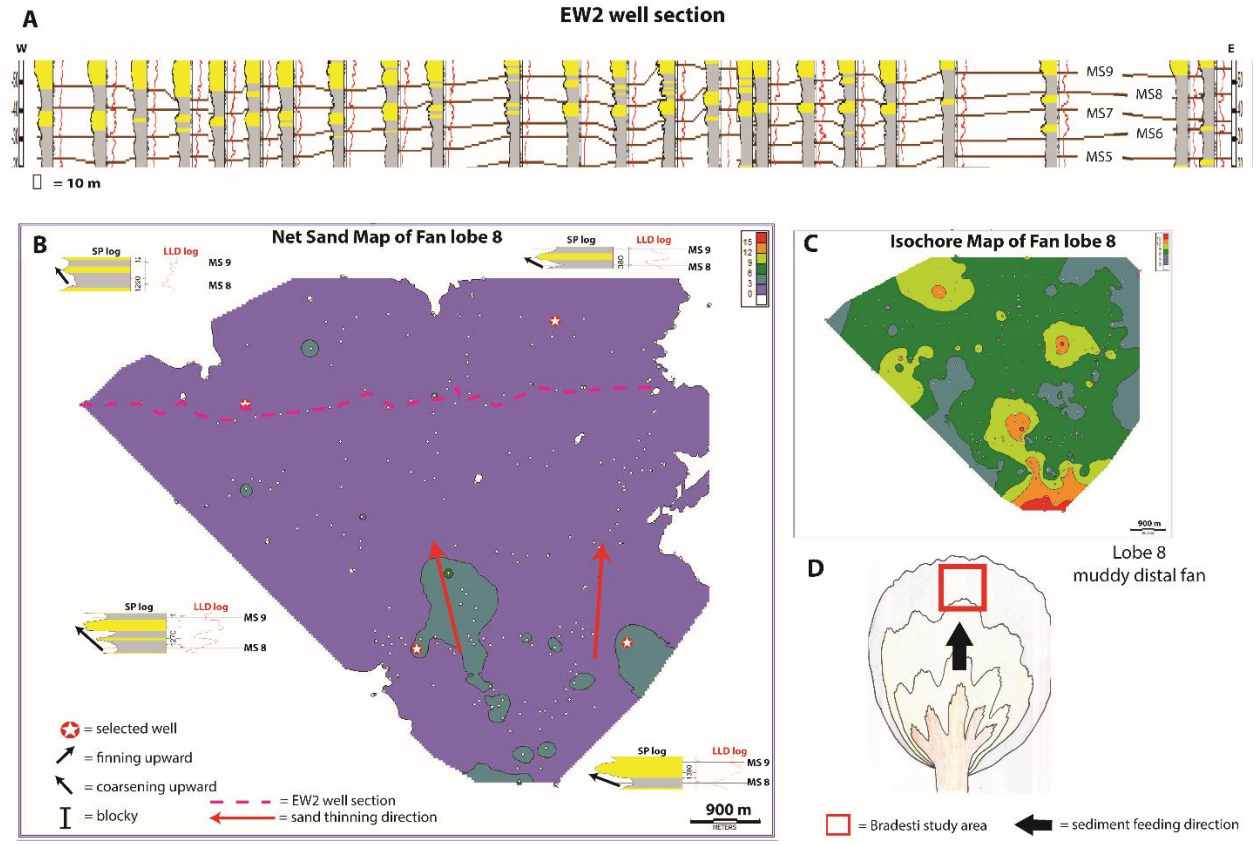


Figure 30: A) East-West2 well section shows well log characteristic of Fan lobe 8 from the east to the west. B) net sand map of Fan lobe 8 with 3 m contour interval C) isochore map of Fan lobe 8 with 3 m contour interval D) sub-depositional environment of Fan lobe 8 inside the study area (red rectangle)

Fan lobe 9 lies between muddy surface 9 and muddy surface 10 (Figure 33A) and is mainly composed of sandstone. The isochore map of Fan lobe 9 indicates overall thickness from 10 to 25 m (Figure 33C). The net sand map shows sandstone thickness from 5 to 20 m without obvious thinning direction (Figure 33B). The SP log characteristics of this lobe are mostly coarsening upward or blocky. The sub-depositional environment of this fan lobe inside the study area is the central or core zone of the fan lobe. The sediment feeding direction is assumed to be from south-west to north-east or from the south to the north similar to the progradation of the previous fan lobe (Figures 32D and 33D).

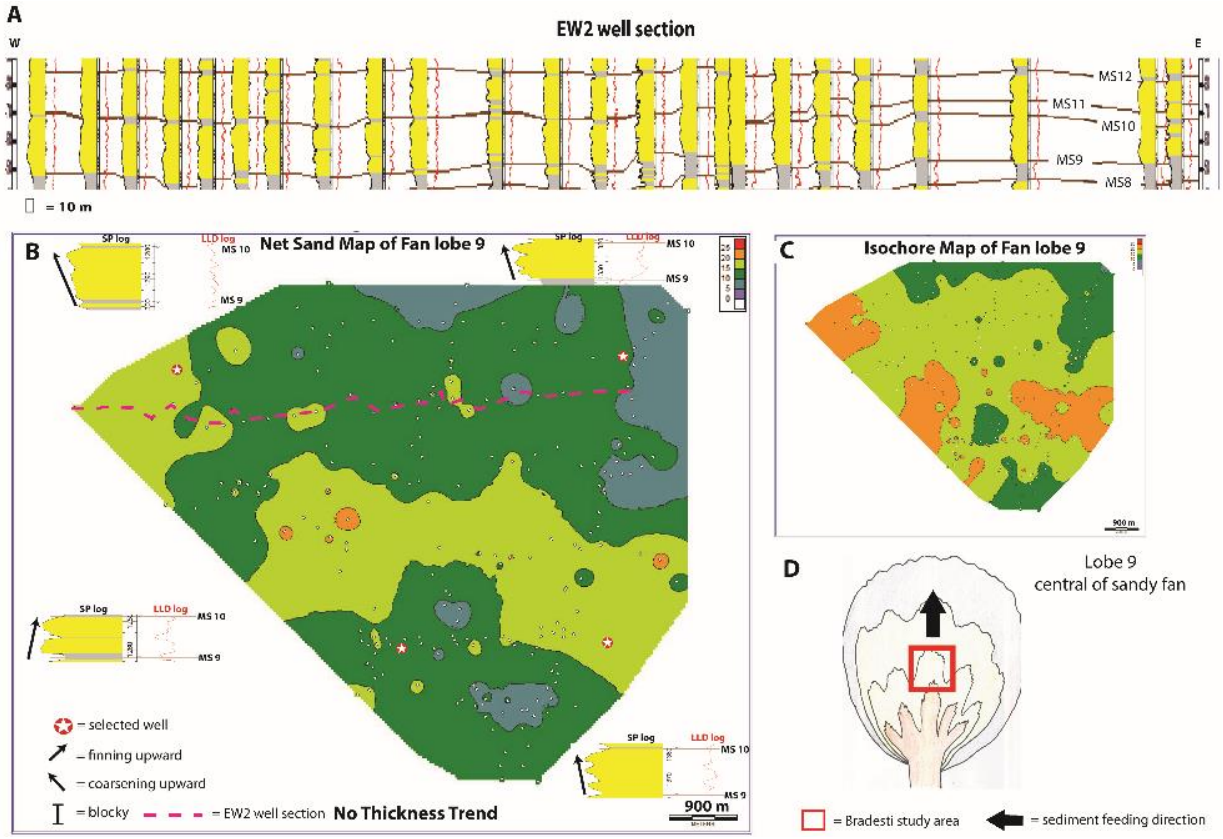


Figure 31: A) East-West2 well section shows well log characteristic of Fan lobe 9 from the east to the west. B) net sand map of Fan lobe 9 with 5 m contour interval C) isochore map of Fan lobe 9 with 5 m contour interval D) sub-depositional environment of Fan lobe 9 inside the study area (red rectangle)

Fan lobe 10 lies between muddy surface 10 and muddy surface 11 (Figure 34A) and is mainly composed of sandstone. The isochore map of Fan lobe 10 indicates overall thickness from 0 to 20 m (Figure 34C). The net sand map shows sandstone thickness from 0 to 15 m with thinning trend toward the northwest (Figure 34B). The SP log characteristics of this lobe are fining upward in the east and coarsening upward in the central-west. One possible interpretation is that channels form SE are forward-stepping the lobe to NW. The sub-depositional environment of this fan lobe inside the study area is the edge of a sandy fan lobe (Figure 34D). The sediment feeding direction is from the southeast to the northwest.

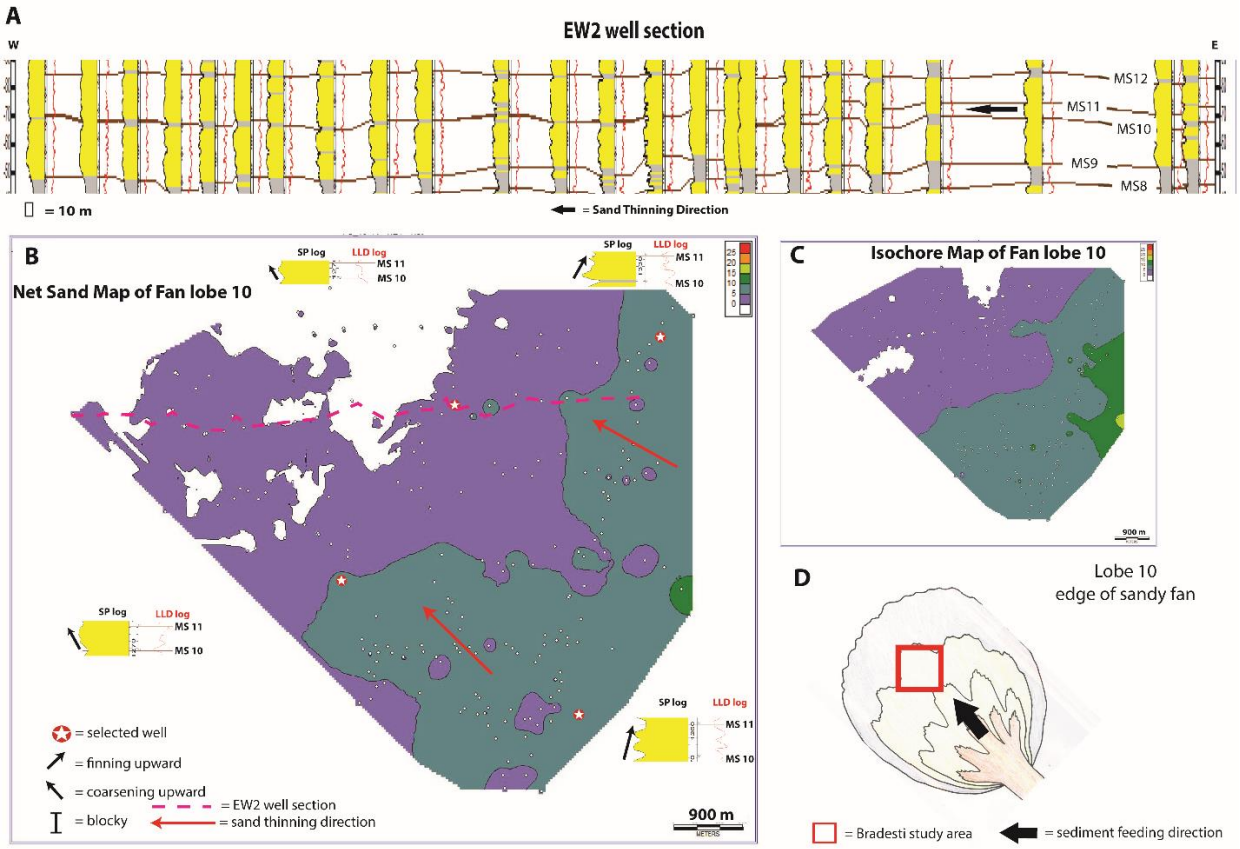


Figure 32: A) East-West2 well section shows well log characteristic of Fan lobe 10 from the east to the west. B) net sand map of Fan lobe 10 with 5 m contour interval C) isochore map of Fan lobe 10 with 5 m contour interval D) sub-depositional environment of Fan lobe 10 inside the study area (red rectangle)

Fan lobe 11 lies between muddy surface 11 and muddy surface 12 (Figure 35A) and is mainly composed of sandstone. The isochore map of Fan lobe 10 indicates overall thickness from 5 to 20 m (Figure 35C). The net sand map shows sandstone thickness from 5 to 20 m with thinning trend toward the east (Figure 35B). The SP log characteristics of this lobe are complicated including fining upward, coarsening upward and blocky. The sub-depositional environment of this fan lobe inside the study area is interpreted as a highly channelized area with the presence of lobate features and thick amalgamated sand inside the lobate features (Figure 35D). The sediment feeding direction is from the west to the east.

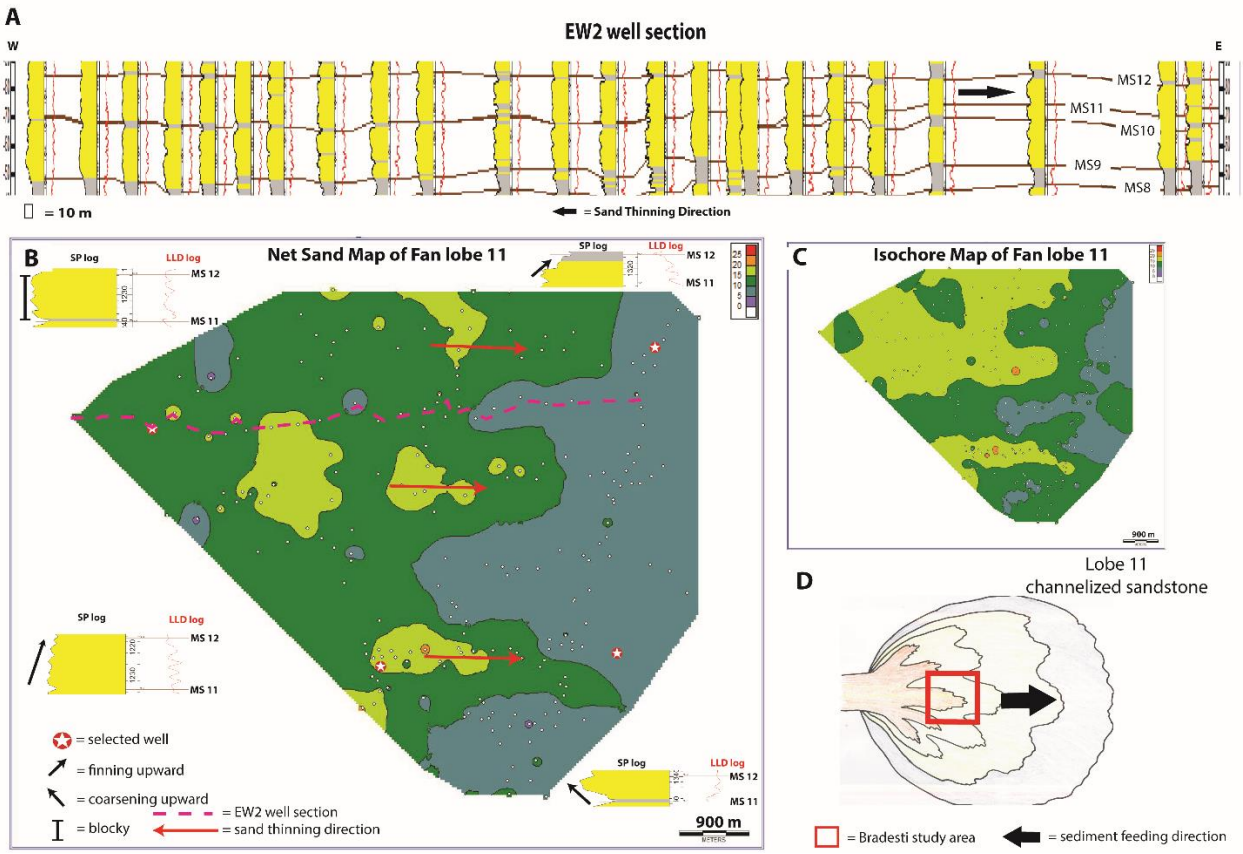


Figure 33: A) East-West2 well section shows well log characteristic of Fan lobe 11 from the east to the west. B) net sand map of Fan lobe 11 with 5 m contour interval C) isochore map of Fan lobe 11 with 5 m contour interval D) sub-depositional environment of Fan lobe 11 inside the study area (red rectangle)

Fan lobe 12 lies between muddy surface 12 and muddy surface 13 (Figure 36A) and is mainly composed of sandstone. The isochore map of Fan lobe 12 indicates overall thickness from 10 to 25 m (Figure 36C). The net sand map shows sandstone thickness from 5 to 25 m without obvious thinning direction (Figure 36B). The SP log characteristics of this lobe are complicated including fining upward, coarsening upward and blocky. The sub-depositional environment of this fan lobe inside the study area is the central or axial part of a sandy fan lobe with some of the logs penetrating channels (Figure 36D). The sediment feeding direction is assumed to be from the west to the east from the previous fan lobe feeding trend.

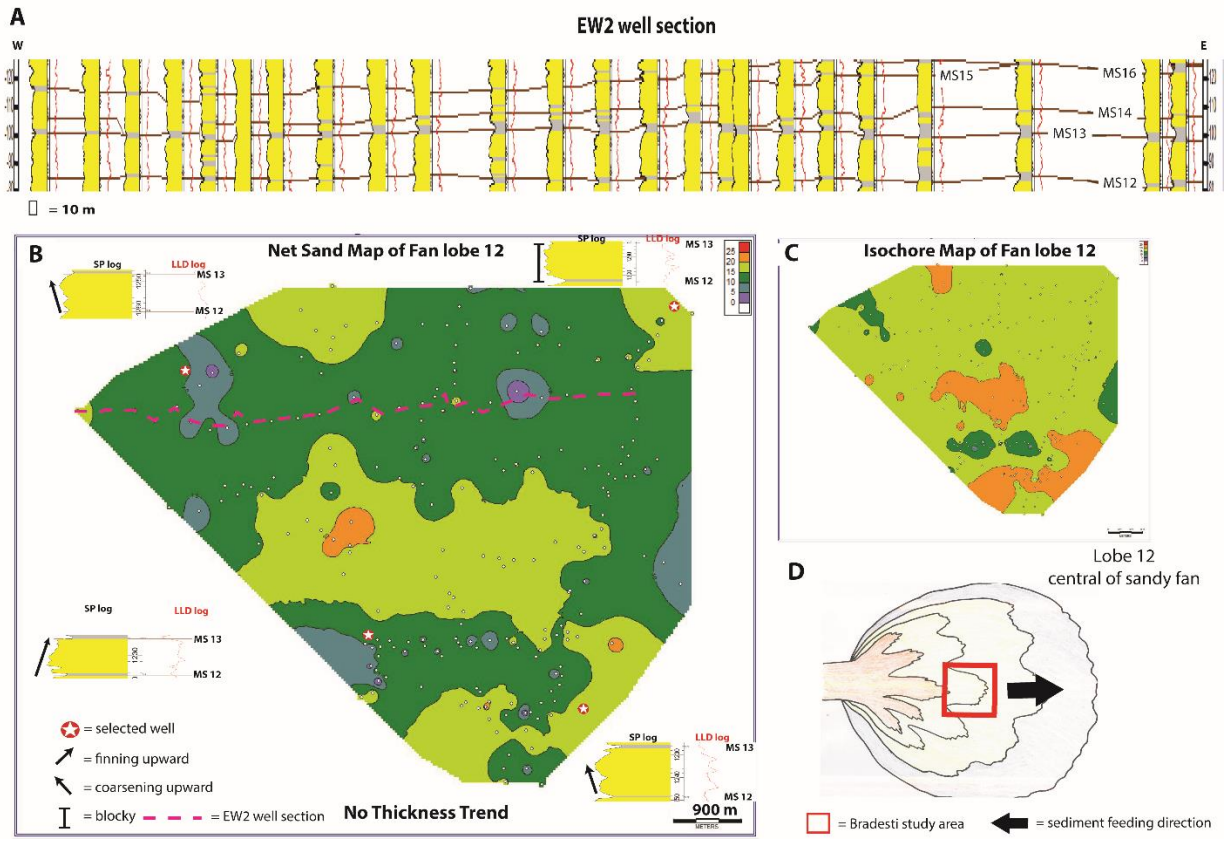


Figure 34: A) East-West2 well section shows well log characteristic of Fan lobe 12 from the east to the west. B) net sand map of Fan lobe 12 with 5 m contour interval C) isochore map of Fan lobe 12 with 5 m contour interval D) sub-depositional environment of Fan lobe 12 inside the study area (red rectangle)

Fan lobe 13 lies between muddy surface 13 and muddy surface 14 (Figure 37A) and is mainly composed of sandstone. The isochore map of Fan lobe 13 indicates overall thickness from 5 to 20 m (Figure 37C). The net sand map shows sand thickness from 5 to 15 m with thinning direction toward the northwest (Figure 37B). The SP log characteristics of this lobe are mostly coarsening upward suggesting lobe forward-stepping. The sub-depositional environment of this fan lobe inside the study area is the edge of sandy fan lobe (Figure 37D). The sediment feeding direction is from the southeast to the northwest.

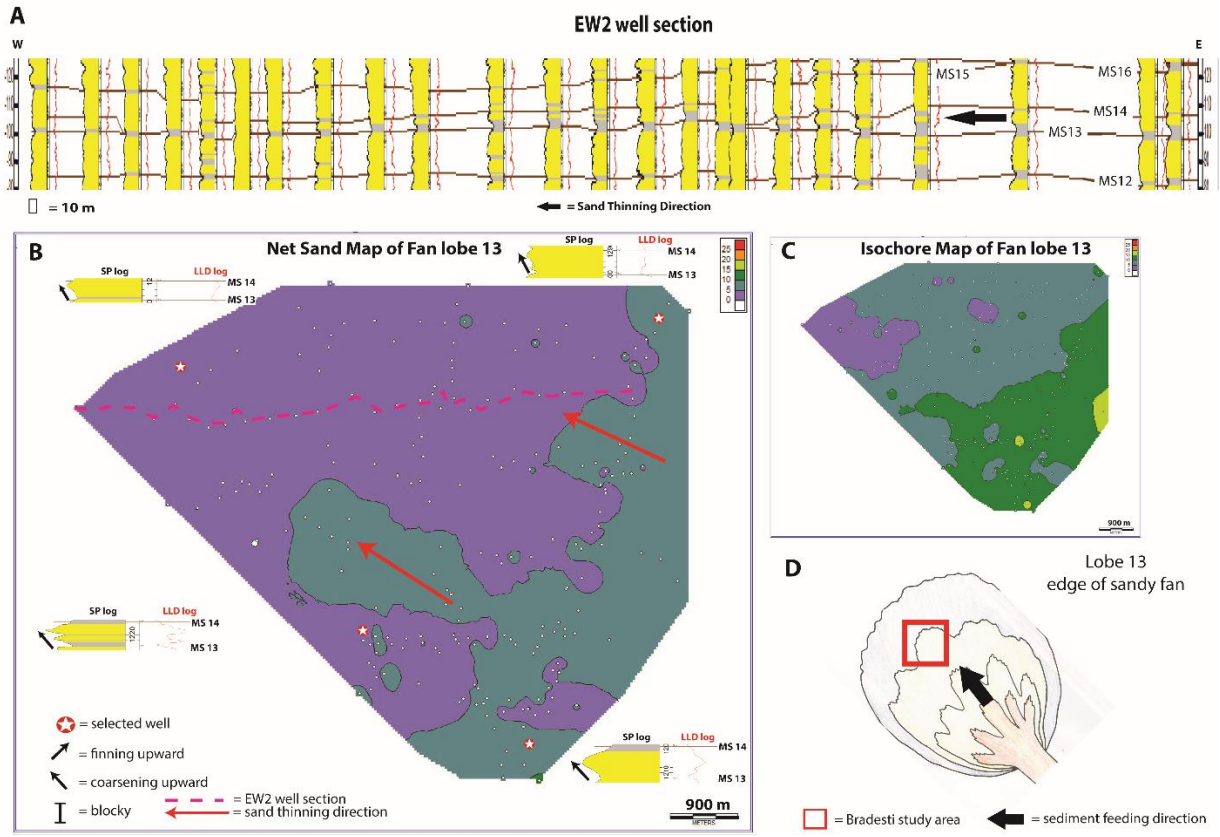


Figure 35: A) East-West2 well section shows well log characteristic of Fan lobe 13 from the east to the west. B) net sand map of Fan lobe 13 with 5 m contour interval C) isochore map of Fan lobe 13 with 5 m contour interval D) sub-depositional environment of Fan lobe 13 inside the study area (red rectangle)

Fan lobe 14 lies between muddy surface 14 and muddy surface 15 (Figure 38A) and is mainly composed of sandstone. The isochore map of Fan lobe 14 indicates overall thickness from 5 to 20 m (Figure 38C). The net sand map shows sand thickness from 5 to 15 m with thinning direction toward the southwest (Figure 38B). The SP log characteristics of this lobe are mostly coarsening upward indicating forward-stepping. The sub-depositional environment of this fan lobe inside the study area is the edge of sandy fan lobe (Figure 38D). The sediment feeding direction is from the northeast to the southwest.

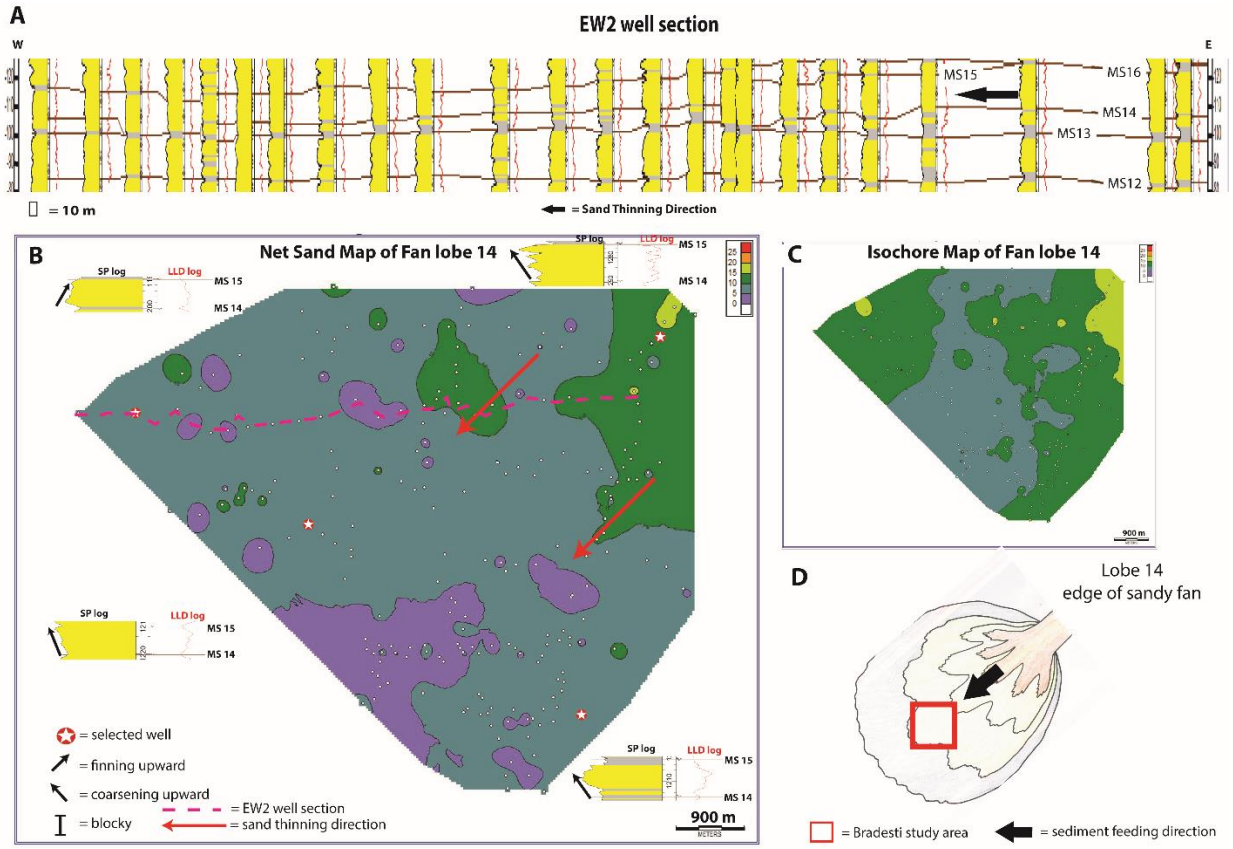


Figure 36: A) East-West2 well section shows well log characteristic of Fan lobe 14 from the east to the west. B) net sand map of Fan lobe 14 with 5 m contour interval C) isochore map of Fan lobe 14 with 5 m contour interval D) sub-depositional environment of Fan lobe 14 inside the study area (red rectangle)

Fan lobe 15 lies between muddy surface 15 and muddy surface 16 (Figure 39A) and is mainly composed of sandstone. The isochore map of Fan lobe 15 indicates overall thickness from 0 to 20 m (Figure 39C). The net sand map shows sandstone thickness from 0 to 15 m with thinning direction toward the southeast (Figure 39B). The SP log characteristics of this lobe are coarsening upward and finning upward in the proximal part then rapidly pinching out toward the east (Figures 39A and 39B). The sub-depositional environment of this fan lobe inside the study area is the edge of sandy fan lobe (Figure 39D). The sediment feeding direction is from the northwest to the southeast.

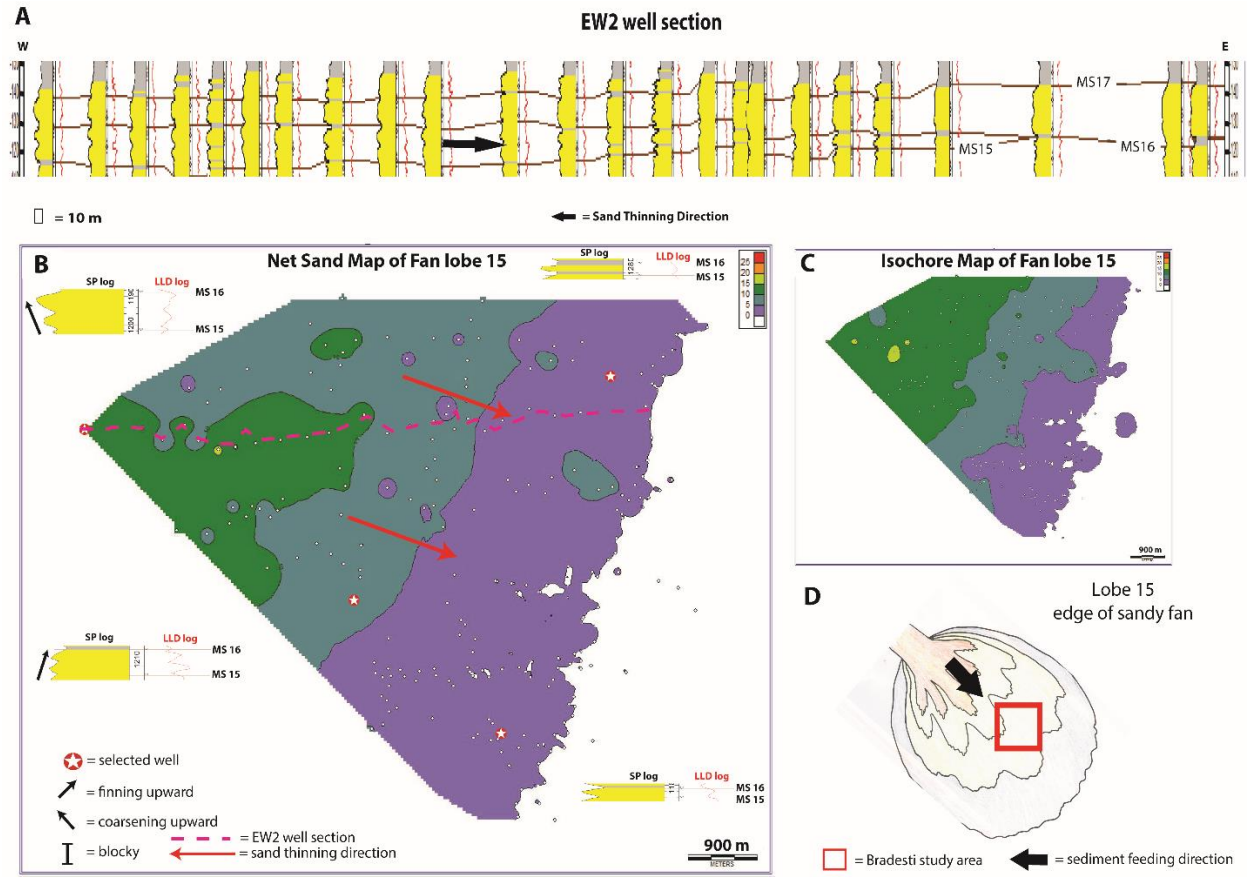


Figure 37: A) East-West2 well section shows well log characteristic of Fan lobe 15 from the east to the west. B) net sand map of Fan lobe 15 with 5 m contour interval C) isochore map of Fan lobe 15 with 5 m contour interval D) sub-depositional environment of Fan lobe 15 inside the study area (red rectangle)

Fan lobe 16 lies between muddy surface 16 and muddy surface 17 (Figure 40A) which is the upper most fan lobe. Fan lobe 16 is mainly composed of sandstone. The isochore map of Fan lobe 16 indicates overall thickness from 5 to 25 m (Figure 40C). The net sand map shows sandstone thickness from 5 to 25 m with thinning direction toward the northwest (Figure 40B). The SP log characteristics of this lobe are complicated including coarsening upward, finning upward and blocky suggesting highly variable alternation of channel axes and edges/ lobes. The sub-depositional environment of this fan lobe inside the study area is the edge of a sandy fan lobe (Figure 40D). The sediment feeding direction is from the southeast to the northwest.

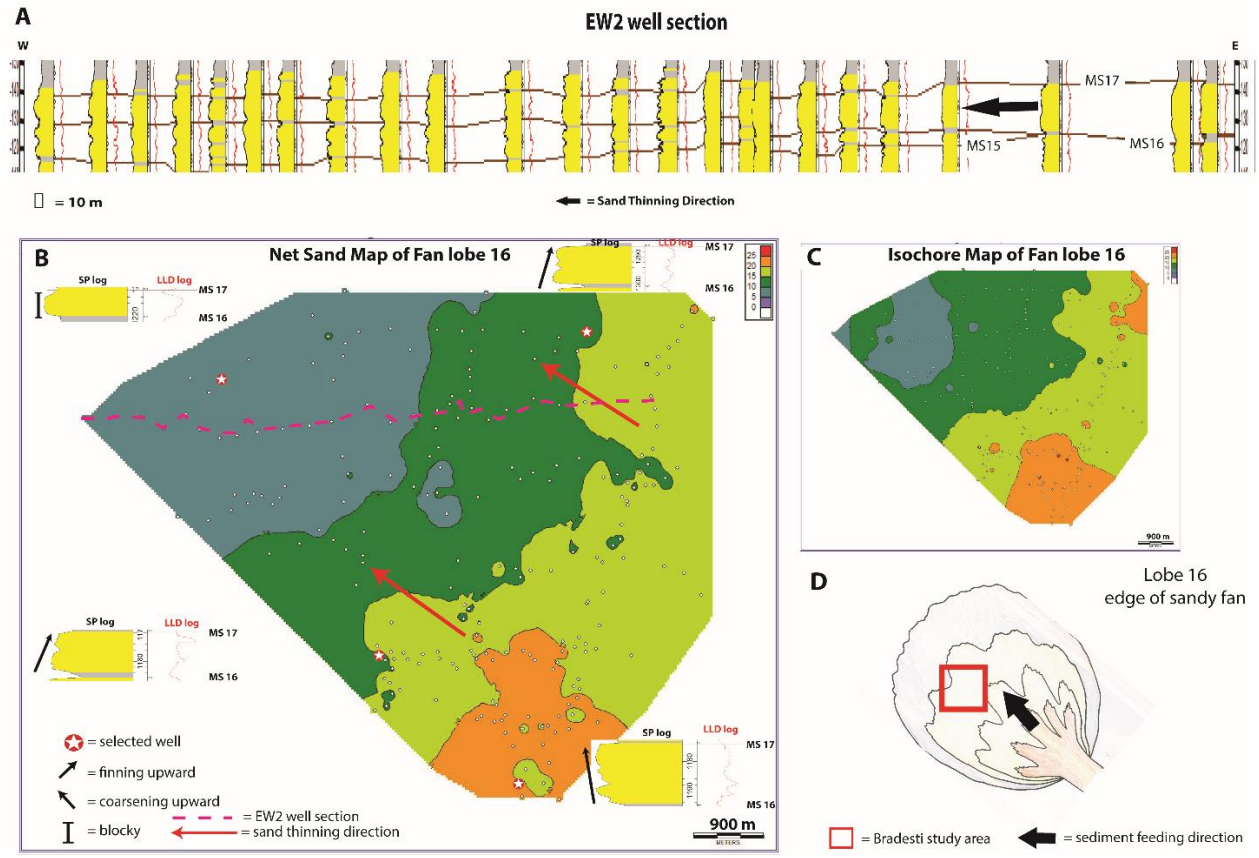


Figure 38: A) East-West2 well section shows well log characteristic of Fan lobe 16 from the east to the west. B) net sand map of Fan lobe 16 with 5 m contour interval C) isochore map of Fan lobe 16 with 5 m contour interval D) sub-depositional environment of Fan lobe 16 inside the study area (red rectangle)

## THE EVOLUTION OF BASIN FLOOR FANS IN THE STUDY AREA

The evolution of the basin-floor fans is reconstructed by evaluating the super-position of successive sub-depositional environments for each fan lobe from Fan lobe 1 (bottom) to Fan lobe 16 (top). The evolution of the basin-floor fans in the study area is shown in Figure 41. The evolution of basin floor fans from the oldest (Fan lobe 1) to the youngest (Fan lobe 16) was caused by four main processes; lateral switching of the sediment source (lobe "rotation"), flip of the sediment source on opposite sides (switching sides), back-stepping and forward-stepping of sediment feeding direction. *Rotation* is the process of sediment feeding movement gradually changing clockwise or counterclockwise from the previous fan lobe but the overall feeding trend is still the same. For example, from Fan lobe 3 to Fan lobe 4, the sediment feeding direction rotated

clockwise from the northeast to the east but overall feeding trend is still from the east. *Switching* is the process whereby sediment feeding direction changes completely (flip on the other side) from the previous fan lobe. To illustrate, from Fan lobe 6 to Fan lobe 7, sediment feeding direction changed from the east to the west. *Back-stepping* refers to a fan lobe moving landward, or more likely the sediment discharge to the lobe decreasing, and more distal deposits in the next fan lobe come inside the study area. For example, from Fan lobe 4 to Fan lobe 5, the sediment feeding trend remains the same, from the east, but the fan lobe received less sediments (moved landward) in Fan lobe 5. *Forward-stepping* process is similar to back-stepping process but the fan lobe feeder moves basinward or the sediment discharge to the basin floor increases. To illustrate, from Fan lobe 5 to Fan lobe 6, the feeding direction is still from the east but Fan lobe 6 moved basinward and has more proximal sub-environment than Fan lobe 5 at the study area location.

Sediment feeding direction of Fan lobe 1 to Fan lobe 6 was from the east and north east, but this then switched to the west in Fan lobe 7. The east-northeast sourced sediments correlate well with the progradation of the clinoforms mapped by Fongngern et al. (2015) and by this current project (Figure 10A) on seismic data. Sediment feeding direction was from the south in Fan lobe 8 to Fan lobe 10. Then, switched to the west again in Fan lobe 11 and 12. Sediment feeding direction of Fan lobe 13 was from the southeast, in Fan lobe 14 from the northeast, in Fan lobe 15 from the northwest and in Fan lobe 16 was from the southeast.

The frequent change in direction, at times in completely opposite directions, in the younger fans 8 to 16 when compared with earlier 1 to 7 fans (Figure 41) can be interpreted as a change in the main sediment supply at the basin margins. This is also reflected by the mapping of the younger seismic clinoforms that have different progradation directions (Figure 16), even though clinoform reflectors were not directly correlated into Bradesti study area. As a summary observation, the frequency of switching of sediment feeding direction, as inferred from the fan lobes, increased from the bottom to the top. However, this bottom to top increase in change of sediment feed direction can also be linked with the "shrinking" of the basin size, due to filling from all sides by clinoforms. If the basin margins became closer as the basin filled it is also more likely that the

basin floor received and accumulated sediments from different directions. Another process linked with decreased size of the basin might be that basin-floor turbidites (gravity flows) extended all the way to the other side of the basin and thickened at the base of the opposite base of slope. This idea is speculative at this point but highly plausible considering that the Dacian Basin gradually became just tens of kilometers wide and basin floor fans have typical dimensions of tens to hundreds of kilometers (Carvajal and Steel, 2006, Koo et al., 2016, Reading and Richards, 1994).

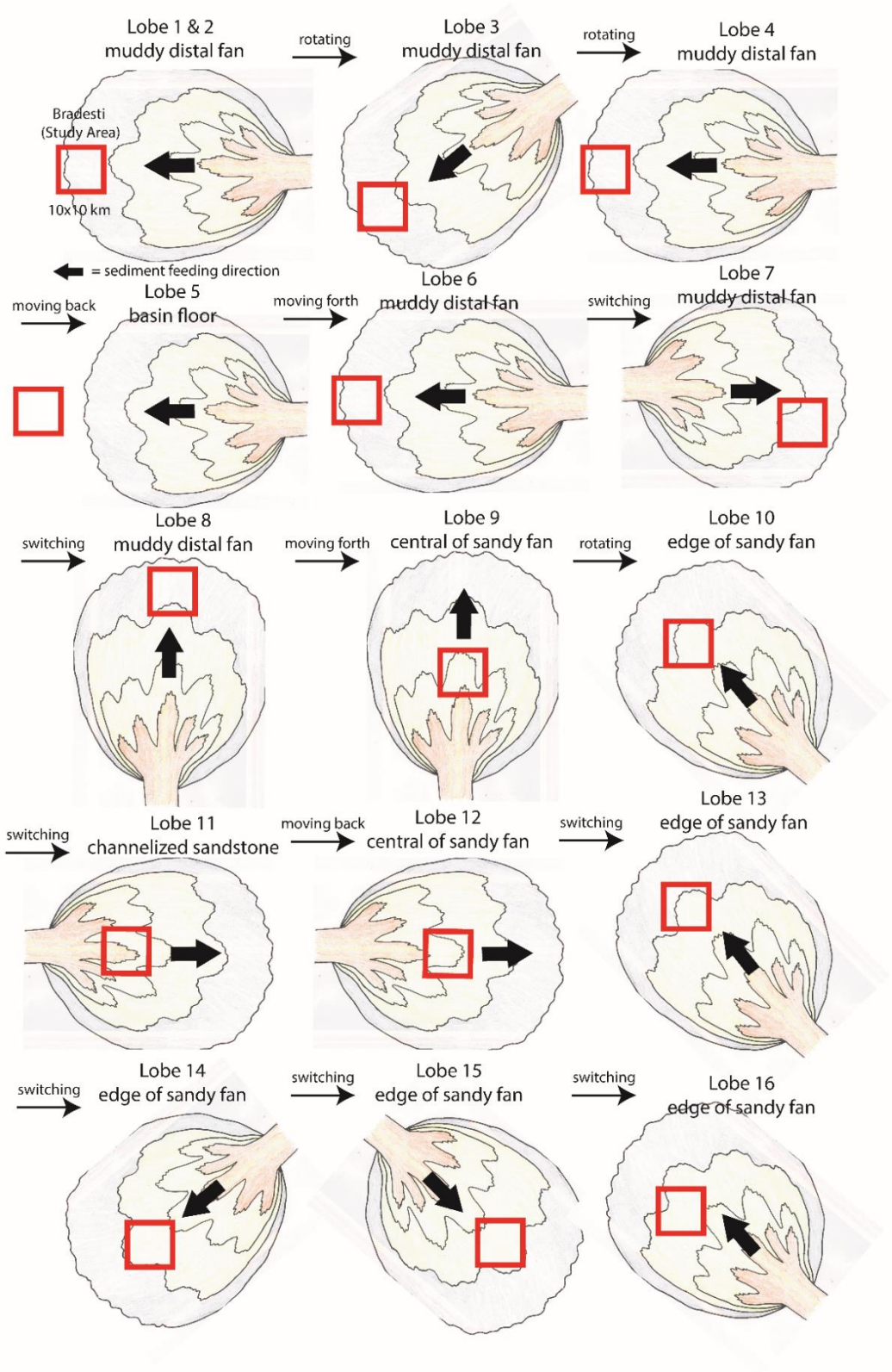


Figure 39: Evolution of basin floor fans in the study area. The red rectangle represents the study area and the arrows represent the sediment feeding direction

## THE OVERALL ARCHITECTURE OF THE FAN

The overall architecture of the Dacian basin-floor fans is shown in six well sections; East-West 1 to 3 in Figure 42, East-West 4 to 6 in Figure 43 and North-South 1 to 3 in Figure 44. The base of the fan succession (FS 1) is picked from the base of the first correlatable sandstone unit throughout the study area. Fan lobes between FS 1 and FS 9 are muddy overall, so FS 9 is the zone of separation between muddy fan lobes below (Fan lobe 1 to Fan lobe 8) and sandy fan lobes above (Fan lobe 9 to Fan lobe 16) (Figures 42 to 44). The top of fan succession is marked by FS 17 at the top of the last correlatable sandstone over the entire study area. The interbedded sandstone and mudstone on top of basin floor fans are interpreted as the base of slope with some slope-channel deposits. The diagnostic characteristic of deepwater slope deposits in the study area is the thick mudstone succession (hundreds of meters above fans) interbedded with lensoid sandstone bodies that are interpreted as slope channels. Examples of slope channels sandstone are seen in N-S2 and N-S3 well cross-sections (Figure 44B and 44C). The slope channel sandstones occur more in the west (Figure 43B). The stacking patterns of lobes at multiple scales is demonstrated in the well cross sections and show inhomogeneous of stacking patterns in both north-south direction (Figure 43B) and east-west direction (Figure 42B).

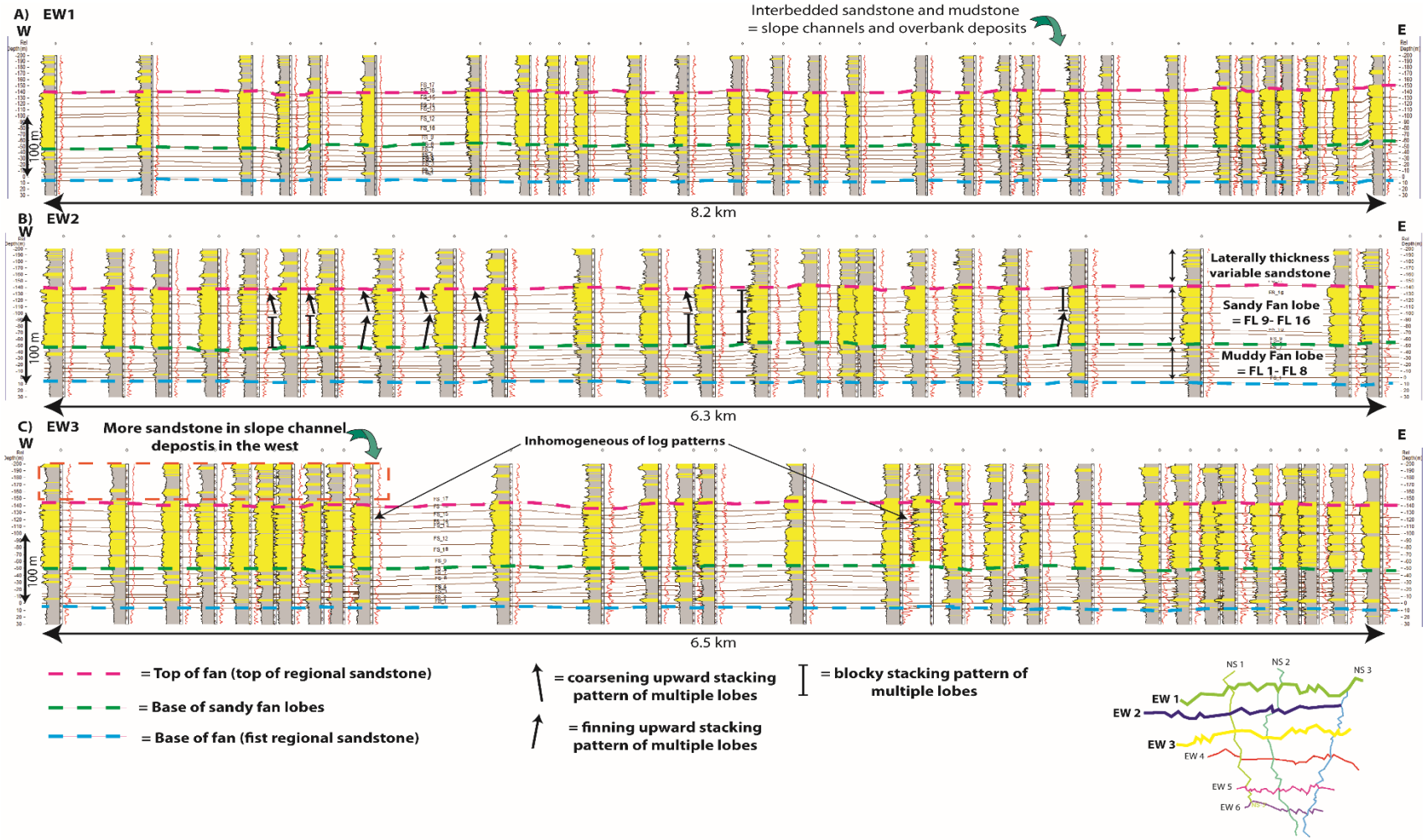


.

Figure 40: A) E-W1 well section B) E-W2 well section C) E-W 3 well section

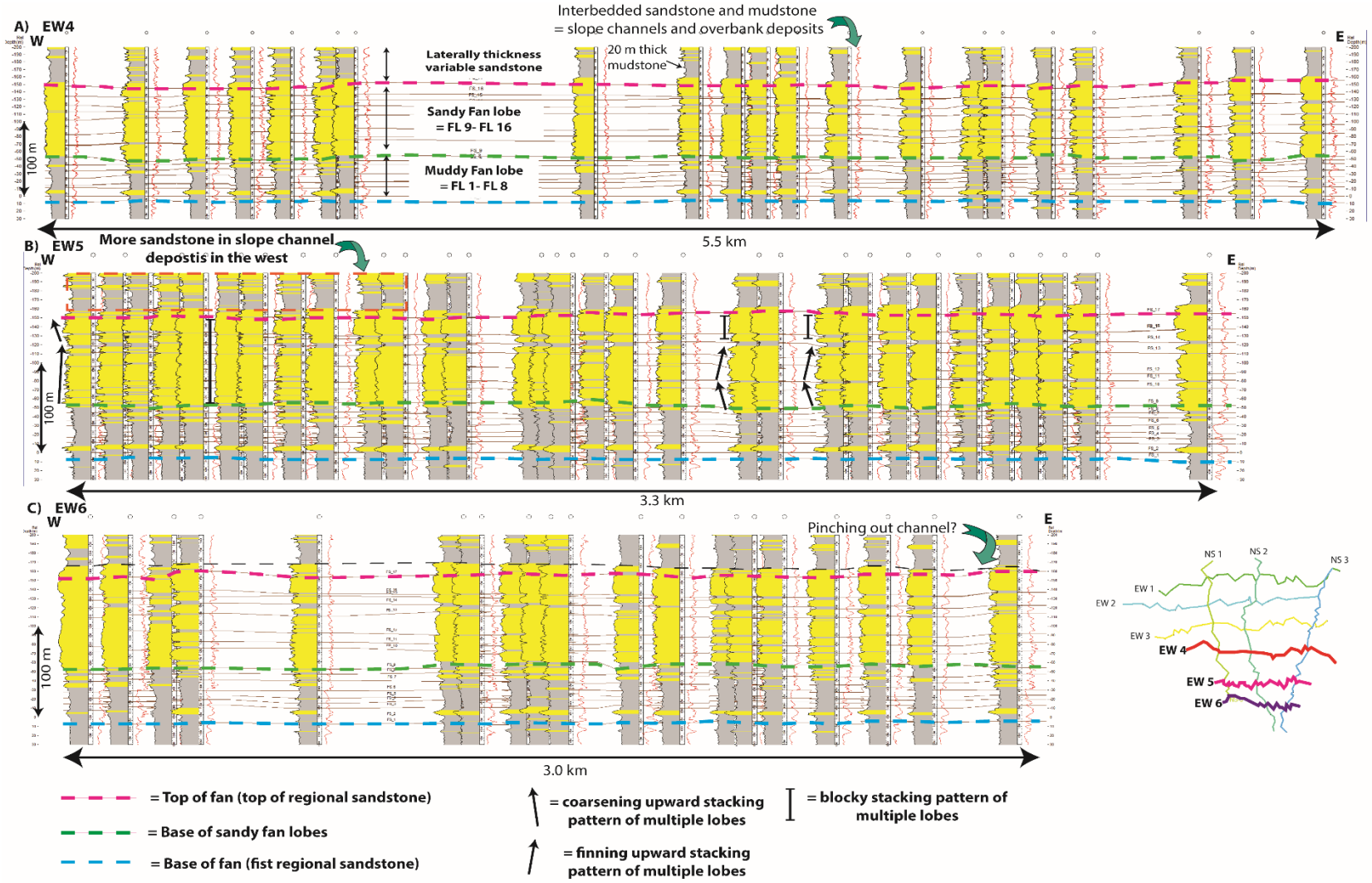


Figure 41: A) E-W4 well section B) E-W5 well section C) E-W6 well section

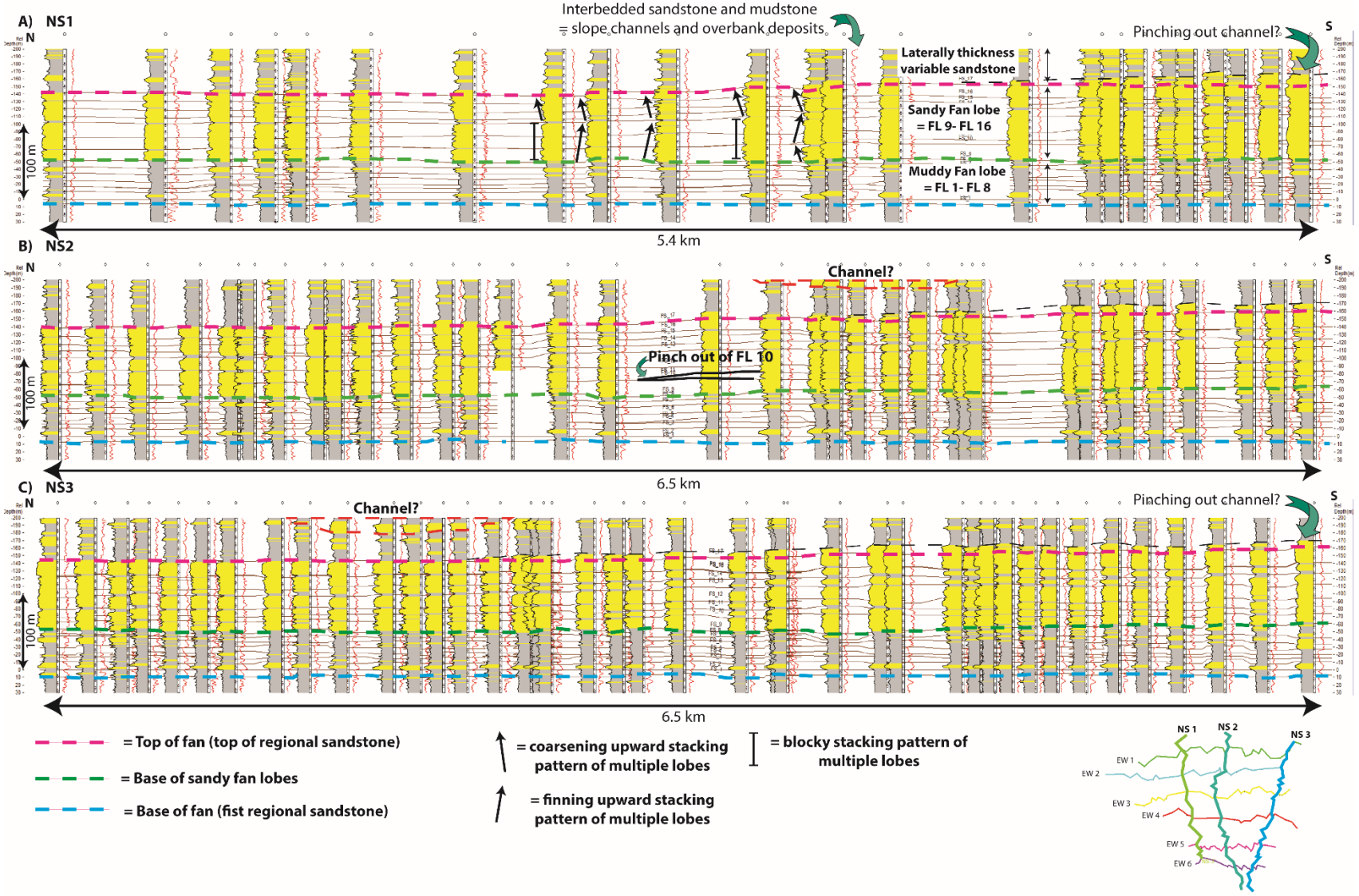


Figure 42: A) N-S1 well section B) N-S2 well section C) N-S3 well section

## THE RELATIONSHIP BETWEEN WELL LOG CHARACTERISTICS AND DIRECTION OF SANDSTONE THINNING

The SP log patterns are overlaid on net sand map of fan lobe 11 and 16 (between muddy surface 11-12) (Figure 45) and 16-17 (Figure 46) since these two fan lobe clearly show a significant thickness trend with a more clear sediment feeding direction. The relationship between the sediment feeding direction and SP log characteristic pattern in the fan lobe 11 shows greater occurrence of fining upward in the proximal part and coarsening upward in the distal part (Figure 45). However, the relationship is not clearly developed in fan lobe 16 that is dominated by a fining upward pattern all over the fan lobe (Figure 46).

The SP log characteristics do not correspond with the expected relationship suggested by the thickness trend. The predicted relationship would be blocky in the central zone of the fan lobe, coarsening upward and fining upward at the edges of fan lobes as usually presented in an "ideal" lobe (Koo et al and Prelat, 2013). However, the expected well log characteristics do not necessarily have the same pattern of distribution in each fan lobe. Prelat et al. (2013) claimed that the thickness patterns (well log characteristics) are influenced by the stacking pattern of lobe elements (Figure 47). In the other words, the relationship between sediment feeding direction and SP log characteristic is variable in each fan lobe despite unidirectional sediment feed and complicated not only by forward-backward movement but also by lateral-stepping (Figure 47)

Moreover, the thinning direction of sandstones used as a first order indication of the sediment feeding direction, adds complexity to the relationship between well log characteristic and feeding direction as well (see previous section discussion and Figure 41). Fan lobes inside the sandy interval shows some pinching out (Fan lobe 10 and Fan lobe 15) that is the evidence of sand body amalgamation and the possible erosion of the previous fan-lobe. Therefore, to some extent, the present sandstone thickness might be a 'relic' of the older, eroded fan-lobe thickness and may not accurately reflect sediment-feeding direction. However, we should also keep in mind that 'erosion' is an integral part of the fan-lobe picture and not necessarily just an external disturbance.

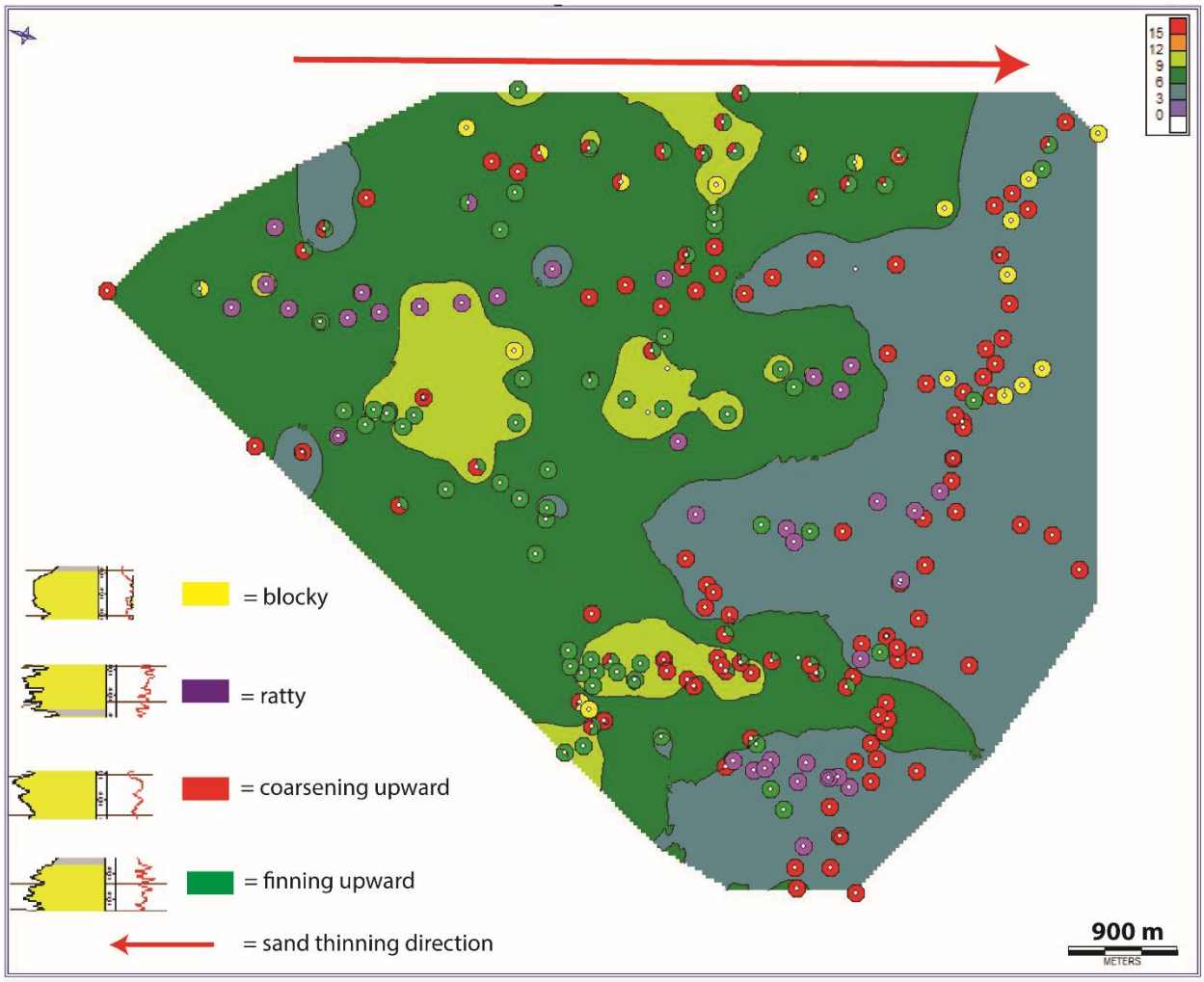


Figure 43: Sand thickness map and the SP log characteristic distribution across Fan lobe 11

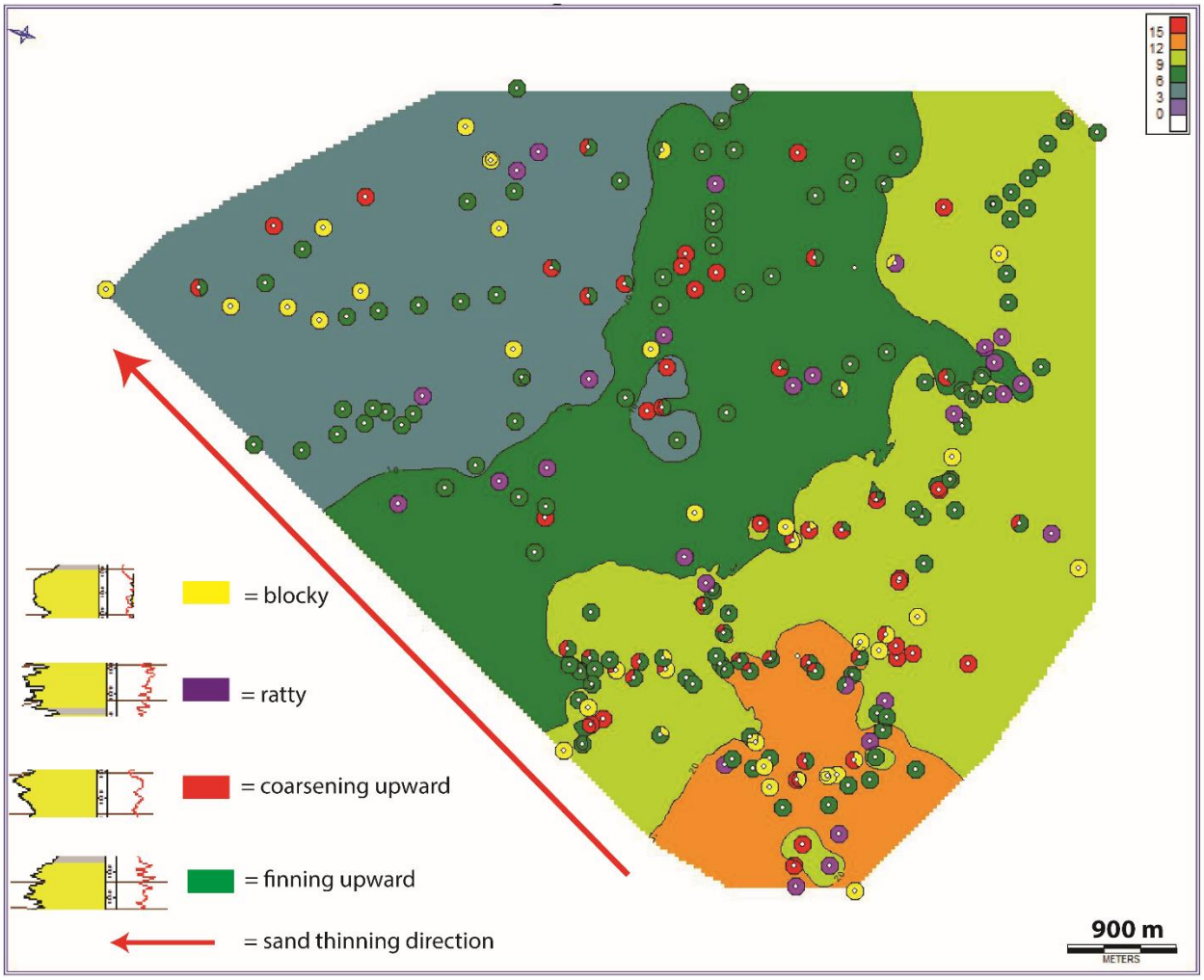


Figure 44: Sand thickness map and the SP log characteristic distribution across Fan lobe 16

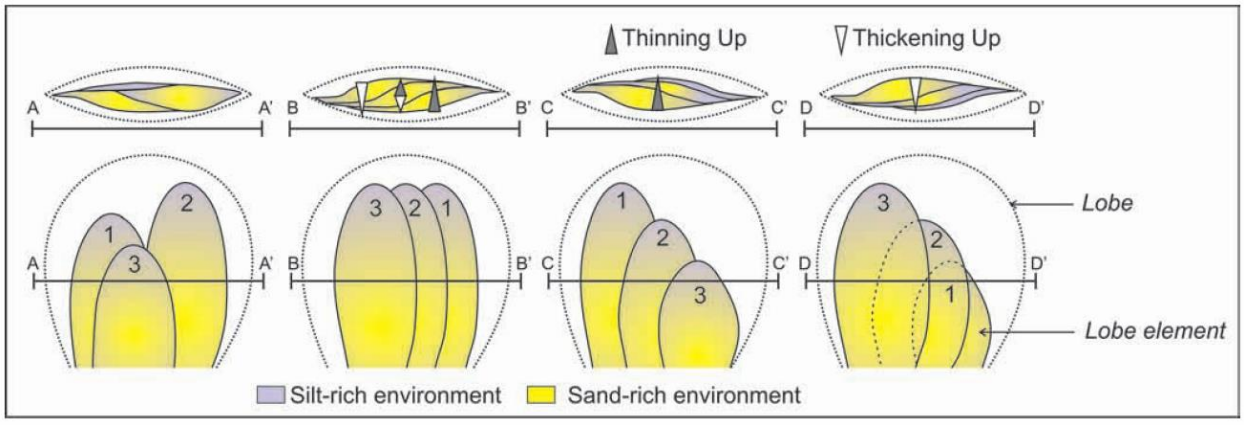


Figure 45: Change of thickness pattern of fan lobes based on the stacking pattern of fan lobe elements (Prelat and Hodgson, 2013)

# Chapter 4: Discussions

Discussion will focus on two points that are specific to large-scale stratigraphic architecture of lacustrine basins, and a third general point related to the abundance of sandy sediment that bypassed from the lacustrine shorelines, bypassed the slopes and accumulated on the basin floor. The first aspect is the multi-directional progradation of the basin margins that is not common to continental margins or to large basins. The second aspect, linked with the first one, is that basin floor fans will be built from sediments fed from multiple directions and is likely to have a complex architecture because of this.

## BASIN FLOOR DEPOSITS IN WESTERN DACIAN BASIN

The seismic and well data, along with the mapping of the western Dacian Basin, show clearly that hundreds of meters thick, deepwater clinoforms prograded from multi-directions (Figure 16) as might be a common thread or feature of closed lake basins or narrow basins. The possibility of multiple directional feeders of sediment in other closed lake basins such as Pannonian Basin in Hungary (Sztano et all, 2013) and Lake Baikal in Russia (Nelson et al 1999) has been previously described. In the Dacian Basin, the large clinoforms prograding from west, north-west, north, north east, south-east, although noticed before on 2D-data (Leveer et al., 2010) have been mapped in detail in the present study. The unusual geometry of western Dacian Basin with thin topset deposits and much thicker bottomsets was also noted earlier by Fongngern et al., (2015), though they did not use well data or extend their mapping significantly into the basin-floor fans. Using over 200 wells closely (100s m) spaced in the center of the basin this study documents that part of the hundreds of meters thick bottomsets are extremely sand-prone and reach 100-150 m thick (Figures 42, 43 and 44). The significant thickness of bottomsets is not unexpected considering that western Dacian Basin was a closed source-to-sink system trapping the entire sediment volume delivered into the basin and the basin floor collected sediments form all around margins. The “all around” sediment feeding was shown by mapping seismic lines with different orientations and also based on thickness patterns of the basin floor fan.

## FREQUENT SANDY SEDIMENT BYPASS FROM LACUSTRINE SHORELINES TO DEEP WATER BASIN FLOOR

Although the Dacian Basin as a closed 'sink' would have received much sediment because of drainage from all sides, as noted above, there is likely another reason for the huge volumes of sand now aggraded on the basin floor. River flooding from land areas into lakes are well-known generators of sediment gravity flows in lakes (Crookshanks and Gilbert, 2008) because the suspended sediment concentration in flooding rivers needed to create plunging underflows in lake water is significantly less than needed in marine basins. This makes it likely that hyperpycnal flow events would have been very frequent from all river flooding along the Dacian Basin shorelines into the deep water of the lake basin. In addition, it was shown by Fongngern et al (2015) that the unusually thin topsets of the Dacian clinoforms were likely controlled by a 'silled' condition at the outflow to the Black Sea; this restriction of aggradation on the topsets would also have enhanced bypass processes on the clinoforms, another factor leading to thickly accumulated sandy bottomsets.

## OTHER LACUSTRINE (CLOSED) BASINS

Lake Baikal in Russia is another example of large (75 by 600 km) lake basin (Figure 48A). It consists of three half-graben rifts that have water depth of 900, 1600 and 1400 m. The lake is bounded by steep faults in the West and gradual ramps on the East (Figure 48E). Sediment is fed to the lake from multiple directions with different sedimentary characteristics. The steep fault boundary in the West provides coarse grained material by multiple small fan deltas (< 10 km diameter) and form sand-rich aprons at the base of the fault boundary while in the East boundary that has less steep ramp provides more fine grained sediment to the lake floor by channelized turbidite fan (5 to > 65 km diameter) (Figure 48D and 48E) (Nelson et al, 1999).

A seismic section across the Lake Baikal in Figure 48B shows the base of slope apron on the west side of the lake (steep border fault) extended a few kilometer away from the toe of slope with seismic characteristic as wedge shape, discontinuous and high amplitude reflectors. The distal apron gradually flattens and continues down to the basin floor which indicates that the sand aprons

laterally feed sediment to the basin floor. Transverse seismic line in Figure 48C shows the sublacustrine channels with dimensions 10-20 m deep and 100-400 m wide. The schematic of cross-section of the lake that shows the depositional environment of the lake is in Figure 48E.

The similarity between Lake Baikal and Dacian Basin is they both are closed lakes and show evidence of multiple directions of sediment fed to the basin. However, the tectonic setting is different. Lake Baikal steeply fault bounded to the west and there is no evidence of the presence of clinoforms on that side of the basin. The dimensions of basin floor fans are also different compared to basin floor fans in Dacian Basin. The size of sand rich apron at the toe of the slope in Lake Baikal is about 5 km wide and 10-20 m thick, while the size of sandstone rich basin floor fans in Dacian basin is at least 10 km wide and about 150 m thick. The reason might be the lack of large rivers/ feeding clinoforms in the western side of Lake Baikal, only short local stream (< 20 km length) that are the main coarse-grained sediment feeder, and therefore less amount of sand transported to the basin floor.

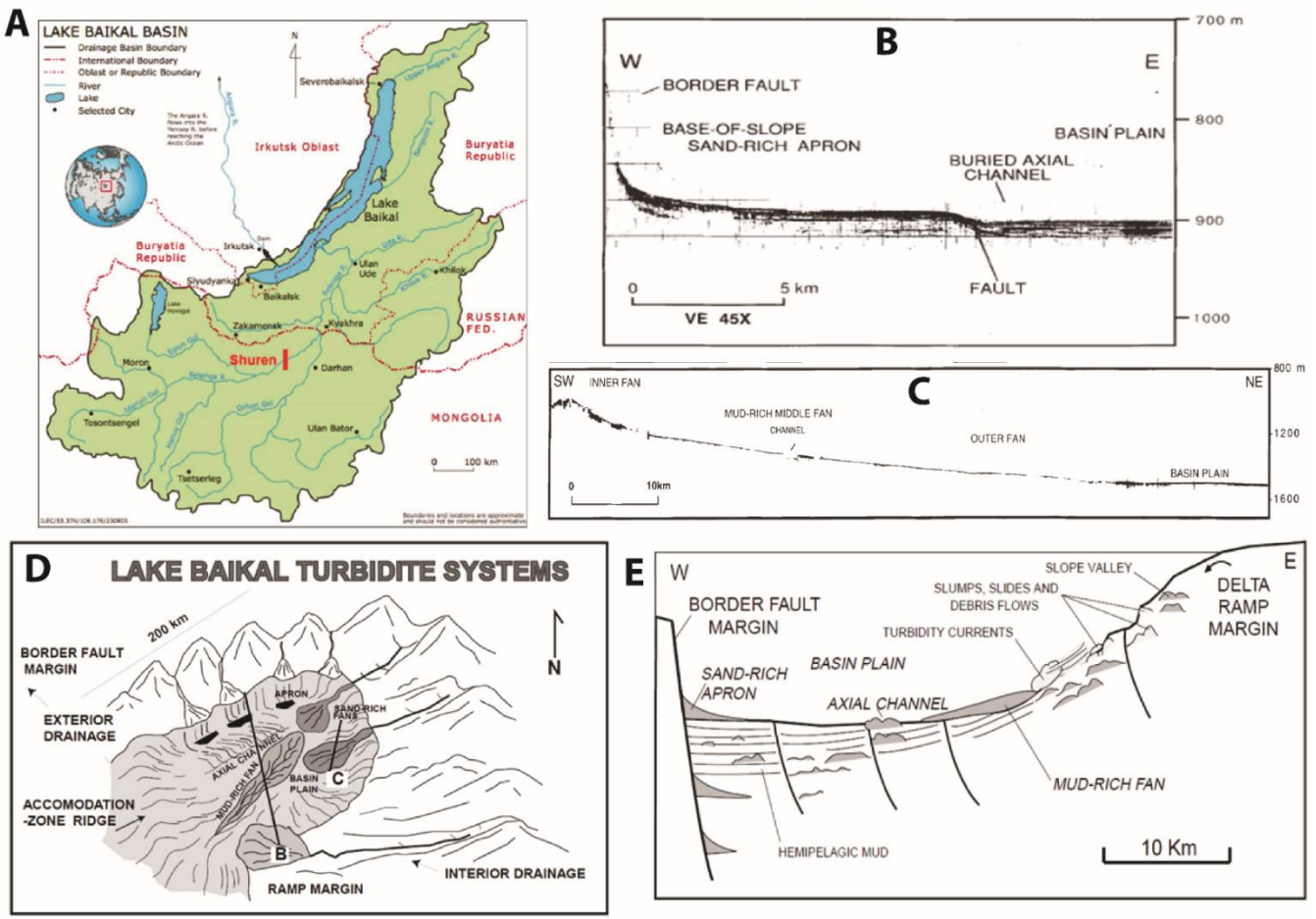


Figure 46: A) Lake Baikal basin with drainage area shows different drainage pattern between the eastern and the western area of Lake Baikal (only one large river in the west) (Gertcyk, 2016). B) East-west seismic line across Lake Baikal shows base of slope sand apron at the toe of steep fault boundary. C) east-west seismic profile of mud-rich fan illustrates channels and fan system on Lake Baikal basin floor. (Nelson et al 1999) D) Turbidite system on Lake Baikal demonstrates sand rich apron deposited on the western side and turbidite fan deposited in the eastern side of the lake. (Nelson et al 1999) E) interpreted cross-section of depositional elements in Lake Baikal (Nelson et al 1999)

Lake Pannon in Hungary was a brackish lake that formed in Late Miocene by post-rift thermal subsidence (Magyar et al, 1999), is located to the west of the Dacian Basin and had a similar evolution. The Pannonian Basin has large (up to 900 m thick) clinoforms mapped on seismic data across the basin (Figure 49E) (Sztano et al., 2013, Magyar et al, 1999). Basin floor fans as a part of bottomset of the large clinoforms are also present in this basin. The seismic amplitude horizon of basin floor fans show that the meandering channel basin floor fans were deposited further into the basin during an aggradation period while basin floor fans were developed at the toe of slope during progradation period (Figure 49D) (Sztano et al., 2013). The size of the sandy fan lobes are 5-15 km long and 4 – 10 km wide. The thickness of each fan lobe ranged from 10 to 50 m. The average size of the fan lobes in Lake Pannon is similar to the lobate features of Bradesti 3-D cube in Dacian Basin (Figure 19). However, the thickness of the fan lobes interpreted in Pannonian are slightly greater than the fan lobes in Dacian Basin that ranged from 10 to 30 m.

Magyar et al. (1999) researched the paleo-Danube shelf margin in the Pannonian Basin during the late Miocene and Early Pliocene (Figure 49A). An example of shelf margin clinoforms is shown in Figure 49B. The height of clinoforms indicates water depth from 200 – 600 m. The individual clinoforms extended about 25 km in strike direction with 5 – 15 km of slope width. The shelf margins are mapped in many seismic lines and are posted with age in Figure 49C. The dip of the slope in Figure 49C shows that the sediment was fed from different directions. In addition to well documented north-south progradation, the Pannonian basin margin was also prograding from east to west or even from the south to north for some time intervals.

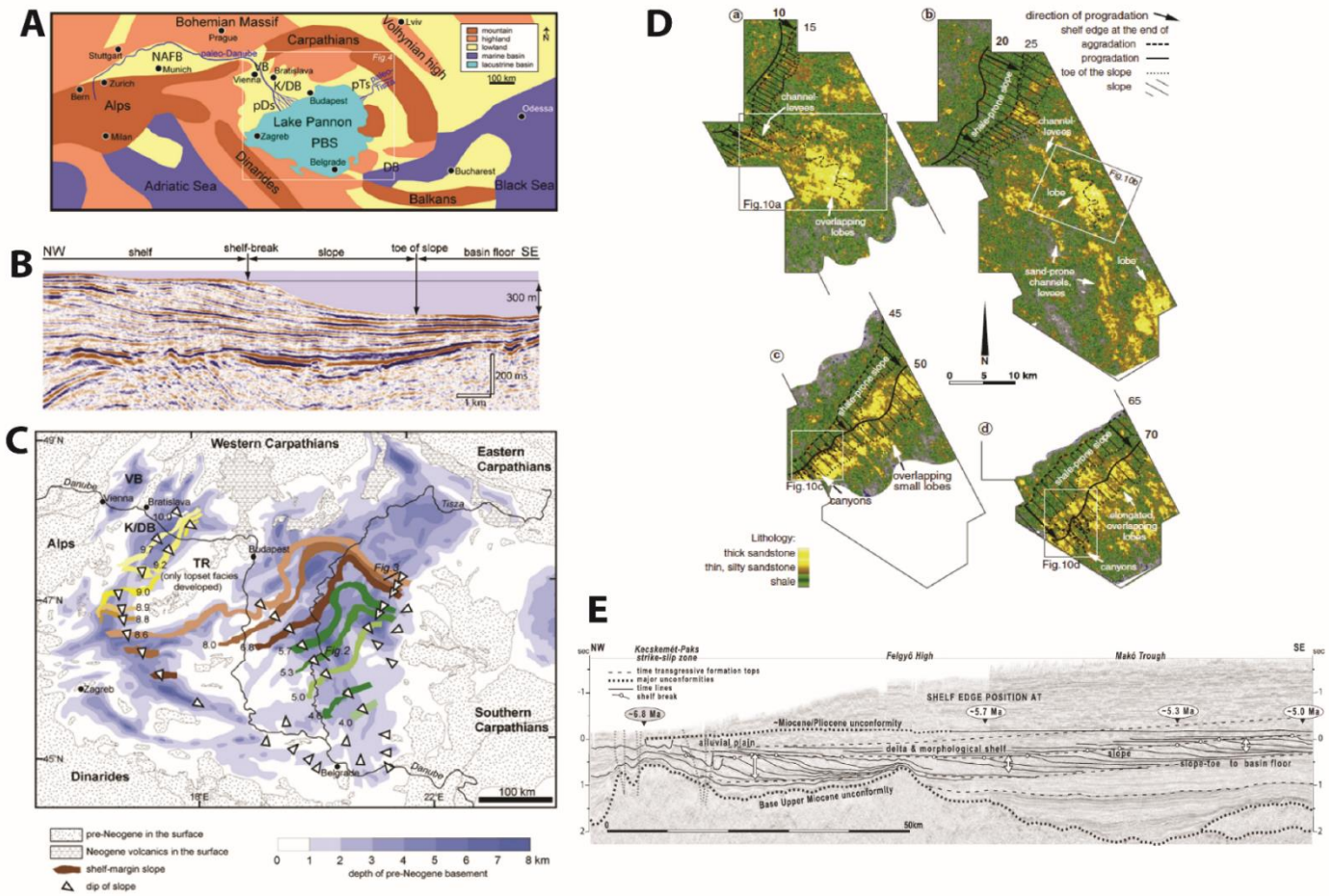


Figure 47: A) The paleo-geography of the Pannaonian Basin at about 9Ma B) Shelf margin clinoforms of the Pannonian Basin C) Shelf margin progradation of the paleo Danube and paleo Tisza shelf across the Pannonian Basin. The width of the ribbon indicate the width of the slope with age in black number. The white arrows represent the dip of the slope (Magyar et al, 2013) D) Amplitude maps of basin floor fans a) and b) are meandering channel fans deposited during the aggradation period c) and d) toe of slope fans deposited during progradation period. E) Seismic line shows prograding clinoforms with height from 400 – 500 m in the South to 900 m in the North of Lake Pannon (Sztano et all, 2013)

Multiple directional feeding of lake sediment is more likely to have multiple sediment sources. As example of multiple source is the large (28,000 $km^2$) Jianghan Basin in China which is the Mesozoic-Cenozoic rift basin (Figure 50A). Detrital zircons dating results of early Eocene formation show three main ages which are 113-158, 400-500 and 700-1000 Ma. The ages of zircons are correlated with the source areas from the east, the north and the south, respectively. Figure 50B is the schematic picture of the provinance of sediment. The simplified depositional environment model of the Jianhan Basin during the early Eocene is in Figure 50C.

Detrital material analysis in Dacain Basin also indicates four regional areas of sediment sourcing: the Eastern Carpathians, the Southern Carpathain, the Balkanian and the Dobrogen source areas (Figure 50D). (Jipa and Olariu, 2009) that potentially have different sediment age-range although such analysis are not done yet.

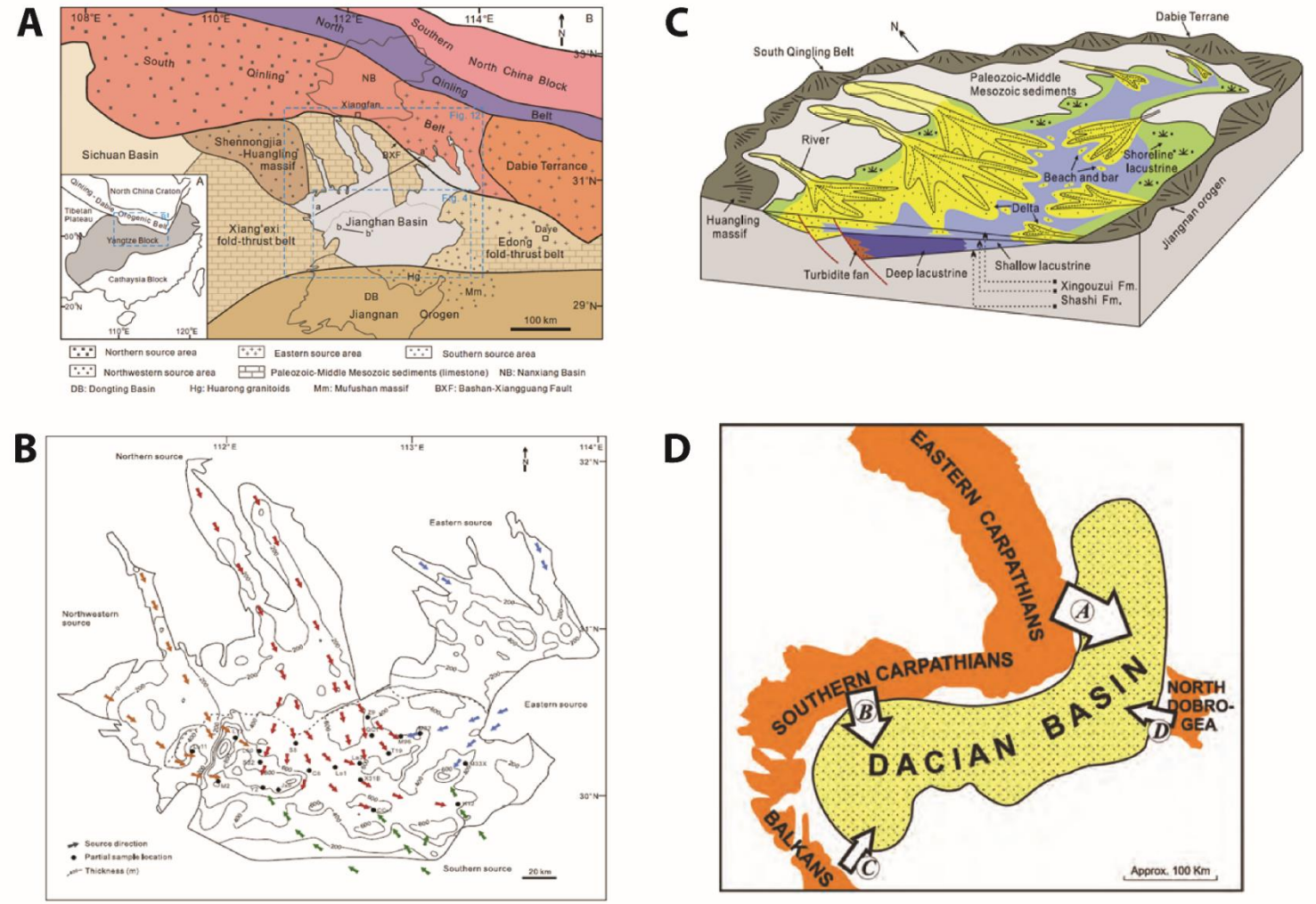


Figure 48: A) Geologic map of Jianghan Basin B) Routing of sediment and possible provenances based on zircon dating results overlying on isopach map of Xinagouzui Formation C) Schematic drawing of paleogeography and depositional environment of Jianghan Basin during the Early Eocene (Wu et al, 2017) D) The sediment source areas of Dacian Basin. (Jipa and Olariu, 2009)

Another example of closed lake basin with deepwater deposits is Lake Malawi, which is one of East Africa Rift basins. The size of this lake is 30 to 80 km wide, 580 km long and water depth over 700 m. Seismic mapping inside this lake found the sigmoidal shaped clinoforms prograding basinward (Figure 51A). The sigmoidal shapes are interpreted as progradational lowstand deltas. Thickness of delta clinoforms is about 50 m and the area of the deltas is around 100 km$^2$ (Figure 51E). Moreover, sand apron (wedge-shaped deposits) as similar to Lake Baikal also present at the toe of steep fault boundary (Figure 51C). Channels also observed in the center of lake with U-shaped in the cross section (Figure 51B). The basin-fill facies at the depocenter of the lake is composed of hemipelagic mud and turbidites onlapping against delta clinoforms (Figure 51D). Even though the size of clinoforms in smaller than in the Dacian Basin, Lake Malawi shows multiple coeval sediment feeding systems similar to the Dacian Basin (Figure 51E).

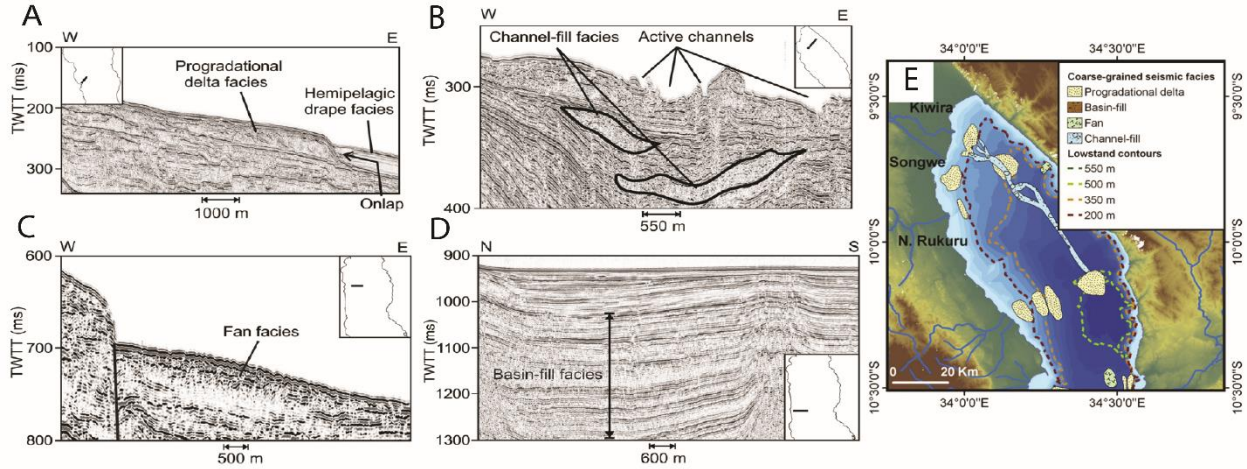


Figure 49: A) seismic section shows progradational deltas facies in Lake Malawi B) active channels and channel facies C) sand facies at the toe of fault boundary D) basin fill facies at the depocenter E) distribution of lowstand coarse-grained deposits in Lake Malawi indicates multiple directional sediment feeding) (Lyons et al, 2011)

## WELL LOG CHARACTERISTICS OF LAKE BASIN FLOOR FANS

Apart from the study of well log charateristics of basin floor fan that was done by Koo et al. (2016), that mentioned earlier in the result chapter. Another example of well log characteristic of basin floor fans in closed lake basin is from Panonian basin. Clinoforms range from 400 to 900

m height occurred in this lake. Basin floor fans in the Pannonian Basin are described as Szolnok Formation with thick stacked sandstone bodies. The gamma ray log of this formation shows similar characteristic as in Dacian basin since they are comprised of various characteristic patterns such as finning upward, coarsening upward and blocky (Figure 52E) (Sztano et all, 2013).

The complexity of basin floor fans architecture is also noted in the study of deep water deposited in Permian Karoo Basin in South Africa. Prelat et al found that the outcrop of basin floor fans lobe have complex bed thickness trends and architecture. The same fan lobe can have both finning upward and coarsening upward characteristic even within the same outcrop (500 m separation of the observation points) (Figure 52A to 52D).

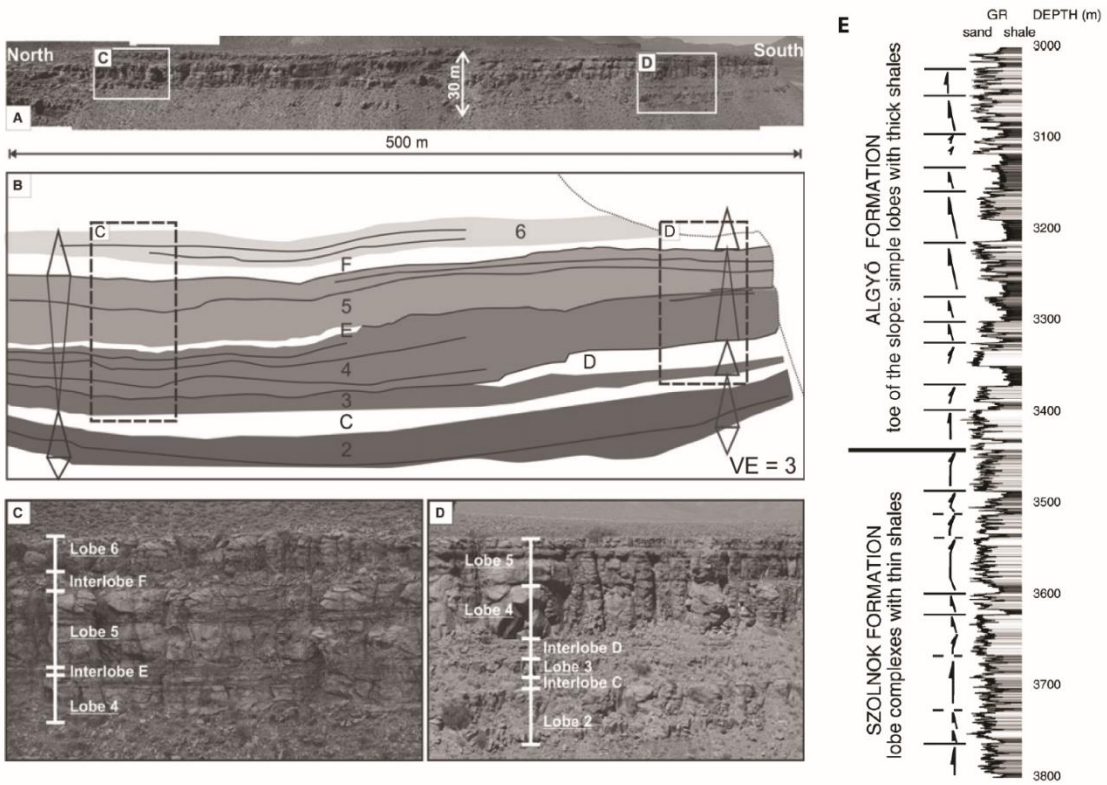


Figure 50: A) the outcrop of basin floor fans lob complex B) the interpretation with triangles represent thinning and thickening direction C) thickening upward characteristic of fan lobe complex D) thinning upward characteristic (Prelat et al, 2009) E) gamma ray log of Szholnok Formation shows basin floor fan lob complex with amalgamated sand bodies with overlying muddier interval of slope deposits. (Sztano et all, 2013)

The well log characteristic of basin floor fans either in marine or lake deposts is the same, the well log characteristic does not show significant difference, both logs show a variety of well log characteristic patterns such as coarsening upward, finning upward and blocky. The composition of sand-mud also similar with thick amalgamated sandstone inside basin floor fans and more mudstone interbedded with sandstone in the slope deposited overlying on the fans deposits (Figure 52E). However, the complexity that added to lake basin floor fans is the multiple sediment feeding direction that might make the evolution of lacustrine fan different from marine basin floor fans.

**DEPOSITIONAL ENVIRONMENT MODEL OF LAKE BASIN FLOOR FANS**

From all mentioned lake basins examples (Figures 48 to 52), it is clear that multiple directional feeding sediment in closed lake basins is common because the turbidity flow runoffs are commonly longer than the lacustrine basin floor. The longer turbidity flows in lakes might be also supported by the higher density difference between turbid flow and ambient water given by low salinity of the water in some lakes. The multiple directional fed clinoforms are more likely to have various sediment provenance since the sediment are transported by different river drainage systems via deltas around the lake. The schematic model of multiple directional feeding are in Figure 53C and 53D. The classic model of point and line fed are illustrated in Figure 53A and 53B.

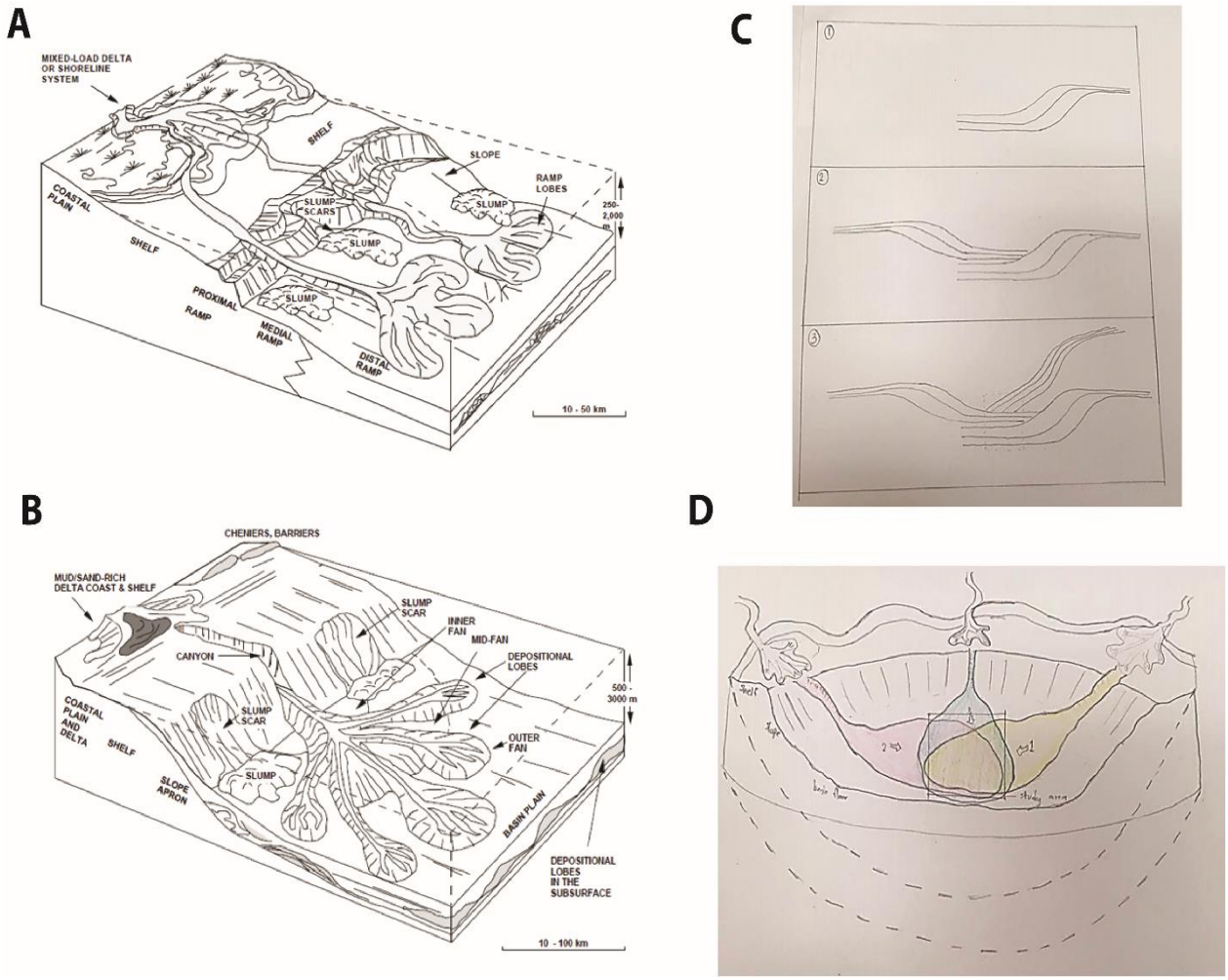


Figure 51: A) depositional model for ramp deposits (Reading and Richards, 1994) B) depositional model of point source fan deposits (Reading and Richards, 1994) C) schematic drawing of amalgamated bottomsets by multiple directional feeding clinofroms. The rectangle represents the study area. D) schematic drawing of multiple directional feeding basin floor fans

# Chapter 5: Conclusion

Seismic interpretation in both 3-D cubes and 2-D lines of seismic data show basin-margin clinoforms prograding from various directions around and down into the deepwater Dacian Basin. The overall thickness of clinothems suggests strong shelf edge progradation with relatively thin (100 m) topsets and thick (300 m) bottomsets. The detailed correlation of closely-spaced (100s of m) well logs illustrates the complexity of basin-floor fans in lake basins. The 150-200 m thick basin floor fans identified on seismic data are subdivided into 16 fan-lobes (averaging 5 m-to 30.m thick) using 217 well logs. In both time and space, fan lobes change their thickness trends and feeding direction. The same variability is also observed for multiple stacked fan lobes of the Dacian basinfloor fans. The SP log characteristics tend to be different in each of the 16 mapped fan lobes, and also varies laterally within the same fan lobe. The thinning direction of fan-lobe sandstone indicates the feeding direction of sediment and the results show that the feeding directions are from around the basin and also vary through time. Furthermore, the frequency of switching of sediment-feeding direction increased with time as well. The relationship between SP log characteristic and sediment feeding direction is complicated and cannot be expressed in a simple interpretation. The multi- directional feeding of sediment from various drainage catchments to the basin floor can possibly lead to complexity to reservoir quality. Furthermore, the complex thinning trends of sandstone bodies increases the difficulty of reservoir modelling and development.

# REFERENCES


*Balla, Z. (1987), Tertiary palaeomagnetic data for the Carpatho-Pannonian region in the light of Miocene rotation kinematics, Tectonophysics, 139, 1-2: 67-98*

*Catuneanu, O., Galloway, W., Kendell, C., Miall, A., Posamentier, H. and Strasser, A., 2011, Sequence Stratigraphy: Methodology and Nomenclature, Newsletters on Stratigraphy, Vol. 44/3, 173-245*

*Crookshanks S. and Gilbert, R., 2008, Continuous, diurnally fluctuating turbidity currents in Kluane Lake, Yukon Territory, the NRC Research, Canada Journal of Earth Sciences, 45: 1123-1138*

*Fongngern, R., Olariu, C., Steel, R. and Krezsek, C., 2015, Clinoforms growth in a Miocene, Para-tethyan deep lake basin: thin topsets, irregular foresets and thick bottomsets, Basin Research, v. 28, p. 770-795*

*Gertcyk, O., 2016, Extreme warning issued that Lake Baikal could drain dry like the Aral Sea, The Siberian Times, Ecology, Case study.*

*Hamor, G., et al., 1988. Neogene paleogeographic atlas of Central and Eastern Europe. Hungarian Geological Institute, Budapest*

*Ilyna, L. B., Nevesska ya, L.A., Paramonova , N.P., 1976. Neogene evolution of mollusks in brackish water basins of Eurasia. Proceedings of Paleontological Institute Akademia Nauk SSSR, 155: 1-289 (In Russian)*

*Jipa, D. and Olariu, C., 2009, Dacian Basin: depositional architecture and sedimentary history of a paraththys sea, National Institute of Marine Geology and Geo-ecology (GeoEcoMar) – Romania*

*Johannessen, E. and Steel, R., 2005, Shelf-margin clinoforms and prediction of deepwater sands, Basin Research, v. 17, p. 521-550*

*Koo, W., Olariu, C., Steel, R., Olariu, M., Carvajal, C. and Kim, W., 2016, Coupling between shelf-edge architecture and submarine-fan growth style in a supply-dominated margin, Journal of Sediment Research, v. 86, p. 613-628*

*Krézsek, C. et al., 2013. Strain partitioning at orogenic contacts during rotation, strike–slip and oblique convergence: Paleogene–Early Miocene evolution of the contact between the South Carpathians and Moesia. Global and planetary change, 103, pp.63–81.*

*Leever, K., Matenco, L., Rabagia, T. Cloetingh, S. Krijgsman, W. and Stoica, M., 2010, Messinian sea level fall in the Dacic Basin (Eastern Paratethys): palaeogeographical implications from seismic sequence stratigraphy, Terre Nova, v.22, p. 12-17*

*Lyons, R., Scholz, C., Buoniconti, M., Martin, M., 2011, Late Quaternary stratigraphic analysis of the Lake Malawi Rift, East Africa: An integration of drill-core and seismic-reflection data, Palaeogeography, Palaeoclimatology, Palaeoecology 303 (2011) 20–37*

*Magyar, I., Geary, D.H., Müller, P., 1999a. Paleogeographic evolution of the Late Miocene Lake Pannon in Central Europe. Palaeogeography, Palaeoclimatology, Palaeoecology 147, 151–167.*

*Magyar, I., Geary, D.H., Sütő-Szentai, M., Lantos, M., Müller, P., 1999b. Integrated biostratigraphic, magnetostratigraphic and chronostratigraphic correlations of the Late Miocene Lake Pannon deposits. Acta Geologica Hungarica 42, 5–31.*

*Magyar, I., Radivojevic, D., Sztano, O., Synak, R., Ujszaszi, K. and Pocsik, M., 2013, Progradation of the paleo-Danube shelf margin across the Pannonian Basin during the Late Miocene and Early Pliocene, Global and Planetary Change, v. 103, p. 168-173.*

*Matenco, L., Bertotti, G., Cloetingh, S., and Dinu, C. (2003) Subsidence analysis and tectonic evolution of the external Carpathian - Moesian Platform region during Neogene times. Sediment. Geol., 156, 71–94.*

*Nelson, C., Karabanov, E., Colman, S. and Escutia, C., 1999, Tectonic and sediment supply control of deep rift lake turbidite systems: Lake Baikal, Russia, Geology, v. 27, no. 2, p. 163-166.*

*Olteanu R., 1989. New Ostracodes in Upper Neogene from Romania, Memoires Inst.Geol., 34: 123-182. Bucureşti.*

*Papa ianopol, I., Marinescu, F., Maca leţ, R., 1995. Stratotypes, faciostratotype, stratotypes de limite. In Marinescu, F., Papaianopol, I. (eds). Chronostratigraphie und Neostratotypen. Neogen der Zentrale Paratethys, IX Dacien: 103-125.*

*Popov, S.V., Rögl, F., Roza nov, A.Y., Steininger, Fritz F., Shcherba , I.G., Kovac , M. (eds) 2004. Lithological-Paleogeographic maps of Paratethys. Late Eocene to Pliocene. 46 pages, maps 1-10 (annex). Courier Forschungsinstitut Senckenberg, 250: 1-46. Frankfurt am Main.*

*Prelat, A. and Hodgson, D., 2013, The full range of turbidite bed thickness patterns in submarine lobes: controls and implications, Journal of the Geological Society, London, Vol. 170, 2013, pp. 209 –214.*

*Prelat, A., Hodgson, D. M. and Flint, S. S., 2009, Evolution, architecture and hierarchy of distributary deep-water deposits: a high-resolution outcrop investigation from the Permian Karoo Basin, South Africa, Sedimentology, v. 56, p. 2132-2154*

*Reading, H. and Richards, M., 1994, Turbidite systems in deep-water basin margins classified by grain size and feeder system, AAPG Bulletin, v. 78, no. 5, p. 792-822*

*Rich, J.L., 1951, Three critical environments of deposition and criteria for recognition of rocks deposited in each of them. Geol. Soc. Am. Bull. 62, 1-20.*

*Saulea, E., Popescu, I., Săndulescu, J.1969. Atlas litofacial. VI – Neogen, 1:200.000 (in Romanian and in French). Institutul Geologic. Bucureşti.*

*Stoica , M., Laz ăr, I., Vasiliev, I., Kri jgsman, W., 2007. Mollusc assemblages of the Pontian and Dacian deposits from the Topolog-Argeş area (southern Carpathian foredeep – Romania). Les associations de mollusques du Pontien et du Dacien de la region de Topolog-Argeş (avan-fosse carpatique meridionale, Roumanie), Geobios, 40: 391-405.*

*Sztano, O., Szafian, P., Magyar, I., Horanyi, A., Bada, G., Hughes, D., Hoyer, D. and Wallis, R., 2013, Aggradation and progradation controlled clinothems and deep-water sand delivery model in the Neogene Lake Pannon, Mako Trough, Pannonian Basin, SE Hungary, Global and Planetary Change, v. 103, p. 149-167.*

*Ustaszewski, K., Schmi d, S., Fügenschuh, B., Tischler, M., Kissling, E., Spak man, W., 2008. A map-view restoration of the Alpine-Carpathian-Dinaridic system for the Early Miocene, Swiss Journal of Geosciences, 101: 273-294.*

*Van Wagoner, J. C., R. M. Mitchum, K. M. Campion, and V. D. Rahmanian, 1990, Siliciclastic sequence stratigraphy in well logs, cores, and outcrops: concepts for high-resolution correlation of time and facies: AAPG Methods in Exploration Series 7, 55 p.*

*Wu, L., Mei, L., Liu, Y., Luo, J., Min, C., Lu, S., Li, M. and Guo, L., 2017, Multiple provenance of rift sediments in the composite basin-mountain system: Constraints from detrital zircon U-Pb geochronology and heavy minerals of the early Eocene Jianghan Basin, central China, Sedimentary Geology, v. 349, p. 46-61*